



1 **Overview: Recent advances on the understanding of the Northern Eurasian environments and of the**  
2 **urban air quality in China - Pan Eurasian Experiment (PEEX) program perspective**

3  
4 Hanna K. Lappalainen<sup>1,2</sup>, Tuukka Petäjä<sup>1,2</sup>, Timo Vihma<sup>3</sup>, Jouni Räisänen<sup>1</sup>, Alexander Baklanov<sup>4</sup>, Sergey  
5 Chalov<sup>5</sup>, Igor Esau<sup>6</sup>, Ekaterina Ezhova<sup>1</sup>, Matti Leppäranta<sup>1</sup>, Dmitry Pozdnyakov<sup>7</sup>, Jukka Pumpanen<sup>8</sup>, Meinrat  
6 O. Andreae<sup>9,42,43</sup>, Mikhail Arshinov<sup>10</sup>, Eija Asmi<sup>3</sup>, Jianhui Bai<sup>11</sup>, Igor Bashmachnikov<sup>7</sup>, Boris Belan<sup>10</sup>, Federico  
7 Bianchi<sup>1</sup>, Boris Biskaborn<sup>12</sup>, Michael Boy<sup>1</sup>, Jaana Bäck<sup>13</sup>, Bin Cheng<sup>3</sup>, Natalia Ye Chubarova<sup>5</sup>, Jonathan  
8 Duplissy<sup>1</sup>, Egor Dyukarev<sup>14</sup>, Konstantinos Eleftheriadis<sup>15</sup>, Martin Forsius<sup>16</sup>, Martin Heimann<sup>17</sup>, Sirkku  
9 Juhola<sup>20</sup>, Vladimir Konovalov<sup>18</sup>, Igor Konovalov<sup>19</sup>, Pavel Konstantinov<sup>5,33</sup>, Kajar Koster<sup>13</sup>, Elena Lapsina<sup>21</sup>,  
10 Anna Lintunen<sup>1,13</sup>, Alexander Mahura<sup>1</sup>, Risto Makkonen<sup>3</sup>, Svetlana Malkhazova<sup>5</sup>, Ivan Mammarella<sup>1</sup>, Stefano  
11 Mammola<sup>22,23</sup>, Stephany Mazon<sup>1</sup>, Outi Meinander<sup>3</sup>, Eugene Mikhailov<sup>24, 25</sup>, Victoria Miles<sup>6</sup>, Stanislav  
12 Myslenko<sup>5</sup>, Dmitry Orlov<sup>5</sup>, Jean-Daniel Paris<sup>26</sup>, Roberta Pirazzini<sup>3</sup>, Olga Popovicheva<sup>27</sup>, Jouni Pulliainen<sup>3</sup>,  
13 Kimmo Rautiainen<sup>3</sup>, Torsten Sachs<sup>28</sup>, Vladimir Shevchenko<sup>29</sup>, Andrey Skorokhod<sup>30</sup>, Andreas Stohl<sup>31</sup>, Elli  
14 Suhonen<sup>1</sup>, Erik S. Thomson<sup>32</sup>, Marina Tsidilina<sup>39</sup>, Veli-Pekka Tynkkynen<sup>34</sup>, Petteri Uotila<sup>1</sup>, Aki Virkkula<sup>3</sup>,  
15 Nadezhda Voropay<sup>35</sup>, Tobias Wolf<sup>6</sup>, Sayaka Yasunaka<sup>36</sup>, Jiahua Zhang<sup>37</sup>, Yubao Qiu<sup>37</sup>, Aijun Ding<sup>38</sup>,  
16 Huadong Guo<sup>37</sup>, Valery Bondur<sup>39</sup>, Nikolay Kasimov<sup>5</sup>, Sergej Zilitinkevich (✉)<sup>1,2,3</sup>, Veli-Matti Kerminen<sup>1</sup> and  
17 Markku Kulmala<sup>1,2,39,40,41</sup>

18

19 <sup>1</sup> Institute for Atmospheric and Earth System Research / Physics, Faculty of Science, University of  
20 Helsinki, Finland

21 <sup>2</sup> Tyumen State University, Department of Cryosphere, 625003 Tyumen, Russia

22 <sup>3</sup> Finnish Meteorological Institute, 00101 Helsinki, Finland

23 <sup>4</sup> World Meteorological Organization, WMO, Geneva, Switzerland

24 <sup>5</sup> Faculty of Geography, Lomonosov Moscow State University, Lenin Hills, 119991, Moscow, Russia

25 <sup>6</sup> Nansen Environmental and Remote Sensing Center/Bjerknes Centre for Climate Research, Bergen,  
26 Norway

27 <sup>7</sup> Nansen International Environmental and Remote Sensing Centre”, Nansen Centre, NIERSC, St.  
28 Petersburg, Russia

29 <sup>8</sup> Department of Environmental and Biological Sciences, PO Box 1627 (Address: Yliopistonranta 1 E), FI-  
30 70211 Kuopio, Finland

31 <sup>9</sup> Max Planck Institute for Chemistry, Mainz, Germany

32 <sup>10</sup> V.E. Zuev Institute of Atmospheric Optics (IAO) SB RAS, Tomsk, 634055, Russia

33 <sup>11</sup> LAGEO, Institute of Atmospheric Physics, Chinese Academy of Sciences (IAP-CAS), Beijing, 100029,  
34 PR, China

35 <sup>12</sup> Alfred Wegener Institute, Helmholtz Centre for Polar and Marine Research, Potsdam, Germany

36 <sup>13</sup> Institute for Atmospheric and Earth System Research /Forest Sciences, University of Helsinki, Helsinki,  
37 Finland



- 38 <sup>14</sup> Institute of Monitoring of Climatic and Ecological Systems SB RAS, Tomsk, 634055, Russia; Yugra State  
39 University, Khanty-Mansiysk, 628012, Russia
- 40 <sup>15</sup> ERL, Institute of Nuclear and Radiological Science & Technology, Energy & Safety, NCSR Demokritos,  
41 Attiki, Greece
- 42 <sup>16</sup> Finnish Environment Institute SYKE, Latokartanonkaari 11, 00790 Helsinki, Finland
- 43 <sup>17</sup> Max-Planck-Institute for Biogeochemistry, Jena, Germany
- 44 <sup>18</sup> Institute of Geography RAS, Moscow, Russia
- 45 <sup>19</sup> Institute of Applied Physics, Nizhny Novgorod, Russia
- 46 <sup>20</sup> Faculty of Biological and Environmental Sciences, University of Helsinki, Helsinki, Finland
- 47 <sup>21</sup> Yugra State University, Khanty-Mansiysk, 634012, Russia
- 48 <sup>22</sup> Finnish Museum of Natural History (LUOMUS), University of Helsinki, Helsinki, 00100, Finland
- 49 <sup>23</sup> Molecular Ecology Group (MEG), Water Research Institute (IRSA), National Research Council of Italy  
50 (CNR), Verbania Pallanza, 28922, Italy
- 51 <sup>24</sup> St. Petersburg State University, 7/9 Universitetskaya nab, St. Petersburg, 199034, Russia
- 52 <sup>25</sup> Multiphase Chemistry and Biogeochemistry Departments, Max Planck Institute for Chemistry, 55020  
53 Mainz, Germany
- 54 <sup>26</sup> Laboratoire des Sciences du Climat et de l'Environnement, IPSL CEA-CNRS-UVSQ, 91190 Gif-sur-  
55 Yvette, France
- 56 <sup>27</sup> Institute of Nuclear Physics, Lomonosov Moscow State University, Moscow, Russia
- 57 <sup>28</sup> GFZ German Research Centre for Geosciences, Telegrafenberg, Potsdam, Germany
- 58 <sup>29</sup> P.P. Shirshov Institute of Oceanology of the Russian Academy of Sciences, Moscow, Russia
- 59 <sup>30</sup> A.M. Obukhov Institute of Atmospheric Physics, Moscow, Russia
- 60 <sup>31</sup> Department of Meteorology and Geophysics, University of Vienna, Vienna, Austria
- 61 <sup>32</sup> Department of Chemistry & Molecular Biology, University of Gothenburg, Göteborg, 41296, Sweden
- 62 <sup>33</sup> Peoples' Friendship University of Russia (RUDN), Laboratory of sSart technologies for sustainable  
63 development of urban environment under global changes, Moscow, Russian Federation
- 64 <sup>34</sup> Aleksanteri Institute, University of Helsinki, Helsinki, Finland
- 65 <sup>35</sup> V B Sochava Institute of Geography SB RAS, Irkutsk, 664033, Russia; Institute of Monitoring of Climatic  
66 and Ecological Systems SB RAS, Tomsk, 634055, Russia
- 67 <sup>36</sup> Japan Agency for Marine-Earth Science and Technology (JAMSTEC), Yokosuka, Japan
- 68 <sup>37</sup> Aerospace Information Research Institute, Chinese Academy of Sciences, Beijing, 100094, China
- 69 <sup>38</sup> Joint International Laboratory of Atmospheric and Earth System sciences (JirLATEST), Nanjing  
70 University, Nanjing, China
- 71 <sup>39</sup> Institute for Scientific Research of Aerospace Monitoring "AEROCOSMOS", Moscow, 105064, Russia
- 72 <sup>40</sup> Aerosol and Haze Laboratory, Beijing Advanced Innovation Center for Soft Matter Sciences and  
73 Engineering, Beijing University of Chemical Technology (BUCT), Beijing, China
- 74 <sup>41</sup> Guangzhou Institute of Geography, Guangzhou Academy of Sciences, Guangzhou, China
- 75 <sup>42</sup> Department of Geology and Geophysics, King Saud University, Riyadh, Saudi Arabia



76 <sup>43</sup> Scripps Institution of Oceanography, UCSD, La Jolla, CA, USA

77

78 **Corresponding author(s):** Hanna Lappalainen, [hanna.k.lappalainen@helsinki.fi](mailto:hanna.k.lappalainen@helsinki.fi), Veli-Matti Kerminen, [veli-](mailto:veli-matti.kerminen@helsinki.fi)  
79 [matti.kerminen@helsinki.fi](mailto:veli-matti.kerminen@helsinki.fi)

80

### 81 **Keywords**

82 Grand Challenges, climate change, land-atmosphere interactions and feedbacks, biogeochemical cycles, Arctic  
83 Ocean, Northern Eurasia, China, Arctic marine ecosystem, atmospheric composition, air quality, Arctic  
84 greening, land use change, permafrost, Pan-Eurasian Experiment (PEEX), Global Earth Observatory, Digital  
85 Earth, Silk Road Economic Belt, Arctic societies, energy policy, boreal region, science diplomacy

86

### 87 **Abstract**

88 The Pan-Eurasian Experiment (PEEX) Science Plan, released in 2015, addressed a need for a holistic system  
89 understanding and outlined the most urgent research needs for sustainable development in the Arctic-boreal  
90 region. Air quality in China and long-range transport of the atmospheric pollutants was also indicated as one  
91 of the most crucial topics of the research agenda. This paper summarizes results obtained during the last five  
92 years in the Northern Eurasian region. It also introduces recent observations on the air quality in the urban  
93 environments in China. The main regions of interest are the Russian Arctic, Northern Eurasian boreal forests  
94 (Siberia) and peatlands and on the mega cities in China. We frame our analysis against research themes  
95 introduced in 2015. We summarize recent progress in the understanding of the land – atmosphere – ocean  
96 systems feedbacks. Although the scientific knowledge in these regions has increased, there are still gaps in our  
97 understanding of large-scale climate-Earth surface interactions and feedbacks. This arises from limitations in  
98 research infrastructures and integrative data analyses, hindering a comprehensive system analysis. The fast-  
99 changing environment and ecosystem changes driven by climate change, socio-economic activities like the  
100 China Silk Road Initiative, and the global trends like urbanization further complicate such analyses. We  
101 recognize new topics with an increasing importance in the near future, such as enhancing biological  
102 sequestration capacity of greenhouse gases into forests and soils to mitigate the climate change and the socio-  
103 economic development to tackle air quality issues.

104



105

106 1. INTRODUCTION

107 Earth system is facing major challenges, including climate change, biodiversity loss, ocean acidification,  
108 epidemics and energy demand on a global scale (Ripple et al., 2017). These “Grand Challenges” are highly  
109 connected and interlinked. This creates a need for an approach for a multidisciplinary scientific program, which  
110 could deliver science based message to fast-tracked policy making (Kulmala et al., 2015). The recent estimates  
111 based on the observed atmospheric concentrations of CO<sub>2</sub>  
112 ([ftp://aftp.cmdl.noaa.gov/products/trends/co2/co2\\_mm\\_mlo.txt](ftp://aftp.cmdl.noaa.gov/products/trends/co2/co2_mm_mlo.txt)) and business-as-usual scenario show that  
113 humankind should find solutions to answer the Grand Challenges. Deep understanding on the feedbacks and  
114 interactions between the land – atmosphere – ocean domains and accounting for social aspects in the regions  
115 of substantial changes are needed for effective technical solutions, mitigation and adaption policy actions. The  
116 northern regions (> 45°N), together with the arctic coastal zone and Siberian region in Russia, are among the  
117 most critical areas for the global climate (Smith 2011; Kulmala et al., 2015; Kasimov et al., 2015).

118

119 The idea of the Pan-Eurasian Experiment (PEEX) ([www.atm.helsinki.fi/peex](http://www.atm.helsinki.fi/peex)), originated from a group of  
120 Finnish and Russian scientists and research organizations in 2012, is a bottom-up research and capacity  
121 building program concentrating on the sustainable development of the Arctic - boreal regions of the Northern  
122 Eurasia under changing climate and socio-economic megatrends (Kulmala et al., 2015, Lappalainen et al.,  
123 2016). The program was laid on four interconnected parts, namely research agenda, research infrastructures,  
124 capacity building and societal impacts (Lappalainen et al., 2014; Kulmala et al., 2016a, Lappalainen et al.,  
125 2017, Kulmala 2018). In addition to a strong involvement of the Russian partners, in 2013 the PEEX China  
126 collaboration was established. China has a strong economic interest on the Arctic regions (Tillman et al. 2018).  
127 Furthermore, China is already facing extensive environmental and air pollution challenges and has a major  
128 interest to find technical solutions for environmental monitoring of the Silk Road Economic Belt Program  
129 (SREB) (Kulmala 2018, Lappalainen et al., 2018). In Russia the program is an umbrella for several bilateral  
130 scientific projects and activities (e.g. Chalov et al., 2015, 2018; Esau et al., 2016; Alekseychik et al., 2017;  
131 Bobylev et al., 2018; Malkhazova et al., 2018; Kukkonen et al., 2020; Ezhova et al., 2018b; Ziltinkevich et  
132 al., 2019; Petäjä et al., 2020 submitted; ; Bondur et al., 2019 a,b,c,d,e,f; Yuanhuizi He et al, 2020), while in  
133 China the primary focus is on the development of atmospheric in-situ stations and advanced air quality  
134 monitoring in megacity environments (e.g. Ding et al., 2016 b; Yao et al., 2018; Ying et al., 2020; Wang et al.,  
135 2020). Furthermore, PEEX is closely collaborating with the Digital Belt and Road (DBAR) Program  
136 coordinated by the Institute for Digital Earth and Remote Sensing (RADI). PEEX collaboration with DBAR  
137 is driven by a need for a novel in situ station network and ground based data as a complementary information  
138 for the remote sensing in the Silk Road economic region. Long-term development on a “Station Measuring  
139 the Earth Surface and Atmosphere Relations” (SMEAR) concept could provide baselines for this (Hari et al.  
140 2016; Kulmala 2015, Kulmala 2018; Lappalainen et al., 2018).

141



142 The PEEEX program is motivated by the need for obtaining scientific information that combines research in the  
143 Arctic and boreal environments, and for understanding large-scale feedbacks and interactions operating in  
144 land-atmosphere-ocean systems (Kulmala et al., 2004; Kulmala et al., 2016a; Vihma et al., 2019) and large-  
145 scale weather impacts related to the Arctic amplification (e.g. Coumou et al., 2014; Vihma et al., 2020). One  
146 of the scientific backbones of PEEEX is the previously coordinated research frameworks and their synthesis.  
147 For example, the latest comprehensive overview on the interactions between the atmosphere, cryosphere and  
148 ecosystems at northern high latitudes was performed by the Nordic Center of Excellence in “Cryosphere-  
149 atmosphere interactions in a changing Arctic climate“, CRAICC) community (Boy et al., 2019). The PEEEX  
150 program can upscale the CRAICC results into a wider geographical context.

151

152 Climate change, as a main driver for environmental changes in the Northern Eurasian Arctic-boreal region and  
153 China, sets environmental boundaries for the future socio-economic activities of these regions in general. The  
154 harsh climate of this region puts a pressure on the ecosystems and living conditions of the local people (e.g.  
155 IPCC, 2019). PEEEX introduced fifteen large-scale research questions, which would also help us to fill the key  
156 gaps in our holistic understanding of land-atmosphere interactions and their connections to societies living in  
157 the northern Eurasian region (Kulmala et al., 2015; Lappalainen et al., 2018). This approach also sets the  
158 framework of the current paper. Here we introduce the recent research progress in the large-scale scientific  
159 themes relevant to the PEEEX region.

160

161 Here we introduce the scientific results from PEEEX scientific output, review the main results from PEEEX  
162 scientific papers and present an analysis of the key gaps in the current scientific understanding. We use the  
163 PEEEX research agenda structure (Kulmala et al. 2016, Lappalainen et al. 2018) as a reference and mirror new  
164 a rising themes and results against this plan. The results are first discussed with a holistic approach and then  
165 we categorize the advances through a set of identified feedbacks and interactions within the Arctic boreal  
166 environment. We follow up with a discussion on the need for a future research infrastructure to be able to  
167 provide relevant data and underline the future socio-economics development of the region setting the  
168 boundaries for proposed new science-based concepts and technical solutions.

## 169 2. RESULTS

170 In the PEEEX Science Plan we indicated four main thematic research domains: the land system, the atmospheric  
171 system, the water system and the society with 15 thematic research areas and related large-scale research  
172 questions (Q) presented in Table 1 (Lappalainen et al., 2015). This is the framework we re-visited and utilized  
173 in the synthesis of new results of the PEEEX community brought together in this paper. Furthermore, we  
174 synthesized the results and discuss their contribution to the large - scale feedbacks and interactions in the Arctic  
175 context in the sections below.

176

### 177 2.1. LAND ECOSYSTEMS

178



179 2.1.1 Changing land ecosystem processes (Q1)

180

181 *High-latitude photosynthetic productivity*

182

183 High-latitude terrestrial ecosystems are crucial to the global climate system and its regulation by vegetation.  
184 These ecosystems are typically temperature limited, and thus also considered especially sensitive to climate  
185 warming. Better understanding of interannual and seasonal dynamics and resilience of the photosynthetic  
186 activity of forest vegetation as a whole is needed for the quantification of GPP and analyzing the carbon balance  
187 of boreal forest. The carbon sink and source dynamics of the boreal forests have been intensively studied  
188 during the last five years at Stations Measuring Atmosphere Ecosystem Relations (SMEAR) II station in  
189 Finland (Hari & Kulmala 2005, Hari et al. 2009). Recent results show that the Norway spruce and Scots pine  
190 ecosystems are rather resilient to a short-term weather variability (Matkala et al., 2020). Overall, the analyses  
191 by Kulmala et al. (2019) and Matkala et al. (2020) on subarctic Scots pine and Norway spruce stands at the  
192 northern timberline in Finland serve as examples of the canopy scale dynamics, showing that these ecosystems  
193 are generally weak carbon sinks but have a clear annual variation. Kulmala et al. (2019) observed that there is  
194 a difference between tree canopy photosynthesis compared to forest floor photosynthesis which starts to  
195 increase after the snowmelt. Thus the models for photosynthesis should also address the snow cover period in  
196 order to better capture the seasonal dynamics of photosynthesis of the Northern forests says Kulmala et al.  
197 (2019).

198

199 The abundance of tree species, stand biomass, increasing tree growth and coverage of broadleaf species may  
200 also affect biogenic volatile organic compound (BVOC) emissions from the forest floor and impact the total  
201 BVOC emissions from northern soils. At least the stand type has been shown to affect BVOCs fluxes from the  
202 forest floor in a hemi boreal - boreal region (Mäki et al., 2019). As a whole, BVOCs emitted by boreal  
203 evergreen trees are connected to the photosynthetic activity with a strong seasonality and have a crucial role  
204 to atmospheric aerosol formation processes over the boreal forest zone. BVOC emissions have low rates  
205 during photosynthetically inactive winter and increasing rates towards summer (Aalto et al., 2015). High  
206 emission peaks caused by enhanced monoterpene synthesis were found in spring periods simultaneously with  
207 the photosynthetic spring recovery (Aalto et al., 2015). This suggests that monoterpene emissions may have a  
208 protective functional role for the foliage during the spring recovery state, and that these emission peaks may  
209 contribute to atmospheric chemistry in the boreal forest in springtime. Vanhatalo et al. (2018) studied the  
210 interplay between needle monoterpene synthase activities, its endogenous storage pools and needle emissions  
211 in two consecutive years at a boreal forest in Finland. They found no direct correlation between monoterpene  
212 emissions and enzyme activity or the storage pool size. Monoterpene synthase activity of needles was different  
213 depending on seasonality and needle ontogenesis. However, the pool of stored monoterpenes did not change  
214 with the needle age (Vanhatalo et al., 2018). Also, clear annual patterns of primary biological aerosol particles  
215 have been measured from a boreal forest, with late spring and autumn being seasons of dominant occurrence.



216 Increased levels of free amino acids and bacteria were observed during the pollen season in the SMEAR II  
217 station in Finland, whereas the highest levels for fungi were observed in autumn (Helin et al., 2017).

218

219 Extensive measurements of Scots pine photosynthesis and modelling resulted in optimized predictions of the  
220 daily behavior and annual patterns of photosynthesis in a subarctic forest (Hari et al., 2017). The study  
221 connected theoretically the fundamental concepts affecting photosynthesis with the main environmental  
222 drivers (air temperature and light), and the theory gained strong support through empirical testing.  
223 Understanding stomatal regulation is fundamental in predicting the impact of changing environmental  
224 conditions on photosynthetic productivity. Lintunen et al. (2020) showed that canopy conductance and soil-  
225 to-leaf hydraulic conductance are strongly coupled, and that soil temperature and soil water content influences  
226 canopy conductance through changes in belowground hydraulic conductance. In particular, the finding that  
227 soil temperature strongly influenced belowground hydraulic conductance in mature, boreal trees may help to  
228 better understand tree behavior and photosynthetic productivity in cold environments. Plant photosynthetic  
229 rate is concurrently limited by stomatal and non-stomatal limitations, and recent modelling (Hölttä et al., 2017)  
230 and empirical (Salmon et al., 2020) studies suggest that stomatal and non-stomatal controls are coordinated to  
231 maximize leaf photosynthesis, i.e. non-stomatal limitations to photosynthesis increase with decreasing leaf  
232 water potential and/or increasing leaf sugar concentration. This new approach allows to include the effect of  
233 non-stomatal limitations in models of tree gas-exchange (Fig. 1).

234

235 Due to climate warming, it seems that trees in high-latitudes have been progressively decreasing their regional  
236 growth coherence in the last decades (Shestakova et al., 2019). Shestakova et al. (2019) showed results that  
237 unequivocally link a substantial decrease in temporal coherence of forest productivity in boreal ecosystems to  
238 less temperature-limited growth that is concurrent with regional warming trends. This emerging pattern points,  
239 for example, to an increasing dependence of the carbon balance on local drivers and the role of forests as  
240 carbon sinks in the northern Ural region.

241

242 Vegetation gross primary production (GPP) is the largest CO<sub>2</sub> flux of the carbon cycle in terrestrial ecosystems  
243 and impacts all of the carbon cycle variables (Beer et al., 2010). Ecosystem models usually overestimate GPP  
244 under drought and during spring, late fall and winter (Ma et al., 2015). Several new methodological  
245 improvements for a better quantification and scaling of GPP have been reported (Zhang et al., 2018; Pulliainen  
246 et al., 2017; Kooijmans et al., 2019). The GPP, measuring photosynthesis, is crucially important for the global  
247 carbon cycle and its accurate estimation is essential for ecosystem monitoring and simulation. Pulliainen et al.  
248 (2017) introduced a new proxy indicator for spring recovery from in situ flux data on CO<sub>2</sub> exchange. This  
249 made it possible to quantify the relation between spring recovery and carbon uptake and to assess changes in  
250 springtime carbon exchange, demonstrating a major increase in the CO<sub>2</sub> sink. Zhang et al. (2018) introduced  
251 a new water-stress factor that effectively mitigates the overestimation of GPP under drought conditions, while  
252 Bai et al. (2018 a,b) developed a method for quantifying the evapotranspiration of crops by using a remote  
253 sensing-based two-leaf canopy conductance model. These methods can provide novel insights into the



254 quantification of GPP under different conditions and, in general, into the impacts of biosphere-atmosphere  
255 relations on a larger scale.

256

257 Methods for satellite-based remote sensing of photosynthesis have been developed recently based on solar-  
258 induced chlorophyll fluorescence signal, such as the OCO-2 product that has an improved spatial resolution,  
259 data acquisition and retrieval precision compared to earlier satellite missions with solar-induced chlorophyll  
260 fluorescence (SIF) capability, and allows for validation of the data directly against ground and airborne  
261 measurements (Sun et al., 2017). Interpretation of the solar-induced chlorophyll fluorescence signal has also  
262 been improved by many *in situ* studies. For example, Liu et al. (2019 a,b ) simulated SIF in realistic 3D birch  
263 stand reconstructed from terrestrial laser scanning data and found a large contribution of the understory layer  
264 to the remote sensing signal.

265

266 *Vegetation changes*

267

268 The normalized difference vegetation index (NDVI) is used for detecting large-scale changes in vegetation  
269 productivity. In the past decades, these changes basically are the increasing NDVI, called “greening”, taking  
270 place in the tundra regions and the decreasing NDVI, called “browning”, in the Northern forest regions (Miles  
271 and Esau, 2016). A deeper analysis behind these changes are needed. For example, in Northern West Siberia  
272 only 18% of the total area had statistically significant changes in productivity either towards greening or  
273 browning, and having these opposite trends for different species within the same bioclimatic zone. The  
274 observed complexity of the patterns of variability and trends in vegetation productivity underlines the new  
275 more detailed studies, how different forest types and species are responding to climate and environmental  
276 change in the Northern environments (Miles and Esau, 2016). Also understanding the variations in small-scale  
277 plant communities, seasonality and biogeochemical properties are needed for modeling the functioning of the  
278 arctic tundra in global carbon cycling. Also the rapid development of the LAI during the short growing season  
279 and the yearly climatic variation address the importance of optimal timing of the satellite data images when it  
280 is compared with the field verification data in the Arctic region (Juutinen et al., 2017).

281

282 Vegetation indices and complex spectral transformations derived from processed long-term satellite data  
283 (1973-2013) for areas around the cities of Arkhangelsk and Zapolyarny (Murmansk oblast) show the changes  
284 in the state of the environment and reveal areas of peak anthropogenic impacts causing significant morphologic  
285 changes in all kinds of geosystems and strongly affecting the Arctic natural ecosystems. These areas are  
286 subjected to peak anthropogenic impact and are associated with specific industrial facilities (Bondur and  
287 Vorobyev, 2015). Region-wide changes in the vegetation cover and the changes in and around several  
288 urbanized areas in Siberia reveal a robust indication of the accelerated greening near the older urban areas.  
289 Many Siberian cities have turned greener while their surroundings have been dominated by wider browning.  
290 The observed urban greening could be associated not only with special tending of the within-city green areas  
291 but also with the urban heat islands and succession of more productive shrub and tree species growing on



292 warmer sandy soils (Koronatova and Milyaeva 2011, Sizov and Lobotrosova 2016). Tundra and forest-tundra  
293 biomes are sensitive to mean summer temperatures which increase production and greening. Taiga biomes are  
294 sensitive to precipitation and soil moisture and increase production in wet summer (Miles et al., 2019).

295

#### 296 *New methodologies determining Earth surface characteristics*

297 Earth surface characteristics are fundamental knowledge for the understanding and quantification land-  
298 atmosphere processes. The methods for determining Earth surface characteristics from satellites are improving.  
299 As an example, a method for recognition of the Earth surface types according to space images using an object-  
300 oriented classification has been developed. The classification relies on Markov stochastic segmentation for  
301 object extraction and supervised classification of the objects (Gurchenkov et al., 2017). Furthermore, a  
302 prototype algorithm for hemispheric scale detection of autumn soil freezing using space-borne L-band passive  
303 microwave observations was developed (Rautiainen et al., 2016) and is currently an operative soil freeze and  
304 thaw product that delivers freely available data (<ftp://litdb.fmi.fi/outgoing/SMOS-FTService/>). The CryoGrid 3  
305 land surface model provides improved descriptions of the possible pathways of ice-wedge polygon evolution  
306 and describes better the complex processes affecting the ice-rich permafrost landscapes (Nitzbon et al., 2019).  
307 In addition, there are new observations for validating satellite observations and permafrost models. Boike et  
308 al., (2016) introduced a new, 16-year permafrost and meteorology data set from the Samoylov Island Arctic  
309 research site, north-eastern Siberia. Terentieva et al. (2016) introduced maps used as a baseline for validation  
310 of coarse-resolution land cover products and wetland data sets in high latitudes. Other examples of available  
311 data for the model validation are “BC emissions from agricultural burns and grass fires in Siberia” by  
312 Konovalov et al. (2018) and permafrost records at the Lena River delta” by Boike et al. (2016).

313

314 Tundra ecosystems are under pressure and intensifying permafrost thawing, plant growth and ecosystem  
315 carbon exchange under the changing climate. The heterogeneity of Arctic landscapes is an extra challenge for  
316 environmental monitoring. For example, remote sensing methods are not able to capture variations in moss  
317 biomass, which is dominating the plant biomass and controlling soil properties in the Arctic. The general  
318 accuracy of landscape level predictions in the land cover type (LCT) is good, but the spatial extrapolation of  
319 the vegetation and soil properties relevant for the regional ecosystem and global climate models still needs to  
320 improved (Mikola et al., 2018). Furthermore, for the future, we need to have a land characterization, in order  
321 to perform quantification and assessment of the ecosystem services at different scales using integrative  
322 techniques and integrated field observations together with remote sensing and modelling at the landscape scale  
323 (Burkhard et al., 2009, Fu and Forsius, 2015). In a smaller scale, the isotopic composition of carbon and oxygen  
324 in peat can be used for the climate reconstruction (Granath et al., 2018).

325

#### 326 2.1.2 Thawing permafrost (Q2)

327

#### 328 *Observations of ground temperature evolution*

329



330 Permafrost regions of the Northern Eurasia are warming along with the climate (IPCC, 2019). During the  
331 Global Terrestrial Network for Permafrost reference decade, 2007 - 2016, the temperature at the depth of zero  
332 annual amplitude increased by  $0.39\text{ °C} \pm 0.15\text{ °C}$  in the continuous permafrost zone and by  $0.20 \pm 0.10\text{ °C}$  in  
333 the discontinuous permafrost zone. At the same time, the mountain permafrost warmed by  $0.19 \pm 0.05\text{ °C}$ . The  
334 global average of the permafrost temperature increased by  $0.29 \pm 0.12\text{ °C}$  (Biskaborn et al., 2019). The observed  
335 trend in the continuous permafrost zone follows the air temperature trend in the Northern Hemisphere.

336

337 The changes in the permafrost region affects climate, hydrology and ecology from local to global scales  
338 (Arneeth et al., 2010; Hinzman et al., 2005). Several local studies focused on the difference introduced by  
339 vegetation, soil and hydrological characteristics at the same site (Göckede et al., 2017, 2019). Göckede et al.  
340 (2017, 2019) presented findings on shifts in energy fluxes from paired ecosystem observations in northeast  
341 Siberia comprising a drained and a corresponding control site. Drainage disturbance had triggered a suite of  
342 secondary shifts in ecosystem properties, including alterations in vegetation community structure, which in  
343 turn influenced changes in snow cover dynamics and surface energy budget. First, the drainage reduced heat  
344 transfer into deeper soil layers, which may lead to shallower thaw depths. Second, the vegetation change due  
345 to the drainage led to an increase in albedo, which decreased the total energy income, or net radiation, into the  
346 system. Third, the drainage reduced water content available for evapotranspiration, which resulted in reduced  
347 latent heat flux and increased sensible heat flux transferring more energy back to the atmosphere. The reported  
348 affects led to surface and permafrost cooling (Göckede et al., 2019).

349

350 Kukkonen et al. (2020) compared temperature data from several shallow boreholes in the Nadym region,  
351 Siberia, and predicted permafrost evolution for different climate scenarios. The Nadym area represents a  
352 typical site located in the discontinuous permafrost zone. Kukkonen et al. (2020) found that the permafrost  
353 thawed most rapidly in low-porosity soils, whereas high-porosity soils in the top layer (e.g., peatland) will  
354 retard thawing considerably. Similarly, the depth of a seasonally frozen layer and the temperature regime of  
355 peat soils in the oligotrophic bog in the southern taiga zone of Western Siberia showed significant differences  
356 at sites with high and low levels of bog waters (Kiselev et al., 2019). Both Kukkonen et al. (2020) and Kiselev  
357 et al. (2019) results are in line with previous conclusions on the importance of volumetric water content and  
358 unfrozen water content for soil thermal properties governing heat transfer and phase change processes  
359 (Romanovsky and Osterkamp, 2000). Locally, the sites with thin snow cover (e.g., hill tops) demonstrated  
360 higher resistance to the thawing (Williams and Smith, 1989; Kukkonen et al., 2020). To follow-up on the  
361 development of permafrost thaw in different soil types require continuous and comprehensive observations  
362 during the coming decades.

363

364 *Changing GHG fluxes and VOCs due to permafrost thaw*

365

366 Biogenic GHG emissions are strongly connected with permafrost conditions and changes in other related  
367 environmental conditions, such as soil temperature and moisture conditions. Here we discuss recent results on



368 the observed emissions from these permafrost perspectives and, later in the section 2.2.1, address the  
369 connections between GHG fluxes and the other environmental factors, like deforestation and forest fires.

370

371 During the permafrost thaw, even small changes in the soil carbon cycle can turn over a terrestrial ecosystem  
372 from a sink to a source (Schuur et al., 2008). Natali et al. (2019) based their analysis on the winter time carbon  
373 loss on the regional in situ observations of CO<sub>2</sub> fluxes and estimated it as 1,662 TgC per year, which is more  
374 than predicted by the process models estimates. Furthermore, Natalie et al. (2019) says that even if the soil  
375 CO<sub>2</sub> loss would be enhanced due to winter warming, the growing season may start earlier and also onset the  
376 carbon uptake under warmed climate conditions. For a better understanding of these connections and the spatial  
377 and temporal dynamics in the Arctic carbon cycle we need more observations from permafrost ecosystems.  
378 Additional flux measurements are urgently needed to understand the variation between the current  
379 measurements and, especially extended measurements on the CH<sub>4</sub> emissions to better quantify their role in the  
380 carbon balance. For example, a new data assimilation system gives Arctic carbon sink equal to -67 g C m<sup>-2</sup>  
381 yr<sup>-1</sup>, but this average value is associated with very high uncertainties. Furthermore, these estimates do not  
382 include methane, which is even more difficult to evaluate (López-Blanco et al., 2019). Based on the field flux  
383 measurements, the Carbon Cycle Report 2018 (Schuur et al., 2018) estimates Eurasian boreal wetland being a  
384 source of 14 Tg CH<sub>4</sub> per year. On the other hand Kirschke et al. (2013) estimations, based on atmospheric  
385 measurements, ends up to the value of 9 Tg CH<sub>4</sub> per year. Locally, methane fluxes measured in 2005-2013  
386 showed significant year-to-year variations. Interestingly, the observed variation in North America, specifically  
387 in the Hudson Bay lowlands, appear to have been driven partly by the soil temperature, while in the Western  
388 Siberian lowlands the variability was dependent on the soil moisture (Thompson et al., 2017). The comparison  
389 of high-resolution modelling of atmospheric CH<sub>4</sub> to CH<sub>4</sub> observations already in 2012 from the East Siberian  
390 Arctic Shelf (ESAS), a potentially large CH<sub>4</sub> source, also confirms that methane releases are highly variable  
391 and inhomogeneous (Berchet et al., 2016).

392

393 Long-term flux measurements provide us insight into the carbon sink - source dynamics. The flux  
394 measurements from the moist tussock tundra in the north-eastern Siberia indicated that drainage effects on the  
395 carbon cycle and how the tundra changed to a weaker CO<sub>2</sub> sink and CH<sub>4</sub> source. Another relevant observation  
396 was that the time outside the growing season influences the carbon balance of ecosystem processes, especially  
397 during the zero-curtain period (Kittler et al. 2017). This is in line with similar studies in Alaska (Commane et  
398 al., 2017; Euskirchen et al., 2017). Therefore, the autumn temperature was identified as a major driving factor  
399 describing the differences between the annual GHG fluxes. Notably, however, the seasonal amplitudes of CO<sub>2</sub>  
400 concentrations in Siberia were found to be significantly higher than those in the North American continent,  
401 likely due to the more intense biological activity here (Timokhina et al., 2015a). A recent study showed that  
402 the Siberian carbon cycle is a major contributor to the Northern Hemisphere amplitude of CO<sub>2</sub> variation (Lin  
403 et al., 2020).

404



405 The observations from the non-permafrost sites may give us a clue on the future dynamics of fluxes as the  
406 permafrost is thawing. The chamber measurements of CH<sub>4</sub> and CO<sub>2</sub> fluxes from a non-permafrost site in the  
407 Siberian peatland in August, 2015, showed that the highest values of methane fluxes were obtained in burnt  
408 wet birch forest and the lowest values in seasonally waterlogged forests (Glagolev et al., 2018). The fluxes can  
409 vary even between different sites of a bog as measured by Dyukarev et al. (2019). Net ecosystem exchange  
410 (NEE), ecosystem respiration (ER) and gross primary production (GPP), based on the measured CO<sub>2</sub> fluxes at  
411 a ridge-hollow complex bog and a model for ridge and hollow sites at oligotrophic bog in Middle Taiga Zone  
412 of West Siberia, showed that a two-year-average NEE at the hollow site was 1.7 times higher than at the ridge  
413 site (Dyukarev et al., 2019). The ecosystem processes are influenced by drying in tundra ecosystems. Kwon et  
414 al. (2019) reported from Alaska that drying in the tundra ecosystems increased contributions of modern soil  
415 carbon to the ecosystem respiration but, at the same time, decreased contributions of old soil carbon. These  
416 changes were attributed mainly to modified soil temperatures at different soil layers due to the altered thermal  
417 properties of organic soils following drainage. Furthermore, the drainage lowered CH<sub>4</sub> fluxes by a factor of 20  
418 during the growing season, with post drainage changes in microbial communities, soil temperatures, and plant  
419 communities also affecting the flux reduction in an Arctic wetland ecosystem (Kwon et al., 2017).

420

421 Voigt et al. (2016) reported that, under warming conditions, the vegetated tundra in north-eastern European  
422 Russia shifted from a GHG sink to a source. The positive warming response was dominated by CO<sub>2</sub>; however,  
423 N<sub>2</sub>O emissions were also significant. N<sub>2</sub>O was emitted not only from bare peat, already identified as a strong  
424 source, but also from the vast vegetated peat areas not emitting N<sub>2</sub>O under current climate conditions. These  
425 results are explained by dynamics between the temperature, nitrogen assimilation by plants and soil microbial  
426 activity, having a strong impact on future GHG balance in Arctic (Voigt et al., 2016; Gil et al., 2017). Studying  
427 N<sub>2</sub>O emissions in the typical permafrost peatland in Finnish Lapland, it was concluded that ca 25% of the  
428 Arctic territory are the areas potentially emitting nitrous oxide (Voigt et al., 2017). It seems that there is positive  
429 feedback mechanism between the permafrost thawing and the moisture regime. Predicting soil response to  
430 climate change or land use is central to understanding and managing N<sub>2</sub>O. According to recent results N<sub>2</sub>O  
431 flux can be predicted by models incorporating soil nitrate concentration (NO<sub>3</sub><sup>-</sup>), water content and temperature  
432 (Pärm et al., 2018).

433

434 In addition to CO<sub>2</sub> and CH<sub>4</sub>, thawing or collapsing of arctic permafrost can release volatile organic compounds  
435 (VOCs). Li et al. (2020a) examined the release of VOCs from thawing permafrost peatland soils sampled from  
436 Finnish Lapland in laboratory. The average VOC fluxes were four times as high as those from the active layer,  
437 and mainly attributed to direct release of old, trapped gases from the permafrost. These results demonstrate a  
438 potential for substantive VOC releases from thawing permafrost and suggests that future global warming could  
439 stimulate VOC emissions from the Arctic permafrost.

440

441 2.1.3 Ecosystem structural change (Q3)

442



443 *Changes in microbial activity*

444

445 Climate change is likely to cause increased tree appearance on open peatlands, but we do not know how this  
446 vegetation change influences the below-ground microbiology and composition. Changes along bog ecotones  
447 at three Russian peatland complexes suggested that tree encroachment may reduce the trophic level of *Testate*  
448 *Amoeba* communities and reduce the contribution of mixotrophic *Testate Amoebae* to primary production.  
449 Thus, it seems that increased tree recruitment on open peatlands will have important consequences for both  
450 microbial biodiversity and microbial-mediated ecosystem processes (Payne et al., 2016). We also need to  
451 understand better the dynamics affecting the bacteria, fungi and other related species in the ground air layer.  
452 Recent studies by Korneykova and Evdokimova (2018) and Korneikova et al. (2018 a,b) showed the influences  
453 of anthropogenic sources (Copper-Nickel Plant) and acidic soils in Russian northern taiga and tundra on the  
454 portion of the airborne fungi and on the structure of algological and mycological complexes (Korneikova et  
455 al., 2018 a,b). New methods were reported on how to improve soils conditions, which were developed on all  
456 kinds of materials made or exposed by human activity that otherwise would not occur at the Earth's surface,  
457 referred as "Technosol engineering" (Slukovskaya et al., 2019) and how to monitor climate change impacts on  
458 the functional state of bogs by using *Sphagnum* mosses (Preis et al., 2018).

459

460 *Effects of forest fires on soils*

461

462 Forest fires, a significant environmental factor in the Northern Eurasian region, change soil chemical and  
463 physical properties and may influence greenhouse gas (GHG) fluxes and emissions of BVOCs. Recent results  
464 indicate that a slower post-fire litter decomposition has a clear impact on the recovery of soil organic matter  
465 following forest fires in northern boreal coniferous forests due to accumulated soil organic matter. The soil  
466 recover relates to slow litter composition and reduced enzymatic and microbial activity (Köster et al., 2016).

467

468 Post-fire studies of the long-term evolution of bacterial community structure and function, are sparse. Sun et  
469 al. (2016) showed that the major drivers influencing bacterial community are soil temperature, pH and  
470 moisture. Furthermore, Köster et al. (2015) analyzed the long-term effects of fire on soil CO<sub>2</sub>, CH<sub>4</sub> and N<sub>2</sub>O  
471 fluxes in pine forest stands in the Finnish Lapland and discussed the role of microbial bio mass in this context.  
472 Köstner et al. (2015) did not detect significant effect on the CO<sub>2</sub> emissions nor on the N<sub>2</sub>O fluxes, but there  
473 were long-lasting strengthening of the CH<sub>4</sub> sink the soil acted as a CH<sub>4</sub> sink, and this change in CH<sub>4</sub> uptake  
474 resulted from the fire was long-lasting. Interestingly, Köster et al. (2018) did not find a similar kind of long-  
475 term effect on the CH<sub>4</sub> sink dynamics in the studies carried out in Siberia.

476

477 Forest wildfires also regulate the BVOC emissions from boreal forest floors by changes in the ground  
478 vegetation. Total BVOC emissions from forest floor decreased after forest fire and then again increased along  
479 with the succession of forests (Zhang-Turpeinen et al., 2020). For a comparison, Bai et al. (2017) showed that



480 biomass burning resulted in increased BVOC emission fluxes and ozone concentration above canopy in a  
481 subtropical forest in China

482

## 483 2.2. ATMOSPHERIC SYSTEM

484

485 Concerning critical atmospheric processes and large-scale climate implications, we concentrate here on  
486 greenhouse gases and aerosol particles over Northern Eurasia and Arctic, urban air quality, and issues related  
487 to the weather and atmospheric circulation. We summarize the recent measurements on the atmospheric  
488 composition relevant to sink and source dynamics in Siberia, on the sources and properties of atmospheric  
489 aerosols in Arctic – boreal environments, including black carbon and dust in the atmosphere and snow, and on  
490 the methodological and model developments related to atmospheric chemistry and physics (Q4, section 2.2.1).  
491 Furthermore, we introduce new results and observations on atmospheric pollution in rural, suburban and mega  
492 city environments in China and Russia (Q5, section 2.2.2). We briefly show some recent results related to  
493 synoptic scale weather in the Arctic boreal regions, such as cold and warm episodes, cyclone density dynamics,  
494 circulation effect on temperature and moisture, cloudiness in Arctic, on clouds and planetary boundary layer  
495 (Q6, section 2.2.3).

496

### 497 2.2.1 Atmospheric composition and chemistry (Q4)

498

#### 499 *Boreal forests carbon balance*

500

501 As already discussed in section 3.1.1, the boreal forests as a carbon sink and the related role of forestation have  
502 been under international debate. It seems that early snowmelt increases springtime carbon uptake of the boreal  
503 forests of Eurasia and North America and shows a major advance in the CO<sub>2</sub> sink (Pulliainen et al., 2017). A  
504 scenario of a complete global deforestation by Scott et al. (2018), combining radiative forcing to CO<sub>2</sub>, surface  
505 albedo and short-lived climate forcers (SLCFs), suggests that global deforestation could cause 0.8 K warming  
506 after 100 years, with SLCFs contributing 8% of the effect. However, deforestation as projected by the RCP8.5  
507 scenario leads to zero net radiative forcing from SLCF, primarily due to nonlinearities in the aerosol indirect  
508 effect. Tuovinen et al. (2019) showed that methane fluxes vary strongly with wind direction in a tundra  
509 ecosystem with heterogeneous vegetation. By combining very high-spatial-resolution satellite imagery and  
510 footprint modelling, they were able to estimate the relation between the main land cover types and the  
511 ecosystem level measurements. CH<sub>4</sub> emissions mainly originated from wet fen and graminoid tundra patches,  
512 whereas the areas of bare soil and lichen acted as strong CH<sub>4</sub> sinks (Tuovinen et al. 2019. Refer to Tsuruta et  
513 al. (2017) posterior mean global total emissions during 2000-2012 were 516±51 Tg CH<sub>4</sub> yr<sup>-1</sup>, which indicates  
514 that the emissions increased by 18 Tg CH<sub>4</sub> yr<sup>-1</sup> from the period 2001-2006 to the period 2007-2012. This  
515 increase be explain by increased emissions from the South America temperate region, the Asia temperate  
516 region and Asia tropics.

517



518 Analysis of the trends and the diurnal, weekly and seasonal cycles of CO<sub>2</sub> and CH<sub>4</sub> mixing ratios derived from  
519 the long-term data of the “Japan–Russia Siberian Tall Tower Inland Observation Network” showed that the  
520 frequency of identified events of elevated concentration differs for CO<sub>2</sub> and CH<sub>4</sub> and may reach up to 20% of  
521 days in some months (Belikov et al., 2019). These observations made it possible to reduce uncertainties in the  
522 biosphere surface CO<sub>2</sub> uptake (Kim et al., 2017). Although the CO<sub>2</sub> uptake in boreal Eurasia estimated by Kim  
523 et al. (2017) was about 30% lower than that obtained without the assimilation of Siberian observation data,  
524 Siberia still remains a key contributor to the terrestrial CO<sub>2</sub> sink in the Northern Hemisphere.

525

526 There are tendencies of significant growth or suppression of soil CO<sub>2</sub> fluxes across the types of human impact  
527 on cryogenic ecosystems in Russia (Karelin et al., 2017). Human footprint on the methane exchange between  
528 the soil and atmosphere is mediated by drainage. However, all types of human impact suppress the sources  
529 and increase the sinks of methane to the land ecosystems. The nitrous oxide (N<sub>2</sub>O) flux grew under the  
530 considered types of human impact. The human footprint on soil greenhouse gases fluxes is comparable to the  
531 effect of climate change at an annual to decadal timescales.

532

533 Wildfires in Siberia lead to a parallel increase of the CO<sub>2</sub> concentration at the Russian Arctic. During 2010–  
534 2017, CO<sub>2</sub> concentrations increased by 20 ppm in Tiksi at a coast of Laptev Sea and by 15 ppm at the Cape  
535 Baranov station (Ivakhov et al., 2019). At the ZOTTO tower site in central Siberia, atmospheric CO<sub>2</sub>  
536 concentration increased an average by 2.0 ppm yr<sup>-1</sup> during 2006–2013, but showed large interannual variations.  
537 The highest increase were found in 2010 and 2012 (3.6 and 4.3 ppm yr<sup>-1</sup>, respectively), when large wildfires  
538 released huge amounts of CO<sub>2</sub> in Siberia (Timokhina et al., 2015b). Repeated wildfires in boreal forests can  
539 combust a portion of the thick organic soil layer characteristic of this ecosystem, and change the forests from  
540 a carbon sink into a carbon source (Walker et al., 2019). In a study on the fire chronosequence of the central  
541 Siberian permafrost soil showed that soils being affected by fires over decades acted as a CO<sub>2</sub> sources (Köster  
542 et al., 2018). The CO<sub>2</sub> emissions from the soil increased with increasing time since the last fire. However, there  
543 were no similar effect on CH<sub>4</sub> emissions, and soils acted as a CH<sub>4</sub> sink without connection to forest fires. In  
544 addition to CO<sub>2</sub>, wildfires also release large amounts of other trace gases and aerosols. Emission factors of  
545 several trace gases and aerosols from Siberian fires measured from the Trans-Siberian railway were reported  
546 by Vasileva et al. (2017). The impact of Siberian fires as elevated aerosol concentrations was at times observed  
547 to extend up on the Arctic coast (Asmi et al., 2016).

548

#### 549 *Arctic methane (CH<sub>4</sub>) balance*

550 Deep understanding of methane emissions dynamics in the Arctic is needed for the identification and  
551 quantification of the GHG-related feedbacks and global methane cycle (Dean et al., 2018). The main source  
552 of methane in Arctic during winter is anthropogenic; on a smaller scale, emissions from oceans including The  
553 Eastern Siberian Arctic Shelf (ESAS) can play an important role. During warm season, the balance is  
554 dominated by emissions from wetlands and freshwater bodies. Thonat et al. (2017) employed CHIMERE  
555 model for the assessment of the methane cycle in Arctic. They reported that all methane sources, except



556 biomass burning, contributed to measurements at six study sites. That study emphasizes the importance of a  
557 joint model-measurements approach for studies of complex phenomena at large spatial scales. Accounting for  
558 OH oxidation and soil uptake, sinks of methane, improved the agreement between observed and modelled  
559 methane concentrations (Thonat et al., 2017). Peltola et al. (2019) up-scaled CH<sub>4</sub> fluxes measured at 25  
560 northern wetland sites and showed three different maps of wetland distribution with the annual methane  
561 emissions varying from 31- 38 Tg(CH<sub>4</sub>) yr<sup>-1</sup>. (For the monthly up scaled CH<sub>4</sub> flux data products see  
562 [doi.org/10.5281/zenodo.2560163](https://doi.org/10.5281/zenodo.2560163)). Multiple sources, together with different spatiotemporal dynamics and  
563 magnitudes, are influencing the total Arctic CH<sub>4</sub> budget and addresses the need for the further improved  
564 assessments (Peltola et al., 2019, Thonat et al., 2017).

565

#### 566 *Northern Eurasian carbon monoxide (CO)*

567 Analysis of the long-term trends in atmospheric composition in remote Northern Eurasia (1998–2016) showed  
568 that the total column carbon monoxide (CO) amount has been stabilized or increased in summer and autumn  
569 months, whereas the total column CH<sub>4</sub> amount has increased since 2007 (Rakitin et al., 2018). The changes in  
570 the global photochemical system, especially changes in the ration between the sources and sinks for minor  
571 atmospheric chemical species, could explain these trends (Skorokhod et al., 2017). A comparative study  
572 (1998–2014) on the atmospheric total column CO amount in the background and polluted regions of Eurasia  
573 indicated that this amount has decreased remarkably in the Moscow urban environments compared to the  
574 background regions (0.9–1.7% per year) (Wang et al., 2018a).

575

#### 576 *Northern Eurasian Ozone (O<sub>3</sub>)*

577 Atmospheric measurements of ozone, its precursors and other pollutants over Siberia are important for the  
578 atmospheric chemistry modelling, satellite products validation and comparisons between Siberia and other  
579 regions of the Northern Hemisphere. Isoprene and monoterpenes together with nitrogen oxides impact  
580 tropospheric O<sub>3</sub> formation and lead to an increase in the daytime ozone-forming potential (OFP) in urban  
581 environment. It was demonstrated that monoterpenes have a major contribution to tropospheric O<sub>3</sub> formation,  
582 especially in cities in Siberia having high atmospheric NO<sub>x</sub> concentration (10-20 ppb) and daytime  
583 temperatures (>25 °C) (Berezina et al., 2019). In contrast, isoprene is dominating the O<sub>3</sub> formation and the  
584 increasing OFP in the Far East cities with the increasing population size. The isoprene-derived OFP can  
585 originate from deciduous vegetation growing in city environments or nearby regions, or from an anthropogenic  
586 isoprene source. The monoterpene-derived OFP was found to be the lowest in medium-size cities and the  
587 highest in small cities (Berezina et al., 2019). The total contribution of benzene and toluene to photochemical  
588 O<sub>3</sub> production was found to be up to 60–70% in urbanized environments, indicating anthropogenic pollutant  
589 sources (Skorokhod et al., 2017). In addition to atmospheric chemistry, the connection between O<sub>3</sub>, UV  
590 radiation and health effects needs to be addressed in the populated urban environments of Siberia. Chubarova  
591 et al. (2019) estimated that winter O<sub>3</sub> depletion in northern regions of Siberia is not critical, but much weaker  
592 O<sub>3</sub> reduction in the early spring can lead to dangerous levels of erythema UV radiation.

593



594 *Sources and properties of atmospheric aerosols in boreal and Arctic environments*

595

596 Atmospheric new particle formation (NPF) is the largest contributor to the number concentration of aerosol  
597 particles in the global troposphere. During the past couple of decades, NPF has been measured in more than  
598 10 boreal forest sites (Kerminen et al., 2018). The annual frequency of NPF event days varies between about  
599 10 and 30% in the boreal forest zone, being the highest in the western part of this region and lowest in the  
600 northern edge and Siberian part of it. Similar high nucleation frequencies were found at two very remote sites  
601 in boreal North America (Andreae et al., 2019). In contrast, annual NPF event frequencies below 2% were  
602 reported from central Siberia (Wiedensohler et al., 2019). Similarly, in the northern Siberia on the Arctic coast,  
603 NPF events were mainly connected with marine and coastal air masses and rarely observed in continental air  
604 masses (Asmi et al., 2016). Seasonally, NPF tend to be most frequent during spring, even though high NPF  
605 event frequencies can also be observed during summer or autumn. Winter-time NPF is rare throughout the  
606 boreal forest region. In the Arctic, NPF appears to be a major aerosol particle source from spring to summer,  
607 after which this source collapses during autumn and practically absent over the whole winter (Freud et al.,  
608 2017). 20 years of NPF observations in a boreal forest at the SMEAR II station in Finland show higher  
609 frequency of NPF events under clear-sky conditions in comparison to cloudy conditions (Dada et al. 2017).  
610 Also oxidized organic vapors showed a higher concentration during the clear-sky NPF event days, whereas the  
611 condensation sinks and some trace gases had higher concentrations during the nonevent days. In spring, a  
612 threshold for the combined values of ambient temperature and condensation sink was found. Above this  
613 threshold, no clear-sky NPF event could be observed.

614

615 The overall importance of atmospheric NPF in boreal and Arctic areas depends on the growth of freshly-  
616 formed particles cloud condensation nuclei. In the boreal forest environment, both observations and model  
617 simulations indicate that the growth particles is tied strongly with the oxidation products of biogenic volatile  
618 organic compounds originating from forest ecosystems (Paasonen et al., 2018; Östrom et al., 2017). The  
619 important compound group in this respect are monoterpenes, even though also sesquiterpenes were found to  
620 have high secondary organic aerosol yields in boreal forest environments (Hellén et al., 2018). The observed  
621 particle growth rates were found to increase with an increasing particle size and to be highest during summer  
622 time (Paasonen et al., 2018). The chemistry of new particle growth in the Arctic atmosphere is not well  
623 characterized, even though available observations suggest that this growth is associated mainly with biogenic  
624 emissions from high-latitude marine areas (Giamarelou et al., 2016; Heintzenberg et al., 2017; Kecorius et al.,  
625 2019).

626

627 Wildfires are an important source of particulate pollutants on a global scale and are affecting both on air quality  
628 and climate (Andreae, 2019; Bondur et al., 2020). Satellite observations indicate that the annual burned area  
629 by wildfires in Russia decreased by a factor of 2.6 during 2005–2016 owing to early detection and suppression  
630 of fire sources, whereas in Ukraine the relative size of burned-out areas increased by a factor of 6–9 from  
631 2010–2013 to 2014–2016 (Bondur et al., 2017; 2019 d). For Siberia, Ponomarev et al. (2016) reported a strong



632 increase both in number and burned areas based on satellite data, 1996-2015. Based on their data, the burned  
633 areas in Siberia doubled from 2005 to 2016. While biomass burning emissions have been measured widely  
634 over Russia (Bondur, 2016; Bondur and Ginzburg, 2016; Bondur et al., 2019 d), there is still a need for further  
635 information on the atmospheric composition of wildfire emissions and related emission ratios from the Siberian  
636 region. Fire experiments provide important information on the emission and aging characteristics of smoke  
637 aerosols (e.g. Kalogridis et al., 2018).

638

639 Luoma et al. (2019) presented a detailed trend analysis for aerosol optical properties at the SMEAR II station  
640 in Finland. They found a statistically significantly decreasing trend for the scattering coefficient, and even a  
641 stronger decreasing trend for the absorption coefficient during 2006 – 2017. These trends are very likely  
642 indicative of decreasing influence of anthropogenic emissions, with the contribution from emissions containing  
643 black carbon decreasing even faster.

644

645 Measurements of carbonaceous aerosols over central Siberia during 2010-2012 showed that in fall and winter,  
646 high concentrations of such aerosols were caused by long-range transport from the cities located in southern  
647 and southwestern regions of Siberia (Mikhailov et al., 2015a). In spring and summer, pollution levels were  
648 high due to regional forest fires and agricultural burning in the Russian-Kazakh region. The variability of the  
649 background concentration of organic aerosols correlated with the air temperature in summer, implying that  
650 biogenic sources dominated the formation of organic particles at that time of the year (Mikhailov et al., 2015b).  
651 Overall, it seems that the atmospheric pollution originating from the biomass burning and anthropogenic  
652 emissions is significantly affecting the Siberian region. In summer, precipitation is removing the pollutants  
653 from the air and leading to relatively clean atmospheric conditions this region (Mikhailov et al., 2017).

654

655 At circumpolar sites over the Arctic, aerosol optical properties were found to vary both seasonally and spatially  
656 (Schmeisser et al., 2018). Arctic haze aerosols in late winter and spring are characterized by increased  
657 concentrations of sulfate, whereas in summer rich organic chemistry seems to be associated with vegetation,  
658 local urban and shipping sources as well as secondary aerosol formation influenced by emissions from low  
659 latitude Siberia (Popovicheva et al., 2019a). In a longer perspective, Arctic observations show large decreases  
660 in both sulfate and black carbon concentrations since the early 1980s (Breider et al., 2017).

661

662 Observations on the elemental composition of surface aerosols on the coastal Kandalaksha Bay of the White  
663 Sea were indicative of the dominance of biogenic aerosol particles during summer time, with heavy metal  
664 concentrations in aerosols being at Arctic background levels (Starodymova et al., 2016). Increases in Ni and  
665 Cu concentrations were observed in air masses arriving from the western part of the Kola Peninsula indicative  
666 of emissions from the smelters in that region.

667

668 *Black carbon and dust in the atmosphere and snow*

669



670 Black carbon (BC) is a potentially large contributor to climate forcing in the Arctic region, however, the  
671 assessment of its pollution is hampered by the lack of aerosol studies in Northern Siberia (Popovicheva et al.,  
672 2019). Spatial variability of Arctic BC was studied using a harmonized dataset from 6 circumpolar Arctic  
673 observatories (Backman et al., 2017). These data suggested significant spatial and seasonal variability  
674 (Schmeisser et al., 2018), addressing a need for more year-round data. BC observations (Sep 2014 – Sep 2016)  
675 at the Hydrometeorological Observatory Tiksi at a coast of the Laptev Sea showed a seasonal variation, with  
676 the highest concentrations (up to  $450 \text{ ng/m}^3$ ) from January to March and the lowest (about  $20 \text{ ng/m}^3$ ) - for June  
677 and September. During winter, stagnant weather and stable atmospheric stratification resulted in accumulation  
678 of pollution, depending also on wind direction and air masses transport (Popovicheva et al., 2019a).

679

680 For Arctic, important sources of BC include industrial regions of Northern Europe, gas flares of the oil fields  
681 in the North Sea and Siberia, and Siberian biomass burning (Shevchenko et al., 2015; Konovalov et al., 2018).  
682 For example in 2012 approximately a quarter of the biogenic BC emissions from Siberia after fire season were  
683 transported into the Arctic (Konovalov et al., 2018). Popovicheva et al. (2017a) analyzed the BC origins over  
684 the Russian Arctic seas together with simulated BC concentrations. Concentrations were observed to be high  
685 ( $100\text{--}400 \text{ ng m}^{-3}$ ) in the Kara Strait, Kara Sea and Kola Peninsula, and extremely high (about  $1000 \text{ ng m}^{-3}$ ) in  
686 the White Sea. It seems that the gas-flaring emissions from the Yamal-Khanty-Mansiysk and Nenets-Komi  
687 regions affected the measurements made in the Kara Strait (northerly  $70^\circ \text{N}$ ) region, while the Near  
688 Arkhangelsk (White Sea) region was connected to the biomass burning in mid-latitudes. The combustion from  
689 the Central and Eastern Europe were also identified as important BC sources.

690

691 Atmospheric aging promotes internal mixing of BC with other aerosol constituents, leading to enhanced light  
692 absorption and radiative forcing. The in-situ observations at Arctic stations demonstrated absorption  
693 enhancement due to the internal mixing of BC, which is a systematic effect and should be considered for  
694 quantifying the aerosol radiative forcing in this region (Zanatta et al., 2018).

695

696 Regional modelling of the Arctic aerosol pollution showed that the main sources of the pollution e.g. BC  
697 deposition over snow originates from long-term anthropogenic emissions and biomass burning and are main  
698 contributors to direct aerosol radiative effects in the region (Marelle et al., 2018). A scenario of the increasing  
699 shipping in the Arctic Ocean in summer 2050 indicates that shipping emissions could become the main source  
700 of surface aerosol and the flaring of the BC. Kühn et al. (2020) assessed the effects of different BC mitigation  
701 measures on Arctic climate and showed that reducing BC emissions by the Arctic Council member states can  
702 reduce BC deposition by about 30 % compared to the current situation. A full execution of recommendation  
703 by the Arctic Council member and observer countries could reduce the annual global premature deaths due to  
704 PM by  $\sim 9\%$  by 2030 (Kühn et al. 2020). Evangelidou et al. (2018) estimated the origin of elemental carbon  
705 (EC) in snow and showed that for western Siberia where gas flaring emissions is a major contributor, the model  
706 underestimation was significant. Furthermore, the model was evaluated by independent BC measurements in  
707 snow over the Arctic showed and, again, the model underestimated BC concentrations, especially in spring.



708  
709 Climatically significant cryosphere effects of light-absorbing, high-latitude dust can be similar to the albedo  
710 and melt effects of BC (Peltoniemi et al., 2015; Svensson et al., 2016, 2018; Meinander et al. 2020ab). Iceland  
711 is the most significant source for European Arctic dust and plays a role in the cryosphere-atmosphere-biosphere  
712 interactions and feedbacks (Boy et al., 2019; Dragosics et al., 2016, Dagsson-Waldhauserova and Meinander  
713 2019). Dust storms from technogenic mining industry tailing dumps on the Kola Peninsula are also an  
714 important source of local atmospheric pollution for neighbor cities, e.g., Apatity and Kirovsk (Amosov et al.,  
715 2020). Besides regional-scale dust storms from deserts in Kazakhstan, Mongolia and China are significant  
716 sources of aerosol pollution not only for these regions, but also for the Northern Asia.

717

718 *Methodological and model developments related to atmospheric chemistry and physics*

719

720 Several methods to characterize the atmospheric chemistry were introduced or improved. Motivated by the  
721 ability of atmospheric ion measurements to identify new particle formation (NPF) events in the atmosphere  
722 (Leino et al., 2016), a new classification method for atmospheric NPF was developed (Dada et al., 2018). The  
723 new method is complementary to the traditional event analysis and it can also be used as an automatic way of  
724 determining new particle formation events from large data sets. Zaidan et al. (2018b) used mutual information  
725 approach to identify key factors contributing to the NPF. This method can be used in the atmospheric studies  
726 also to discover other interesting phenomena and relevant variables. The NPF is directly observed by  
727 monitoring the time evolution of ambient aerosol particle size distributions. A new machine learning-based  
728 approach, a Bayesian neural network (BNN) classifier, points out the potential of these methods and suggest  
729 further exploration in this direction (Zaidan et al., 2018a).

730

731 The condensation sink, being proportional to the surface area of an aerosol population, is one of the major  
732 parameters controlling NPF. A simple model for the time evolution of the condensation sink in the atmosphere  
733 for intermediate Knudsen numbers was developed to describe the coupled dynamics of the condensing vapor  
734 and the condensation sink (Ezhova et al., 2018a). The model gives reasonable predictions of condensation sink  
735 dynamics during periods of particle growth by condensation in the atmosphere. A new empirical relation  
736 between the atmospheric cloud condensation nuclei (CCN) concentration and aerosol optical properties was  
737 derived (Shen et al., 2019), making it possible to estimate CCN concentrations at sites with continuous  
738 observations of aerosol optical properties.

739

740 Empirical models of solar radiation were developed and used for calibrations of solar radiometers (Bai, 2019).  
741 This method can be used to calibrate all kinds of solar radiometers. A solar radiation model combined with  
742 ceilometer and pyranometer measurements was used to classify clouds at SMEAR II (Ylivinkka et al., 2020)  
743 It opens new possibilities for studies of aerosol-cloud interactions.

744



745 Che et al. (2016) made an inter-comparison of three satellite (AATSR Level 2) aerosol optical depth (AOD)  
746 products (SU, ADV and ORAC) over China. The SU algorithm performs very well over sites with different  
747 surface conditions in mainland China from March to October, but slightly underestimates AOD over barren or  
748 sparsely vegetated surfaces in western China. The ADV product has the same precision and error distribution  
749 as the SU product. The main limits of the ADV algorithm are underestimation and applicability. The ORAC  
750 algorithm has the ability to retrieve AOD at different ranges, including high values of AOD, but its stability  
751 decreases significantly with an increasing AOD, especially when  $AOD > 1.0$ .

752

753 One of the major problems for both interpretation of satellite data and applications of empirical models of solar  
754 radiation is related to elevated aerosol layers in the atmosphere. It was demonstrated that their origin can be  
755 attributed at a higher confidence when back trajectories are combined with lidar and radiosonde profiles  
756 (Nikandrova et al., 2018).

757

758 A progress has been made with regards to black carbon measurement methods. A representative value for the  
759 multiple scattering enhancement factor, a fundamental quantity correcting atmospheric black carbon  
760 measurement using an aethalometer, was derived for the first time in the Arctic environment (Backman et al.,  
761 2017). By analyzing BC measurements made with an Aethalometer in Nanjing, Virkkula et al. (2015) showed  
762 that the compensation parameter of a widely-used data processing method depends both on single-scattering  
763 albedo and backscatter fraction of the aerosol. The multiple-scattering correction factor of quartz filters and  
764 the effect of filtering particles mixed in snow was estimated by Svensson et al. (2019) who applied the method  
765 for analyzing light absorption and BC in snow samples taken from the Finnish Lapland and the Indian  
766 Himalayas.

767

768 Measurement of atmospheric sub-10 nm particle number concentrations has been of substantial interest  
769 recently. A new high flow differential mobility particle sizer (HF-DMPS) was built, calibrated and operated  
770 in field conditions for one month (Kangasluoma et al. 2018). The counting uncertainties of the HFDMPs were  
771 reduced by about 50% as compared to the traditional DMPS. The HFDMPs detected about two times more  
772 particles than the DMPS in size range of 3–10 nm. Below 3 nm, the HF-DMPS is currently limited by the  
773 inability of diethylene glycol to condense on biogenic particles. For collecting BVOC samples, a novel  
774 collection method offering portability and improved selectivity and capacity was developed. A solid-phase  
775 microextraction (SPME) Arrow sampling (Barreira et al. 2018) can be used for static and dynamic collection  
776 of BVOCs in the field conditions. A significant improvement on sampling capacity was observed with the new  
777 SPME Arrow system over SPME fibers. A fully automated online dynamic in-tube extraction (ITEX)–gas  
778 chromatography/mass spectrometry (GC/MS) method was introduced for continuous and quantitative  
779 monitoring of VOCs in air (Lan et al. 2019). The stability and suitability of the developed system was validated  
780 with a measurement campaign, and the ITEX method provided 2–3 magnitudes lower quantitation limits than  
781 established methods. Parshintsev et al. (2015) introduced a new, fast analysis method for the desorption  
782 atmospheric pressure photoionization high-resolution (Orbitrap) mass spectrometry (DAPPI-HRMS). The



783 DAPPI results agreed with the aerosol particle number measured with an established method and was found  
784 to detect different compounds and giving complementary information about the aerosol samples.

785

786 Fragmentation of molecular clusters inside mass spectrometers is a significant uncertainty-source in many  
787 chemical applications. A novel model, capable of quantitatively predicting the extent of fragmentation of  
788 sulfuric acid clusters was developed (Passananti et al. 2019). The fragmentation cannot be described in terms  
789 of rate constants under equilibrium conditions, because clusters accelerate under electric fields (Zapadinsky et  
790 al. 2019). A model describing an energy transfer to the cluster internal modes caused by collisions with residual  
791 carrier gas molecules was developed. The model can be used to interpret experimental measurements done  
792 with atmospheric pressure interface mass spectrometers.

793

794 Recently, new atmospheric aerosol instruments have been deployed in the PEEX area. At the Beijing  
795 University of Chemical and Technology (BUCT), the Aerosol and Haze Laboratory (AHL) was established, a  
796 permanent laboratory with a focus on characterizing air pollution in a comprehensive manner from a long-term  
797 perspective. Several chemical compounds are measured continuously by the state-of-the-art instruments at  
798 AHL in connection to atmospheric trace gases, aerosol particle size distributions and mass concentrations,  
799 particle chemical composition on the levels from molecules, clusters and nanometer to micrometer sized  
800 particles. The first results showed increased cluster mode particle number concentrations during NPF events,  
801 whereas during haze days accumulation mode particle number concentrations were high (Zhou et al., 2020).  
802 During these measurements, an evidence was found on significant nighttime sulphuric acid production,  
803 yielding gaseous sulphuric acid concentrations of  $1.0$  to  $3.0 \times 10^6 \text{ cm}^{-3}$  (Guo et al., ACPD 2020).

804

805 Besides Beijing, measurements have been performed in several other locations inside the PEEX area. We used  
806 novel instrumentation to measure new particle formation and its precursors at the background Fonovaya station  
807 in Tomsk region (Russia, Siberia), at the Värriö subarctic research station (Finland), in Ny-Ålesund (Svalbard,  
808 Norway) and on the German icebreaker, the Polarstern, during the MOSAIC project. As an example, the first  
809 results from Fonovaya station are shown in Fig. 2. Thanks to these deployments, in the next years we will be  
810 able to understand the identity of NPF precursors in those remote places. This will help to elucidate the human  
811 impact on aerosol formation and therefore aerosol-cloud interactions at high latitudes. In Siberia, we will  
812 finally understand why new particle formation occurs infrequently, and hopefully also identify the human role  
813 in this phenomenon. In the Arctic, we will understand the marine influence on new particle formation and will  
814 find out the detailed mechanism that leads to the formation of the initial clusters.

815

816 Model developments were made at several scales. Aerosol-radiation and aerosol-cloud interactions are among  
817 the main sources of uncertainties in climate models, and detailed information on anthropogenic aerosol number  
818 emissions is needed to improve this situation. Anthropogenic aerosol number emissions in current large-scale  
819 models are usually converted from the corresponding mass emissions in pre-compiled emission inventories  
820 using very simplistic methods. In the global aerosol-climate model ECHAM-HAM, the anthropogenic particle



821 number emissions converted originally from the AeroCom mass emissions were replaced with recently-  
822 formulated number emissions from the Greenhouse Gas and Air Pollution Interactions and Synergies (GAINS)  
823 model (Xausa et al., 2018). However, revisions are still needed in the new particle formation and growth  
824 schemes currently applied in global modeling frameworks.

825

826 For regional and urban scales, a fully integrated /online coupled meteorology-chemistry-aerosol model Enviro-  
827 HIRLAM was developed (Baklanov et al., 2017) and tested for several applications in Europe, Russian Arctic  
828 and China (Shanghai) (Mahura et al., 2018, 2019). Key issues for seamless integrated chemistry–meteorology  
829 modeling for Earth System prediction were analyzed and formulated (Baklanov et al., 2018), highlighting the  
830 scientific issues and emerging challenges that require proper consideration to improve the reliability and  
831 usability of these models for three main application areas: air quality, meteorology, and climate modeling.  
832 Baklanov et al. (2018) also presents a synthesis of scientific progress in the form of answers to nine key  
833 questions, and provides recommendations for future research directions and priorities in the development,  
834 application, and evaluation of online coupled models.

835

#### 836 2.2.2 Urban air quality and megacities (Q5)

837

838 The rapid urbanization and growing number of megacities and urban agglomerations requires new types of  
839 research and services that make the best use of science and available technology. There are urgent needs for  
840 examining what the rising number of megacities means for air pollution, local climate and the effects these  
841 changes have on global climate (Baklanov et al., 2016). Such integrated studies and services should assist cities  
842 in facing hazards, such as storm surge, flooding, heat waves and air pollution episodes, especially in changing  
843 climates (WMO, 2019). We discuss here the recent observation on the atmospheric pollution in China and  
844 Russia.

845

#### 846 *Air quality in China – recent observations*

847

848 China is one of the regions with highest concentrations of fine  $PM_{2.5}$  in the world (Wang et al., 2017a). This  
849 has serious consequences on air pollution and the associated visibility reduction (haze) and adverse health  
850 effects (Zhao et al., 2017). The number of haze days in China has been growing during the recent decades, but  
851 detailed understanding of the factors governing the occurrence of haze is still not clear. A key feature of haze  
852 formation seems to be an increased inorganic fraction of the aerosol, suggesting that the reduction of nitrate,  
853 sulfate and their precursor gases would improve air quality and visibility in China (Wang et al., 2019). In  
854 northern China,  $PM_{2.5}$  concentrations declined over the period 2013–2017, and approximately half of the inter-  
855 annual variability in this region was attributed to atmospheric circulation changes (Li et al., 2020b). The  
856 maximum daily 8-h average  $O_3$  concentrations increased over most of northern China during the same time  
857 period, with again large influences due to atmospheric circulation on daily basis (Liu et al., 2019b).

858



859 Measurements in urban China demonstrated a relative frequent occurrence of atmospheric new particle  
860 formation (NPF), characterized typically by high particle formation rates and strongly size-dependent growth  
861 of newly-formed particles (Kulmala et al., 2016b; Wang et al., 2017b; Chu et al., 2019). Since the first reported  
862 sub-3 nm particle measurements in China a few years ago (Xiao et al., 2015), new insight into the formation  
863 pathways of molecular clusters and their growth have been obtained, including the relative roles of gaseous  
864 sulfuric acid, amines, ammonia and organic vapors in these processes (Yao et al., 2018; Yan et al., 2021).  
865 While high pre-existing particle loadings appear to suppress NPF during severe haze periods in Chinese  
866 megacities, it is unclear how NPF is possible at all under less but still quite polluted conditions typical for these  
867 environments (Kulmala et al., 2017). Overall, the available observations suggest NPF to be a major source of  
868 aerosol particles in urban China, with potentially large effects on haze formation (Kulmala et al., 2021) and  
869 cloud properties (Chu et al., 2019).

870

871 Urban measurements of particle number size distributions give deep understanding into the sources and  
872 atmospheric processing of fine particles. The longest urban continuous record is from the SORPES station in  
873 the Yangtze River Delta (Qi et al., 2015), whereas the broadest size range (1.5 nm – 1  $\mu$ m) was measured in  
874 the winter Beijing atmosphere (Zhou et al., 2020). The latter study found clear differences in particle sources  
875 in different size ranges: NPF was in general the largest source of clusters and nucleation mode (<25 nm)  
876 particles, while traffic contributed to all the size ranges and dominated both cluster and nucleation modes on  
877 haze days. Aitken mode (25–100 nm) particles originated mainly from local emissions, with additional  
878 contributions from regional and transported pollution as well as from the growth of nucleation mode particles.  
879 Regional and transported pollution were identified as the main source of accumulation mode (>100 nm)  
880 particles.

881

882 Air pollution and chemical transformation, including annual and seasonal variations of the concentrations of  
883 atmospheric constituents, were analyzed for North China for 2005–2015 by Bai et al. (2018a). A  
884 photochemical link relating the production of fine PM and O<sub>3</sub> was detected. In particular, the VOCs  
885 contribution in chemical and photochemical reactions was found to be prominent in summer. An intensive  
886 measurement campaign (SORPES station, Yangtze River Delta) was carried out to investigate sulfate  
887 formation and associated nitrogen chemistry (Xie et al., 2015). That study highlighted the effect of NO<sub>x</sub> in  
888 enhancing the atmospheric oxidizing capacity, and indicated a potentially very important impact of increasing  
889 NO concentrations on particulate pollution formation and regional climate change in East Asia. In Changzhou,  
890 a highly-populated city in the Yangtze River Delta, primary organic aerosol concentrations outweighed  
891 secondary ones, indicating an important role of local anthropogenic emissions in aerosol pollution (Ye et al.,  
892 2017). The measurement also showed the abundance of organic nitrogen compounds in water-soluble organic  
893 aerosol, suggesting that these compounds are likely associated with traffic emissions.

894

895 Aerosol impacts on warm cloud properties were investigated over three major urban clusters in Eastern China  
896 and East China Sea using multi-sensor satellite observations (Liu et al., 2017, 2018). In addition to the amount



897 of aerosol, evidence was provided that aerosol types and environmental conditions need to be considered to  
898 understand the relationship between cloud properties and aerosols. Aerosol-cloud interactions were found to  
899 be more complex and of greater uncertainty over land than over ocean.

900

901 The atmospheric boundary layer (ABL), and especially its dynamic behavior, is central to the evolution of  
902 near-surface air pollution. Using atmospheric observations combined with theoretical arguments, Petäjä et al.  
903 (2016) proposed a feedback mechanism connecting ABL properties with PM. According to such mechanism,  
904 high concentrations of PM enhance the stability of an urban boundary layer (BL) decreasing its height, thus  
905 causing further accumulation of pollution inside BL. Ding et al. (2016a) and Wang et al. (2018b) demonstrated  
906 an important role of BC aerosols in this feedback using model simulations combined with observations. A tight  
907 connection between the BL height and pollutant concentration, and indications of the presence of the above  
908 feedback mechanism, was also found based on comprehensive observations made on a 325-m tower in Beijing  
909 (Wang et al., 2020). In line with the proposed mechanism, Shen et al. (2018) showed that aerosol optical  
910 properties evolve clearly during the development of multi-day pollution episodes in heavily polluted regions,  
911 such as East China. In order to understand these feedbacks, Kulmala (2018) emphasized the crucial role of  
912 continuous, comprehensive measurements on a network of flagship stations in tackling the air pollution  
913 problem in urban China and megacities elsewhere in the world. The first such station in China, the SORPES  
914 station located in the Yangtze River Delta, has been operating since 2011 (Ding et al., 2016b).

915

916 *Anthropogenic emissions and environmental pollution in Russia*

917

918 In the complex situation of the plurality of emissions, an important research task remains in the Moscow  
919 megacity environment for the assessment of the air quality and potential sources through aerosol composition  
920 analyses. Moscow aerosol pollution has been studied using a special AeroRadCity-2018  
921 experiment (Chubarova et al., 2019) and satellite data with the application of new MAIAC/MODIS aerosol  
922 algorithm with a 1-km resolution (Zhdanova et al., 2020). An advanced source apportionment for this  
923 environment was performed using combined Fourier-transform infrared spectroscopy data and statistical  
924 principal component analysis (Popovicheva et al., 2020b). The main principal component loadings revealed  
925 the source impacts of transport, biomass burning, biogenic, dust and secondary aerosol in spring. Identification  
926 of biomass burning-affected periods discriminated the daily aerosol composition change with respect to air  
927 mass transport and number of fires detected in the surrounding areas. Measurements of particulate BC were  
928 conducted at an urban background site (Meteorological Observatory of MSU) during spring period of 2017-  
929 2018 (Popovicheva et al., 2020c). The mean BC concentrations displayed significant diurnal variations, with  
930 a poorly prominent morning peak and minimum at daytime. BC mass concentrations were higher at nighttime  
931 due the shallow boundary layer and intensive diesel traffic. Aerosol optical thickness (AOT) over Moscow  
932 showed a pronounced seasonal cycle, with a summer maximum and winter minimum (Chubarova et al.,  
933 2016a). It was found that during 2001–2014, the monthly-mean values of AOT declined by 1–5% per year,  
934 and this decline was attributed the decreased emissions of aerosols and their precursors.



935

936 In general, the atmospheric environment over remote areas of Siberia and Northern Asia is relatively clean  
937 compared with other surrounding regions of Asia and Eastern Europe (Baklanov et al., 2013). However, air  
938 pollution from Siberian industrial centers poses significant environmental threats. For Siberian cities (e.g.,  
939 Norilsk, Barnaul, Novokuznetsk), the air quality is among the worst in the Russian and European cities. Similar  
940 to Arctic cities, stable atmospheric stratification and temperature inversions dominate for more than half a  
941 year. This leads to pollution accumulation near the surface, and influences ecosystems and people. Moreover,  
942 not only severe climatic conditions, but also manmade impacts on the environment in industrial areas and large  
943 cities have intensified. The impacts manifest themselves as the pollution of environment, land use changes,  
944 hydrodynamic regimes and local climate. Ultimately, these impacts feedback to people affecting their health  
945 and well-being.

946

947 Although anthropogenic emissions and environmental pollution in the Barents Euro-Arctic region are  
948 relatively low in comparison with other industrially developed areas of Europe, there are several severe ‘hot  
949 spots’, mostly in the Russian part of this region. The Kola Peninsula, despite the presence of areas with  
950 undisturbed nature in the eastern part, is the most industrially developed and urbanized region in the Russian  
951 Arctic. The main polluters are the smelters of the Severonickel (Monchegorsk, central part of the peninsula)  
952 and the Pechenganickel (Nickel and Zapolyarnyi near the Russian-Norwegian border) enterprises. For  
953 comparison, the emissions of SO<sub>2</sub> only from the Nickel smelter are 5-6 times larger than the total Norwegian  
954 emissions (NILU, 2013). In 2015 the Norilsk Nickel in Siberia - the biggest mining and the metallurgical  
955 complex - emitted about 1.9 million tons of SO<sub>2</sub> (GGO, 2016). With the nickel factory (located in the southern  
956 part of the city), the copper factory (just to its north), and the metallurgical plant (12 km to the east), the city  
957 of Norilsk is caught between heavy industry no matter which way the wind will blow. The Blacksmith Institute  
958 declared in 2007 that Norilsk is one of the top 10 worst-polluted places in the world. The impacts of emissions  
959 are manifested as deterioration of forest ecosystems, acidification of soils and surface waters (Derome and  
960 Lukina, 2011), even at considerable distances from the smelters. Heavy metals and alkaline pollutants  
961 contaminate areas around the sources of pollution within a few hundred kilometres, while acid sulphates can  
962 be transported over long distances (Mahura et al., 2018).

963

964 A recent analysis on the total deposition and loading on the population in North-Western Russia and the  
965 Scandinavian countries from the continuous sulfur emissions from the Cu-Ni smelters in Murmansk indicates  
966 the dominance of wet deposition, especially in winter time (Mahura et al., 2018). North-Western Russia is  
967 more influenced by the Severonickel emissions compared to countries of the Scandinavian Peninsula. The cities  
968 of the Murmansk region (Kola Peninsula) are under higher impacts. On a yearly scale, the individual loadings  
969 on population are at the largest level (up to 120 kg/person) in the Murmansk region, much lower (15 kg/person)  
970 in northern Norway, and the smallest (< 5 kg/person) in eastern Finland, Karelia Republic and Arkhangelsk  
971 region. Distinct seasonal variability was identified, with the lowest contribution during summer and highest  
972 contribution during winter-spring in Russia, spring - in Norway, and autumn - in Finland and Sweden.



973

974 Referring to a “Russian urban emission statistical analysis” for 2017 (GGO, 2019), the highest atmospheric  
975 emissions of PM were observed in Siberian and Ural cities. In Novokuznetsk the observed PM was the highest  
976 (> 30 000 tons per yr) while emissions from other cities such as Angarsk, Omsk and Chelyabinsk were less (>  
977 20 000 tons per yr). For the gaseous compounds, such as SO<sub>2</sub>, the maximum emissions included very high  
978 from Siberian cities (e.g. Norilsk, Novosibirsk, Novokuznetsk, Omsk, Ufa, Irkutsk, Angarsk) and from North-  
979 West European Russia cities (Zapolyarny, Nickel, Monchegorsk). High NO<sub>2</sub> emissions were observed in  
980 Novosibirsk, Omsk, Angarsk and Chelyabinsk. The CO integral urban emissions depend on a city size. These  
981 varied from less than 10 Gg yr<sup>-1</sup> (for small regional centers like Vladimir, Kursk, Samara) to 406 and 804 Gg  
982 yr<sup>-1</sup> for large metropolitan areas such as St. Petersburg and Moscow. As a whole, analysis of spatio-temporal  
983 variation of the trace gases in the boundary layer over Russian cities indicated significant emission variations  
984 between the urban environments and remote sites (Elansky et al., 2016).

985

986 Cities, being not isolated systems, may distribute as much pollution to the surrounding areas as they receive it  
987 from the outside or from remote regions. The analysis of the transboundary atmospheric transport between  
988 Russian Siberia and bordering countries (e.g. China, Kazakhstan, Mongolia) is part of a mutual risk assessment  
989 for urban areas/ cities and their surroundings. For example, city of Ulaanbaatar (Mongolia) suffers from high  
990 levels of pollution due to excessive airborne PM emanating from coal combustion mixes with traffic emissions  
991 and resuspended soil resulting in variable chemical source profiles (Gunchin et al., 2019). Long-range transport  
992 from remote sources might be also additional contributor. Moreover, there are indications (Jaffe et al., 2004)  
993 that such transport of biomass burning emissions from Siberia could lead to pollution episodes and impact on  
994 surface ozone as far as in western North America.

995

996 2.2.3 Weather and atmospheric circulation (Q6)

997

998 The observed evolution of weather and climate represents the combined effects of external forcing (changes  
999 in the concentrations of greenhouse gases and aerosols etc.) and internal variability, related to a large extent to  
1000 the atmospheric circulation. It is also affected by local factors, particularly urban heat islands in cities. Here  
1001 we discuss these interconnected processes, focusing on cold and warm episodes, cyclone density and  
1002 atmosphere-ocean interaction, effects of circulation on temperature and moisture, cloudiness in the Arctic, and  
1003 boundary layer dynamics relevant to the Arctic-boreal region.

1004 *Cold and warm episodes*

1005 The Arctic warming, and the Arctic amplification, have been associated with changes in atmospheric large-  
1006 scale circulation together affecting the European winter temperatures. In large parts of Europe, severe cold  
1007 (warm) winter events are significantly correlated with warm (cold) Arctic episodes (Vihma et al., 2020). Air  
1008 mass trajectory analysis revealed that air masses associated with extreme cold (warm) events typically



1009 originate over continents (sea areas). Despite Arctic and European-wide warming, winter cooling has occurred  
1010 in northeastern Europe in cases of air masses arriving from the southeast (Vihma et al., 2020).

1011

1012 *Cyclone density dynamics and atmosphere-ocean interaction*

1013 Transporting large amounts of heat and moisture from mid-latitudes to the central Arctic, synoptic-scale  
1014 cyclones are vital for the Arctic climate system. Recent findings, based on atmospheric reanalysis, above all  
1015 the global ERA-Interim reanalysis available from 1 January 1979 to 31 August 2019, are summarized below.  
1016 During 1979–2016 in winter (Dec, Jan, Feb), the cyclone density increased in the areas around Svalbard and  
1017 in northwestern Barents Sea, but decreased in southeastern Barents Sea (Wickström et al., 2020). This is related  
1018 to a shift to more meridional winter storm tracks in the Norwegian, Barents and Greenland Seas. The shift is  
1019 favored by a positive trend in the Scandinavian Pattern and, in the areas north of Svalbard, by a significant  
1020 increase in the Eddy Growth Rate (Wickström et al., 2020).

1021

1022 Numerical model simulations of the storm activity in the White, Baltic and Barents Seas were analyzed for the  
1023 period 1979-2015 (Myslenkov et al., 2018). A high interannual variability in the storm number was observed  
1024 for all studied seas. No significant trends in the storm number during the period 1979-2015 were found in the  
1025 studied sea areas. On average, the connection with global atmospheric circulation is stronger for the Baltic Sea  
1026 than for the other two seas. Also, the future changes of wind wave climate were analyzed. According to the  
1027 RCP8.5 scenario, in the second part of the 21st century the number of storm events will rise in the Baltic and  
1028 Barents Seas.

1029

1030 In the Bjerknes compensation, changes in atmospheric heat transport co-occur with opposing changes in ocean  
1031 heat transport. Observations and model simulations indicate a central role for ocean-atmosphere heat exchange  
1032 in the Barents Sea area in maintaining this compensation in the Arctic (Bashmachnikov et al., 2018 a,b).

1033

1034 *Circulation effect on temperature*

1035 The effect of atmospheric circulation on temperature trends in years 1979-2018 was studied by Räisänen (2019,  
1036 2020) using a trajectory-based method. He found that circulation trends had reduced the annual mean warming  
1037 during this period in western and central Siberia locally by over 1°C, with a much larger cooling effect in  
1038 autumn and winter (Fig 3). His findings also confirmed a circulation-induced amplification of warming over  
1039 the Barents and Kara seas particularly in winter. Yet in most areas the circulation-related temperature trends  
1040 have varied strongly from month to month, leaving only a relatively small effect on the annual mean  
1041 temperature trends. The residual warming obtained after subtracting the circulation effect therefore tends to  
1042 have a smoother seasonal cycle than the observed temperature trends, in better agreement with the multi-model  
1043 mean trends in the CMIP5 simulations (Taylor et al., 2012).

1044

1045 *Circulation effect on moisture*



1046 The effects of large-scale circulation on moisture, cloud and longwave radiation mostly occur through the  
1047 impact of horizontal moisture transport (Nygård et al., 2019). Evaporation is typically not efficient enough to  
1048 shape those distributions, and much of the moisture evaporated in the Arctic is transported southward (Nygård  
1049 et al., 2019). Strong moisture transport events avail a large part of the northwards moisture transport. The  
1050 meridional net transport is only a small part of the water vapor exchange between the Arctic and mid-latitudes  
1051 (Naakka et al., 2019). When a high-pressure pattern across the Arctic Ocean from Siberia to North America is  
1052 lacking, the amount of moisture, clouds, and downward longwave radiation is anomalously high near the North  
1053 Pole (Nygård et al., 2019). Using vertically-integrated water vapor as a metric, the Arctic (north of 70°N) has  
1054 since 1979 experienced a robust moistening trend that is in absolute numbers the smallest in March and the  
1055 largest in August (Rinke et al., 2019). However, the relative trends are the largest in winter. Although different  
1056 atmospheric reanalysis are consistent in spatiotemporal trend patterns, they scatter in the trend magnitudes.

1057

1058 Analysis of moisture and aridity estimated using the web-GIS "CLIMATE" and the ECMWF ERA-Interim  
1059 reanalysis data for Southern Siberia (50-65 °N, 60-120 °E) from 1979 to 2010 with a  $0.75^\circ \times 0.75^\circ$  grid  
1060 resolution showed that the mountain regions of Eastern Siberia have been becoming more arid each month  
1061 during the last 30 years (Ryazanova and Voropay, 2017). In Western Siberia, aridity increased in May and  
1062 decreased in June, while in the other months positive and negative trends were found. The greatest differences  
1063 in the trends of the aridity index (Si), air temperature, and precipitation were observed in July.

1064

1065 *Cloudiness in Arctic*

1066

1067 The climatology and inter-annual variability of Arctic cloudiness remains a wildcard in regional climate  
1068 change projections. Both climate models and satellite data products need in situ observations for calibration  
1069 and validation. Chernokulsky et al. (2017) and Chernokulsky and Esau (2019) collected and processed manual  
1070 cloud observations from meteorological stations in the PEEEX area. The cloud records in the Arctic are available  
1071 since the end of the 19<sup>th</sup> century. Since 1936, the cloud observations representatively cover the Eurasian Arctic.  
1072 It permits reconstructions of cloud type and cloud cover climatology as well as to study inter-decadal  
1073 variability of cloudiness. A problem of a special interest is related to co-variability of the total cloud cover and  
1074 sea ice concentration or extent. Both clouds and sea ice affect the surface heat balance through surface albedo,  
1075 but their feedback mechanisms, dynamical impacts and climate sensitivities are different. Chernokulsky et al.  
1076 (2017) found that the annual-mean total cloud cover (TCO) decreases during warmer climate periods with a  
1077 lower sea ice concentration, but increases over sea ice in the Barents Sea as more moisture is transported into  
1078 the Arctic at higher temperatures. Furthermore, the increasing TCO reduces deficit of the surface heat and the  
1079 intra- and inter-annual variability of TCO over solid ice is higher than that over open water (Chernokulsky et  
1080 al. 2017). Long-term cloud climatological analysis based on meteorological observations of the total and low  
1081 cloud cover and of the cloud types from the Barents Sea to the Chukchi Sea showed that significant transitions  
1082 between cloud types has been taken place especially the low-level stratus and stratocumulus types has been  
1083 transformed to the convective cloud types (Chernokulsky and Esau, 2019). Chernokulsky and Esau (2019)



1084 addressed that their results are relevant for understanding Arctic cloud processes and feedbacks, and that new  
1085 knowledge is needed to connect the changes in the Arctic radiation balance with the Arctic cloud cover—cloud  
1086 type climatology.

1087

1088 *Boundary layer dynamics and urban heat islands*

1089

1090 On the background of accelerated and amplified Arctic warming, anthropogenic heat release and metabolism  
1091 of cities add up to persistent warm temperature anomalies in the urbanized areas (Fig. 4). Indeed, if the climate  
1092 change forcing approaches  $2 \text{ W m}^{-2}$ , the urban heat forcing could be  $10\text{-}100 \text{ W m}^{-2}$  (Konstantinov et al., 2018).  
1093 The urban heating trapped in the shallow PBLs is potent to rise the local temperatures by  $1^\circ\text{C}$  to  $10^\circ\text{C}$  and even  
1094 more. This local climate phenomenon is known as the urban heat island (UHI) (Esau et al., 2020). A series of  
1095 *in situ* and satellite UHI studies in the northern cities revealed strong and persistent warm temperature  
1096 anomalies in almost all of 28 northern West Siberian cities (Miles and Esau, 2017), in 5 cities covered by the  
1097 UHIARC network (Konstantinov et al., 2019; Varentsov et al., 2018a) and in 57 Scandinavian cities (Miles  
1098 and Esau, 2020). The mean wintertime temperature anomalies, the UHI intensity, varied from  $0.8 \text{ K}$  to  $1.4 \text{ K}$   
1099 and had extreme intensities of up to  $7 \text{ K}$  during cold anticyclone weather conditions. The complete dataset of  
1100 surface UHI intensity derived from MODIS LST data products is freely available and published in Miles  
1101 (2020). Such a UHI induced strong mediation of cold temperature spells might cause significant socio-  
1102 economic and environmental impacts in the cities (Konstantinov et al. 2018, Fig. 4). A survey of other UHI  
1103 studies in 11 Arctic cities and towns confirmed that even relatively small cities at high latitudes may exhibit  
1104 intensive UHIs. A recent analysis confirms the important role of the surrounding temperature in explaining  
1105 spatial-temporal variation of UHI intensity (Miles and Esau, 2017). The major contribution to the UHI was  
1106 revealed for water, sparse vegetation, grassland and scrubland. The mechanisms and pathways of the UHI  
1107 maintenance requires involvement of numerical experiments with turbulence-resolving models to advance the  
1108 understanding of the local climate features (Urban Heat Islands - UHIARC dataset see  
1109 [http://urbanreanalysis.ru/uhi\\_arc.html](http://urbanreanalysis.ru/uhi_arc.html)). We would need a denser meteorological network, especially high  
1110 quality temperature data, to better understand the urban climatology and the thawing processes in urban soils  
1111 and to better assess climatic trends relevant to Arctic societies and welfare (Konstantinov et al. 2018).

1112

1113 Urban climate anomalies may cause more extreme weather and climate phenomena in densely populated  
1114 megacities. The Moscow agglomeration – the largest megacity in the boreal continental climate within the  
1115 PEEEX domain – demonstrates profound effect of interactions between the UHI and urban winds, known as a  
1116 cross-over effect (Varentsov et al. 2018b). The UHI creates an urban heat “dome” with near-surface air inflow  
1117 into the urban central districts and air outflow at higher levels in the atmosphere. The air uplift in the urban  
1118 dome is connected to the increase in summer rainfall at the lee side and over the central urban districts. Stable  
1119 atmospheric stratification over rural area is strengthened by the downwind air motions coming from the urban  
1120 region.



1121  
1122 Atmospheric boundary layer over the Arctic Ocean has been studied on the basis of tethered sonde sounding  
1123 observations over sea ice (Palo et al., 2017) and research aircraft observations over the open ocean and sea ice  
1124 (Suomi et al., 2016). Palo et al. (2017) found that in spring and summer, the occurrence and properties of  
1125 temperature inversions were controlled by the surface melt and warm air advection rather than surface net  
1126 radiation. During snow/ice melt, temperature inversions were frequently surface-based, and equally strong as  
1127 winter inversions over the Arctic Ocean. To better understand atmospheric boundary layer processes in the  
1128 Arctic, Suomi et al. (2016) developed a method to measure wind gusts from a research aircraft. It allows wind  
1129 gust observations at altitudes not reached by traditional weather mast observations. The observed gust factors  
1130 strongly depended on the surface roughness, which differed for sea ice and the open ocean.

1131

### 1132 2.3 ARCTIC-BOREAL AQUATIC SYSTEM

1133

1134 We discuss the recent results on the Arctic sea ice dynamics and thermodynamics, snow depth and sea ice  
1135 thickness, sea ice research supporting navigation, and rare elements in the snow and the ocean sediments,  
1136 especially from the perspective of improvements in the observation and modelling methods (Q7, section 3.3.1).  
1137 We introduce new results on the Arctic marine ecosystem and focus on the primary production and carbon  
1138 cycle (Q8, section 3.3.2.). In section 3.3.3 for the Arctic – boreal lakes and rivers, we discuss the browning of  
1139 lakes and lake sediment with a special attention on the Selenga River system of Lake Baikal (Q9).

1140

#### 1141 2.3.1 Changing water systems, snow, sea ice and ocean sediments (Q7)

1142

##### 1143 *Sea ice and thermodynamics with atmospheric and ocean dynamics*

1144

1145 Referring to the earlier discussion in section 2.2.3 on atmospheric circulation, we address here how the sea ice  
1146 dynamics closely interacts with atmospheric and ocean dynamics. A rapid decrease in the Arctic Ocean ice  
1147 cover, particularly in the Barents and Kara Seas, has occurred since the late 1970s simultaneously with a  
1148 cooling of winters in central Eurasia (McCusker et al., 2016). This unexpected winter cooling is related to  
1149 increasing northeasterly winds over the southeastern flank of an anomalous high that has developed over the  
1150 northwestern coast of Russia (McCusker et al., 2016; Mori et al., 2019, Räisänen 2020). However, the causality  
1151 between the atmospheric circulation changes and the Arctic sea ice decrease is debated. Observations suggests  
1152 a strong correlation between these two, but climate model simulations forced by reduced ice cover produce a  
1153 much weaker circulation change than observed, resulting in only weak cooling in central Eurasia (Mori et al.,  
1154 2014, 2019; McCusker et al., 2016). This suggests that either most models are underestimating the sensitivity  
1155 of the atmospheric circulation to sea ice decrease, supported by Romanowsky et al. (2019), or that the  
1156 circulation change has not been primarily caused by decreasing sea ice. In the latter case, the correlation  
1157 between the reduced ice cover and atmospheric circulation would mainly reflect the effect of circulation on  
1158 sea ice. In support of this, Blackport et al. (2019) showed that reduced sea ice coincides with anomalous heat



1159 flux from the atmosphere to the ocean, and that on the sub-seasonal time scale, anomalies in atmospheric  
1160 circulation tend to precede rather than follow those in sea ice. Thus, while reduced sea ice might partly explain  
1161 the observed changes in atmospheric circulation (Mori et al., 2019), the effect of circulation on sea ice appears  
1162 to be stronger than the effect of sea ice on circulation.

1163

1164 Considering atmosphere-ice interactions, Jakobson et al. (2019) studied the linkages between sea ice  
1165 concentration (SIC), atmospheric stratification, surface roughness and wind speed at the 10-m height (W10)  
1166 and 850-hPa level (W850). In all the seasons except summer, a reduction in SIC favored reduced atmospheric  
1167 stratification and aerodynamic surface roughness, which resulted in a stronger W10. The effect was the  
1168 strongest in autumn, and positive trends in W10 and its ratio to W850 typically occurred in regions with the  
1169 strongest negative trends in SIC. The relationships were stronger on inter-annual than sub seasonal time scales.  
1170 Large-scale atmospheric circulation, characterized, e.g., by the Dipole Anomaly (DA), has also contributed to  
1171 sea ice dynamics. A positive polarity in DA has contributed to the recent rapid loss of summer sea ice in the  
1172 Pacific part of the Arctic Ocean by bringing warmer air masses from the south and transporting more ice  
1173 towards the north enhancing the ice-albedo feedback (Lei et al., 2016). Another example of ice dynamics  
1174 affecting the ice-albedo feedback was the weakened Transpolar Drift Stream in summer 2013. It reduced sea  
1175 ice transport out of the Arctic Ocean, and restrained ice melt because of the low air temperatures, weakened  
1176 albedo feedback, and a relative small oceanic heat flux in the central Arctic (Lei et al., 2018).

1177 Solar radiation, being the main forcing factor for sea ice melt in summer, is difficult to parameterize in  
1178 thermodynamic models. This is due to the large variability of the optical properties of sea ice in space and  
1179 time. A two-stream model provides a time-efficient parameterization of the apparent optical properties (AOPs)  
1180 for ponded sea ice, accounting for both absorption and scattering, and has a potential for being implemented  
1181 into sea-ice thermodynamic models to explain the role of melt ponds in the summer decay of Arctic sea ice  
1182 (Lu et al. 2016). This model was used to investigate the role of solar radiation in the Arctic sea ice during the  
1183 melting season considering layers of melt ponds, underlying sea ice, and ocean beneath the ice. It was found  
1184 that the energy absorption profiles depend strongly on the incident irradiance and ice scattering, but only  
1185 weakly on the pond depth. It seems that the incident solar energy is largely absorbed by the melt pond rather  
1186 than by the underlying sea ice (Lu et al., 2018a).

1187 The model was further applied to investigate the influence of a surface ice lid on the optical properties of a  
1188 melt pond. The thickness of the ice lid determines the amount of solar energy absorbed. Visual inspections on  
1189 the color of refreezing melt ponds also help to judge the significance of the influence of the ice lid. This will  
1190 allow for an accurate estimation on the role of surface ice lid during field investigations on the optical  
1191 properties of melt ponds (Lu et al., 2018a). The modelled pond color agrees with field observations from the  
1192 Arctic sea ice in summer. The analysis of pond color is a new potential method to obtain ice thickness in  
1193 summer, however, more validation data and improvements to the radiative transfer model would be needed  
1194 (Lu et al., 2018b).

1195



1196 *Snow depth/mass and sea ice thickness*

1197 Snowpack on sea ice has a crucial role in insulating the sea ice from the colder atmosphere, accordingly  
1198 reducing sea ice growth in winter, effectively reflecting the incoming solar radiation, reducing sea ice melt in  
1199 spring and summer and contributing to its formation. The replacement of snow fall by rain strongly enhances  
1200 the ice-albedo feedback in the Arctic Ocean (Dou et al., 2019). Shalina and Sandven (2018) refined the  
1201 description of snow depth on sea ice in the central Arctic, providing new snow depth data for the Arctic  
1202 marginal seas. High autumn and winter precipitation and thinning Arctic sea ice make snow-ice formation  
1203 prevalent in the Atlantic sector of the Arctic (Merkouriadi et al., 2017).

1204

1205 Advance has been made in applying thermistor string based autonomous high-resolution Snow and Ice Mass  
1206 Balance (IMB) Array (SIMBA) buoys to measure snow depth and ice thickness (Figs. 5, 6.). SIMBA has a  
1207 lower cost, allowing deployment in large numbers (Lei et al., 2015). The determination of snow depth and ice  
1208 thickness from SIMBA temperature profiles has so far been largely a manual process. A SIMBA-algorithm  
1209 was developed to process SIMBA data automatically (Liao et al., 2018), assuming a fixed snow-ice interface.  
1210 Snow-ice formation results in snow-ice interface moving upward. The SIMBA-algorithm was further  
1211 developed to tackle the moving interfaces (Cheng et al., 2020). The developed SIMBA-algorithm works well  
1212 in cold condition for lakes and Polar Oceans. For Polar Oceans, the snow and ice are close to isothermal during  
1213 summer, which prevents the identification of interfaces on the basis of the temperature gradient. Under such  
1214 conditions, thermodynamic modelling yields valuable information on snow depth and ice thickness (Tian et  
1215 al., 2017).

1216 A challenge in sea ice thermodynamic modelling is the uncertainty in the magnitude of the oceanic heat flux  
1217 at the ice base, especially for land-fast sea ice. Yang et al. (2015) applied a one-dimensional thermodynamic  
1218 model to investigate impact factors on land-fast sea ice in the East Siberian Sea. The modelled snow cover was  
1219 less than 10 cm, having a small influence on the ice thickness, but surface albedo and oceanic heat fluxes were  
1220 critical.

1221

1222 Also in the terrestrial Arctic and boreal zone, there is a need for a better efficiency and coverage of an *in-situ*  
1223 snow observation network. Snow cover and snow mass are fundamental parameters for global energy and  
1224 water cycles, and the changes in the regional snowpack have societal impacts like on amount of drinking water  
1225 or capacity for the hydropower generation (Bormann et al., 2018). Snow depth data in the Arctic region are  
1226 available from the synoptic weather stations and snow mass data are systematically collected from the snow  
1227 courses, as demonstrated in Extended Data (fig. 2) by Pulliainen et al. (2020). The use of automatic and cost-  
1228 effective measurements together with harmonized snow measurement practices is the way forward. A survey  
1229 on a harmonized snow monitoring in Europe demonstrated that crucial parameters for operational services,  
1230 such as parameters characterizing precipitating and suspended snow, are measured by 74% of the European  
1231 snow network contributors (COST Action ES1404), but the parameters characterizing the snow  
1232 microstructural properties, electromagnetic properties and composition are currently measured by only 41%,  
1233 26% and 13%, respectively, of the network contributors (Pirazzini et al., 2018). The observations at the



1234 continental scale, so far, demonstrate a widespread snow-cover retreat since the 1970s across the Northern  
1235 Hemisphere, particularly in the Arctic (Derksen et al., 2012; Bormann et al., 2018). On the contrary, the results  
1236 from the mountains are mixed and there is no consistent picture of what is happening at the regional scale  
1237 (Bormann et al., 2018). Pulliainen et al. (2020) provided new insight into the seasonal snow mass and its trend  
1238 by using a bias-corrected GlobSnow 3.0 estimates. Pulliainen et al. (2020) is now able to demonstrate different  
1239 continental trends based on the 39-year satellite record: a decrease in North America, a negligible trend in  
1240 Eurasia, and a high regional variability in both areas.

#### 1241 *Sea ice research supporting navigation*

1242

1243 Recent research has addressed emerging opportunities for Arctic navigation and the importance of operational  
1244 sea ice analysis. Lei et al. (2015) is showing the trends along the Arctic Northeast Passage (NEP) and  
1245 demonstrates the increase of the spatially-averaged length of the open period (the ice concentration less than  
1246 50%) from 84 days in the 1980s to 114 days in the 2000s. The summer sea ice along the High-Latitude Sea  
1247 Route (HSR) north of the eastern Arctic islands has also decreased during the last decade, with the ice-free  
1248 period reaching 42 days in 2012. The HSR avoids shallow waters along the coast, which easier the access to  
1249 for deeper-draft vessels (Lei et al., 2015). Considering operational sea ice analyses for the Bohai Sea, work  
1250 has been done to combine thermodynamic modelling and Earth Observation (EO) data from synthetic aperture  
1251 radar (SAR) and microwave radiometers (Karvonen et al., 2017). The SAR-based discrimination between sea  
1252 ice and open-water works well, and areas of thinner and thicker ice can be distinguished. However, a larger  
1253 comprehensive training dataset is needed to set up an operational algorithm for the estimation of sea ice  
1254 concentration and for the weighting scheme for sea ice thickness (Karvonen et al., 2017).

1255

1256 Multi-decadal Arctic sea-ice state estimates are important for the strategic planning of Arctic navigation. These  
1257 estimates are usually based on climate models with a thermodynamic-dynamic sea-ice models. An up-to-date  
1258 assessment of large-scale sea-ice models was with the aid of sea-ice models as a climate model component, a  
1259 comprehensive review was carried out by Leppäranta et al. (2020). Specifically, Uotila et al. (2015) found that  
1260 a model with the subgrid-scale sea-ice thickness distribution reproduces more realistic sea ice and upper ocean,  
1261 due to better captured spring evolution, than a model with just single sea-ice thickness category. In terms of  
1262 validity of initial conditions for multi-decadal predictions, Uotila et al. (2019) analyzed a set of ocean  
1263 reanalysis products, including Arctic sea ice, and found that the multi-model set mean is a useful product as a  
1264 state estimate. This finding increases confidence toward the use of the combination of ocean reanalysis for  
1265 both initialization of multi-decadal predictions and analysis of multi-decadal variability.

1266

#### 1267 *Ocean floor and Sediments: composition and fluxes*

1268

1269 A significant content of illite and muscovite among layer silicates in most of the ice-rafted sediments samples  
1270 taken from selected Arctic regions suggests that sources of the sedimentary material are mainly mineralogically  
1271 similar to modern bottom sediments of the East Siberian and Chukchi seas, as well as presumably sediments



1272 of the eastern Laptev Sea. A significant kaolinite fraction in the samples from the North Pole area can be  
1273 caused by the influx of ice-rafted fine-grained sedimentary material from the Beaufort or Chukchi seas, where  
1274 kaolinite is supplied from the Bering Sea. The samples contained variable proportions of erosion products of  
1275 both mafic and felsic magmatic rocks and/or sufficiently mature sedimentary rocks (Maslov et al., 2018 a).

1276

1277 Quantification of CH<sub>4</sub> sources is fundamental information for the climate change mitigation (Fletcher and  
1278 Schaefer 2019). Methane stored in ocean floor reservoirs can reach the atmosphere in the form of bubbles or  
1279 dissolved in water. Methane hydrates could destabilize with rising temperature further increasing greenhouse  
1280 gas emissions in a warming climate. Subsea permafrost and hydrates in the East Siberian Arctic Shelf (ESAS)  
1281 are acting as a substantial carbon pool, and source of methane to the atmosphere. Annual methane emissions  
1282 of the region varies from 0.0 to 4.5 TgCH<sub>4</sub> yr<sup>-1</sup> estimated by Berchet et al. (2016). Yasunaka et al. (2018)  
1283 estimated the monthly air-sea CO<sub>2</sub> fluxes in the Arctic Ocean and adjacent seas located north of 60 degrees N  
1284 for the period 1997 - 2014 and end up to a net annual Arctic Ocean CO<sub>2</sub> uptake of 180 ± 130 TgC per year.

1285

1286 The Zeppelin Observatory data for 2014 suggest CH<sub>4</sub> fluxes from the Svalbard continental platform below 0.2  
1287 Tg yr<sup>-1</sup>. All estimates are in the lower range of values previously reported (Pisso et al., 2016). Platt et al. (2018)  
1288 reported a potential region with ocean-atmosphere CH<sub>4</sub> flux locating north of Svalbard but addressed that at  
1289 the time of the measurements the meteorological conditions were unique including a short episode of the highly  
1290 sensitive to emissions over an active seep site, without sensitivity to land-based emissions.

1291

1292 *River runoff affecting the hydrological processes at coastal marine environments*

1293

1294 The Arctic Ocean (including the Hudson Bay) receives 55.6 % of its river inflow from Russia, mostly via 19  
1295 large rivers (Shiklomanov and Shiklomanov, 2003). This freshwater inflow of approximately 2920 km<sup>3</sup> per  
1296 year (Shiklomanov, 2008) is associated with large sediment and heat transports, which together affect the  
1297 hydrography, marine climate, and ecosystems across the Siberian shelf seas (Magritsky et al., 2018). A major  
1298 part of seasonal and interannual variations in river runoff is anthropogenic, due to regulation in large reservoirs  
1299 (Georgiadi et al., 2016). In addition, Magritsky et al. (2018) detected an increased runoff trend of 5-10 %,  
1300 compared to a reference period of 1936 to 1975, in most of the major Russian rivers discharging into the Arctic  
1301 Ocean. The trend is mostly due to a climate-induced increase since the second half of 1980s (Magritsky et al.,  
1302 2018). However, due to gaps in the monitoring programs, these estimates have a large uncertainty: focusing  
1303 on river discharge from the six largest Eurasian rivers to the Arctic Ocean, estimates of the increase range from  
1304 7% (Peterson et al., 2002) to 1.5 % (Shiklomanov and Lammers, 2009).

1305

1306 Permafrost thawing has resulted in releases of old carbon storages, but so far there is no clear evidence on the  
1307 impact of permafrost thawing on the net emissions of CO<sub>2</sub> and CH<sub>4</sub> to the atmosphere (IPCC, 2019). A potential  
1308 explanation of no or weak net increase is that part of the methane released has been taken by rivers instead of  
1309 emitted to the atmosphere. Increased amounts of organic carbon in rivers impact the regional and global



1310 biochemical and methane cycles (Shakhova et al., 2007; Wild et al., 2019). With the accelerating permafrost  
1311 thaw, also the atmospheric emissions are expected to increase, in particular for CO<sub>2</sub> but also for CH<sub>4</sub>. Expected  
1312 future changes in river ice regime are consistent with the expected changes in the duration of the cold season  
1313 and accumulated negative air temperatures. Significant changes are expected for the rivers of the Kola  
1314 Peninsula and the lower reaches of the rivers Northern Dvina and Pechora, whereas the lowest changes are  
1315 expected for the central parts of Eastern Siberia (Agafonova et al., 2017). Due to anthropogenic activities  
1316 (above all industry, municipal services, and filling of reservoirs), water withdrawal from Russian Arctic rivers  
1317 and related groundwater systems is approximately 20.6 km<sup>3</sup> per year, and it is expected to increase to 37 km<sup>3</sup>  
1318 per year by 2025 to 2030 (Magritsky et al., 2018). Features of these changes at the marine margin of the Lena  
1319 River delta are different compared to changes in the delta head area.

1320

1321 The hydrological representativeness of a glacier is a new characteristic, and of practical importance for basin-  
1322 wide tasks of hydrology and glaciology. For its evaluation, it is proposed to replace the seasonal air  
1323 temperatures with the glacier summer mass balance (BS) or to include BS in the multiple regression equations  
1324 for calculating the runoff of rivers fed by melting of snow and ice. This method can be recommended for at  
1325 least of some glaciers in the existing network of the World Glacier Monitoring Service (WGMS) (Konovalov  
1326 et al., 2019).

1327

1328 2.3.2 Marine ecology (Q8)

1329

1330 *Living marine organisms weaken or even subdue CO<sub>2</sub> accumulation*

1331 The important climatological role of the world's oceans is to reduce the CO<sub>2</sub> accumulation into the atmosphere  
1332 through its absorption. This mechanism is ordinarily viable as the partial pressure of dissolved CO<sub>2</sub> in marine  
1333 surface waters is less than the content of CO<sub>2</sub> in the overlying atmosphere. Due to the organic pump, a net  
1334 draw down of atmospheric CO<sub>2</sub> into the ocean is put into effect. It proceeds in the process of sinking of  
1335 particulate organic carbon of algal origin: organically bound CO<sub>2</sub> is released through remineralization and  
1336 further accumulated in the deep ocean. In contrast, owing to the processes of carbonate counter pump, CaCO<sub>3</sub>  
1337 is exported downward and, at depth, dissolves causing a net release of CO<sub>2</sub> to the atmosphere (Balch et al.,  
1338 2016). However, there are living marine organisms that are able to weaken or even subdue CO<sub>2</sub> accumulation,  
1339 at least within their habitat. Among this group of marine organisms, the leading role belongs to  
1340 coccolithophores. Among marine bio systems, coccolithophores (class Primmnesiophyceae) are most productive  
1341 calcifying algae (Taylor et al., 2017). They both produce particulate inorganic carbon (in the form of calcite)  
1342 and promote the increase of CO<sub>2</sub> partial pressure (*p*CO<sub>2</sub>) in the ambient marine surface waters. Thus, the  
1343 biological activity of coccolithophores can exercise a direct influence on both the CO<sub>2</sub> flux exchange at the  
1344 atmosphere-ocean interface and the marine carbonate chemistry system (CCS). The rain ratio, i.e. the ratio of  
1345 particulate inorganic carbon to organic carbon, determines the intensity and direction of CO<sub>2</sub> flux at the



1346 atmosphere-ocean interface. In the case of coccolithophores, the rain ratio is above unity within their habitat  
1347 area, which potentially can have climatic consequences but also drive alterations in marine CCSs (Balch 2018).  
1348  
1349 *Emiliania huxleyi* is the most widespread coccolithophorid algal species in Earth's oceans, which, in light of  
1350 the above, naturally explains why this is one of the best-studied marine algae. Of all other coccolithophores,  
1351 *E. huxleyi* is probably most successful in forming extensive blooms in world-wide marine waters ranging from  
1352 oligotrophic to eutrophic. Unlike diatoms and dinoflagellates, this alga is phenomenally immune to both light-  
1353 limitation and very high light intensities. As high levels of incident light/irradiance enhance calcification  
1354 (which is predominantly a light-dependent reaction), it is supposed that the calcification machinery enables *E.*  
1355 *huxleyi* cells to resist photodamage through dissipating excess energy. This specialty is important in case of  
1356 nutrient-depleted waters, especially in combination with the high affinity of *E. huxleyi* for nutrients including  
1357 nitrogen but especially phosphorous. The property of both mixotrophic nutrition, and resistance, at least partial,  
1358 to zooplankton grazing and virus attacks (due to cell's coverage by calcite scales/coccoliths) contribute to this  
1359 alga ability to sustain a variety of unfavorable conditions and retain steadfastly its ecological niche (Godrijan  
1360 et al., 2020). Thus, the elaborate biology of *E. huxleyi* cells imparts to them the intrinsic and rather rare property  
1361 of pursuing growth-maximizing and loss-minimizing life strategies. This property reveals itself through  
1362 multiple manifestations, two of which are vastness and sustainability of *E. huxleyi* bloom areas. A typical  
1363 bloom surface is not less than thousands of square kilometers, but in many marine environments it is far larger  
1364 (Kondrik et al., 2018b). For example, in some years, the value of *S* in the North and Norwegian Sea can be  
1365 well above 100 000 km<sup>2</sup>, in the Bering Sea maximum bloom area (*S*) values were registered at 250 000 km<sup>2</sup>,  
1366 particularly large *E. huxleyi* bloom areas (up to 380 000 km<sup>2</sup>) were observed in the Barents Sea (Kondrik et  
1367 al., 2017). Within the subpolar and polar zones of the Northern Hemisphere, in the waters around the Great  
1368 Britain, in the North, Norwegian, Labrador, Greenland, Barents, and Bering seas *E. huxleyi* blooms occur  
1369 annually although with largely varying intensity (Pozdnyakov et al., 2017). The duration of blooms in the  
1370 Northern Atlantic and the Barents Sea is on average about three-four weeks. The moment of onset of the *E.*  
1371 *huxleyi* bloom area maximum shifts from June-July to September-October for the seas located at the temperate,  
1372 subpolar and polar latitudes of the Northern Hemisphere, respectively. This sequence mimics the flow pattern  
1373 of the Gulf Stream. In the Bering Sea, the temporal pattern of *S* variations reveals two periods (1998-2001 and  
1374 2018-2020) of extraordinary intense *E. huxleyi* outbursts. It is hypothesized that this phenomenon was driven  
1375 by massive advection of Fe-depleted North Pacific waters due to a significant weakening of the Alaskan  
1376 Current. The latter is supposed to be a teleconnected aftermath of exceptionally strong El Niño events in 1996-  
1377 1997 and 2017, respectively (Pozdnyakov et al., 2020).  
1378  
1379 Satellite-borne estimations made during 1998-2018 showed that *E. huxleyi* outbursts resulted in the release of  
1380 inorganic carbon (PIC) in the form of CaCO<sub>3</sub> in surface water in the amounts ranging from ~10 to several  
1381 hundreds of kilotons. In the Barents Sea, the released PIC content varied between ~100 kt and 250-300 kt,  
1382 whereas in the Bering Sea, during the two periods of exceptional activity, the PIC content was as high as 500  
1383 kt (Kondrik et al., 2017). There is ample evidence that the release of PIC was accompanied by a significant



1384 increase in CO<sub>2</sub> partial pressure ( $\Delta p\text{CO}_2$ ) within the bloom area: between 1998 and 2016, the mean and  
1385 maximum values of the ratio  $\Delta p\text{CO}_2/(\Delta p\text{CO}_2)_{\text{background}}$ , varied in the range  $\sim (20\text{-}40)\%$ , and  $\sim (30\text{-}60)\%$ . The  
1386 highest numbers were registered in the Bering and Barents seas (Kondrik et al., 2018a; 2019). Also, there is  
1387 space borne evidence for the atmospheric columnar  $\Delta\text{CO}_2$  enhancement ( $(\Delta\text{CO}_2)_{\text{atm}}$  over *E. huxleyi* blooms:  
1388 numerous case studies in the aforementioned North Atlantic seas as well as in the Barents and Black seas  
1389 proved that  $(\Delta\text{CO}_2)_{\text{atm}}$  could reach 2-3 ppm (Kondrik et al., 2019; Morozov et al., 2019).

1390

1391 Notwithstanding the remarkable ability of *E. huxleyi* to grow under conditions unfavorable for algae of other  
1392 functional groups (e.g. diatoms, flagellates, cyanobacteria), a highly irregular pattern of the registered two-  
1393 decadal (1998-present) time series of *S*, PIC, and  $\Delta p\text{CO}_2$  are indicative of susceptibility of this alga outbursts  
1394 to environmental conditions (Nissen et al., 2018; Kazakov et al., 2019; Silkin et al., 2019). Statistical  
1395 prioritization of non-biogenic forcing factors (FFs) shows that the latter are sea- and time-period specific  
1396 (Pozdnyakov et al., 2019). Thus, in the Barents Sea, sea water temperature (SWT) is the highest-ranked FF,  
1397 followed by PAR (photosynthetic active radiation). In the Bering Sea, beyond the aforementioned periods  
1398 (1998-2001 and 2018-present), sea surface salinity (SSS) is the FFs leader, with PAR as a runner up, whereas  
1399 SWT is only third in the row. Although these assessments are done without explicitly considered nutrients  
1400 concentrations (NCs), implicitly NCs were among the FFs. Indeed, arguably, variations in SWT, SSS, CHL,  
1401 MLD, and surface current speed/advection (tested as FFs) indirectly account for the variations in NCs as well  
1402 in such CCSs parameters as alkalinity and basicity (Durairaj et al., 2015; Pozdnyakov et al., 2019, and  
1403 references therein).

1404

1405 In the long run, under conditions of CO<sub>2</sub> steady accumulation in the atmosphere, this factor should be closely  
1406 considered (Rivero-Calle et al., 2015). The action of rising atmospheric CO<sub>2</sub> is expected to proceed through a  
1407 number of direct and indirect interactions (Fig. 7), both of which should ultimately cause alterations in the rain  
1408 ratio. Increase in atmospheric CO<sub>2</sub> leads to rising of global temperature, and further on to strengthening of  
1409 stratification, intensification of irradiance within the euphotic zone, cutting of nutrient fluxes from below.  
1410 Although the increase of CO<sub>2</sub> fluxes into the surface ocean causes a reduction of pH and CO<sub>3</sub><sup>2-</sup> levels in water,  
1411 the large pool of HCO<sub>3</sub><sup>-</sup> remains to support the calcification machinery. Thus, it will lead to the establishment  
1412 of environmental conditions unfavorable for non-calcifying phytoplankton (NCP), but beneficial (or at least  
1413 enduring) for coccolithophores in general and *E. huxleyi* specifically. Reduction of NCP and uncontested  
1414 growth of *E. huxleyi* drives a further reduction in dissolved CO<sub>2</sub> consumption by other groups of  
1415 phytoplankton, increase in *p*CO<sub>2</sub> in the surface ocean and intensification of CO<sub>2</sub> fluxes into the atmosphere.  
1416 Concurrently, through a system of feedback interactions, alterations in the rain ratio are bound to affect the  
1417 carbon fluxes at the water-atmosphere interface. Therefore, the scenario of further heightening of atmospheric  
1418 CO<sub>2</sub> in the future, in all probability, implies more vast proliferation of *E. huxleyi* in the world's oceans.

1419

1420 In combination with statistic-based-mathematical models of *E. huxleyi* blooms (Pozdnyakov et al., 2019), the  
1421 available IPCC climate models permit mid-term projections of the forthcoming changes (Gnatiuk et al., 2020).



1422 However, our knowledge on the reciprocal influence of climate change and both the structure and functioning  
1423 of marine ecosystems (even at the level of primary producers!) is still insufficient to confidently prognoses the  
1424 future dynamics of the *E. huxleyi* phenomenon. More studies are required even to fully understand the  
1425 mechanism of intracellular light-dependent reaction of calcification, its dependency on both seawater  
1426 carbonate chemistry and environmental FFs (Vihma et al., 2019). Creation of respective multidecadal  
1427 databases (as in Kazakov et al., 2019) as well as further delivery of satellite and *in situ*/shipborne/laboratory  
1428 data are necessary to improve our capacity to assess with certainty the climatological and ecological role of *E.*  
1429 *huxleyi* blooms on regional and global scales (Fig.7).

1430

### 1431 2.3.3 Lakes and rivers (Q9)

#### 1432 *Organic carbon in lakes*

1433

1434 Spatial variability, an essential characteristic of lake ecosystems, has often been neglected in field research and  
1435 monitoring. The detected spatial "noise" strongly suggests that besides vertical variation also the horizontal  
1436 variation should be considered in the ecosystem monitoring and, most importantly when the role of dissolved  
1437 organic carbon (DOC) on the CO<sub>2</sub> flux is estimated (Manasypov et al., 2015; Leppäranta et al., 2018). In  
1438 natural waters with increasing level of colored dissolved organic matter (CDOM) concentration, the water  
1439 color is shifted towards brown. The key "permanent" landscape variables, the coverage by lakes and peatland  
1440 in the catchment area can be strongly correlated with lake elevation above the sea level. A high lake coverage  
1441 indicates a low CDOM concentration, while a high peat coverage indicates the opposite (Arvola et al., 2016).  
1442 For example in Finland, recent results from inland water studies have not shown any overall, consistent large-  
1443 scale changes in CDOM concentrations over the last 101-year period (Arvola et al., 2017). Rather, CDOM  
1444 changes in individual lakes have been related to changes in land use in the drainage basin. Manasypov et al.  
1445 (2015) reported results from Siberian lakes, representing discontinuous permafrost zone, and addressed that  
1446 although the concentration of most elements in the lakes are lowest in spring, the maximal water coverage of  
1447 land made it as an significant reservoir of DOC. The soluble metals in the water column that can be easily  
1448 mobilized to the hydrological network.

1449

1450 In very shallow freezing lakes, the volume liquid water is much reduced due to ice growth, and rejection of  
1451 nutrients and pollutants in the ice growth causes major enrichment of the water body. This has major  
1452 implications to the ecosystem of these lakes (Yang et al., 2016; Song et al., 2019). Freezing rejects some 80-  
1453 90 % of the impurities in freshwater lakes. On the other hand, ice cover accumulates atmospheric deposition  
1454 over several months but releases them into the water body within one month's melting phase. Rejection of  
1455 nutrients and pollutants in lake ice growth causes major enrichment of the water body in shallow lakes and  
1456 notable increases in nutrient concentrations in a shallow lake during seasonal ice growth (Fang et al., 2015).

1457

#### 1458 *Lake carbon balance*

1459



1460 Arctic and boreal lakes are an important natural source of CH<sub>4</sub> to the atmosphere (Bastviken et al, 2011).  
1461 Methane is mainly produced in the bottom sediments and/or hypolimnion, where most of anaerobic  
1462 decomposition of organic matter take place, and then is either oxidized to CO<sub>2</sub> in the water column or emitted  
1463 to the atmosphere. At Kuivajärvi, a typical meso humid lake located in Southern Finland, it was found that  
1464 91% of available CH<sub>4</sub> was oxidized in the active CH<sub>4</sub> oxidation zone during hypolimnetic hypoxia (Saarela et  
1465 al., 2020). In warm springs, the early onset of thermal stratification with cold and well-oxygenated  
1466 hypolimnion delays the period of hypolimnetic hypoxia and thus limiting the production of methane. At  
1467 Kuivajärvi measured CO<sub>2</sub> fluxes (F-CO<sub>2</sub>) showed that the lake acted as net source of carbon during two open-  
1468 water periods (Mammarella et al., 2015). During day time, with typically high wind speed, shear-induced water  
1469 turbulence controls the water-air gas transfer efficiency, and thus enhancing the vertical diffusive fluxes across  
1470 the water-air interface. However, during calm nighttime conditions, buoyancy-driven turbulent mixing,  
1471 associated with penetrative cooling of surface water, controls the gas exchange, and simple wind speed-based  
1472 transfer velocity models strongly underestimate F- CO<sub>2</sub> (Mammarella et al., 2015). Kiuru et al. (2018)  
1473 developed a model simulating CO<sub>2</sub> dynamics of a boreal lake in warming climate. The simulations for 2070-  
1474 2099 showed a 20–35% increase in the CO<sub>2</sub> flux from the lake compared to the reference period 1980–2009.

1475

1476 *Lake ice cover*

1477 Wei et al. (2016) studied the Lake Inari (67.14 N, 25.73 E), Finnish Lapland, in winters 1980/1981 - 2012/2013,  
1478 and observed an increasing trend of the air temperature during the freezing season, associated with an  
1479 increasing trend of water precipitation in winter. Low temperature with less precipitation lead to the formation  
1480 of columnar ice, while strong winds together with the heavy snowfall favored of granular ice formation.  
1481 Karetnikov et al., (2017) analyzed long-term ice conditions of Lake Ladoga, in Russia, in a period of 1913–  
1482 2015 and showed that the mean freezing and breakup dates were November 26 and May 15, respectively, and  
1483 that the annual frequency of complete freeze over of the lake was 0.83. The period from 1990 to present was  
1484 much milder than the preceding years. The annual increase in ice concentration depended on the accumulated  
1485 freezing-degree-days (AFDD) and the hypsographic curve, while the ice thickness increased with the square  
1486 root of AFDD.

1487

1488 An analysis of a Siberian thermokarst lake located in the Lena River Delta, characterized as a floating ice lake,  
1489 showed that temporal dynamics and magnitude of heat fluxes and surface energy balance closures are  
1490 substantially different depending on the lake surface conditions (Franz et al., 2018). Sensible heat and latent  
1491 heat fluxes, modelled using available heat bulk transfer models (Woolmay et al, 2015; Verburg and Antenucci,  
1492 2010; Andreas et al, 2002) tend to underestimate the measured fluxes and show less variability over freezing  
1493 ice cover, melting ice in Spring, as well as over open water in Summer. However, the performance of these  
1494 models depends also on the accuracy on meteorological and hydrological input parameters, which should be  
1495 carefully measured especially during challenging winter conditions.

1496



1497 The seasonal lake ice cover is a sensitive indicator of climate variations in the Arctic (Kirillin et al., 2012;  
1498 Leppäranta, 2015). To work more on this question, Lake Kilpisjärvi (surface 37.1 km<sup>2</sup>, max depth 57 m), a  
1499 tundra lake in northern Finland has been under an intensive ice-related field programs in recent years. The  
1500 research covered all year but was focused on the melting period in May–June. The heat budget over the ice  
1501 season was dominated by the radiation balance. Turbulent fluxes were significant before the freeze-up in fall,  
1502 but in the ice season they were small. The evolution of ice thickness served as a very good approximation for  
1503 the total surface heat flux (Leppäranta et al., 2017) (Fig.8). In the melting stage, solar radiation, the strongest  
1504 forcing of the water body beneath ice cover, breaks the stability and initiates convective turbulent mixing. This  
1505 brings heat from the deeper water to ice enhancing melting at the ice bottom (Kirillin et al., 2018). Thus the  
1506 common assumption of the heat flux from the water to ice to be due to molecular conduction does not hold in  
1507 the melting stage but it is much higher. The ice–water interaction under lake ice has not been well covered in  
1508 earlier studies of ice growth and melting.

1509

1510 Ice melting process was studied in detail in Lake Kilpisjärvi. The melting progressed in the upper and lower  
1511 surfaces and in the interior, with proportions depending on the solar flux and optical properties of the ice and  
1512 therefore case-dependent. About one-third of the solar flux which penetrated the ice returned to ice bottom  
1513 providing heat for melting. This was consistent with the under-ice results in Kirillin et al. (2018). In 2013 a  
1514 rapid ice breakage event completed the ice breakup in short time with final breakage at the ice porosity 40-  
1515 50%. A lake ice melting model should include the thickness and porosity of ice, with porosity connected to an  
1516 ice strength criterion (Leppäranta et al., 2019).

1517

#### 1518 *Lake Baikal and Selenga River delta*

1519 The Selenga River, the main tributary of Lake Baikal, has a catchment area of 450 000 km<sup>2</sup> in the boundary  
1520 region between Northern Mongolia and Southern Siberia. This area is well known by its climate, land use and  
1521 dynamic socioeconomic changes which might have negative impacts on the ecosystems of Lake Baikal and  
1522 thus was selected as PEEEX field laboratory within PEEEX subprogram Selenga-Baikal Network  
1523 ([www.atm.helsinki.fi/peex/index.php/baikal-selenga-network-basenet](http://www.atm.helsinki.fi/peex/index.php/baikal-selenga-network-basenet)). In the recent past hydroclimatic  
1524 development both with land use changes lead to contaminant influx from mining areas and urban settlements  
1525 increase. Additional hydrological modifications due to the construction of dams and abstractions/water  
1526 diversions from the Selenga's Mongolian tributaries could lead to additional alterations (Karthe et al., 2017b).  
1527 In addition to Selenga River, a key issue for improved understanding of regional impacts of the environmental  
1528 change is to disentangle the influence of climate change from that of other pressures within the catchment  
1529 (Lychagin et al., 2017). The PEEEX subprogram Selenga-Baikal Network aims at integrated field-based and  
1530 modeling knowledge to develop basin-wide conceptual framework of riverine fluxes (Kasimov et al., 2017a;  
1531 Karthe et al., 2019).

1532

1533 As a PEEEX field laboratory, the regional large-scale assessments made it possible to predict the comprehensive  
1534 nature of hydrological and geochemical changes driven by climatic processes and human impacts. Heavy



1535 metals in water and sediments (Kasimov et al., 2020a, 2020b) and fish communities (Kaus et al., 2017) were  
1536 measured since 2011 in over 50 locations around catchment. The mining zones are potential hotspots for  
1537 increasing metal loads to downstream river systems. Several metals (Al, Cd, Fe, Mn, Pb and V) are exported  
1538 from mining sites to the downstream river system, as shown by net increasing mass flows. Based on novel  
1539 partitioning coefficient approach (Fig. 9) contrasting patterns with domination of both particulate and dissolved  
1540 phases in different parts of the basin were found. Such heterogeneity of metal partitioning is likely to be found  
1541 in many large river systems.

1542  
1543 Multiscaling modeling ranged from basin wide (Malsy et al., 2017; Frolova et al., 2017) to specific subregions,  
1544 like the particular segments of river system (Kaus et al., 2017; Thorslund et al., 2017; Garmaev et al., 2019)  
1545 or its delta (Chalov et al., 2017 a, b; Shinkareva et al., 2019), identified reaction of hydrogeochemical pathways  
1546 on climate change. Mean flow reduction in the Selenga River by an average of 3-5% in the 2020s-2030s and  
1547 4-25% in the 2080s-2090s is the crucial driver of ongoing and future hydrogeochemical change. Increase in  
1548 temperatures with permafrost thaw and the expansion of agricultural, mining and urbanization processes may  
1549 induce up to 6% increase in the particulate modes and 3% in the dissolved modes of some metals in the river  
1550 system (Chalov et al., 2018). Possible changes in the number or magnitude of high-flow events, caused by  
1551 climatic or other anthropogenic factors, could influence total sediment deposition, which was primarily found  
1552 to occur during relatively short high-flow events. Such potential changes also have important implications for  
1553 the possible spreading of polluted sediments (Pietron et al., 2015) and its storage in the Selenga River Delta,  
1554 which is an important wetland region forming the geochemical barrier which mitigate pollution of Lake Baikal  
1555 by riverine fluxes (Voropay and Kichigina, 2018, Chalov et al., 2015).. The Selenga delta region sequester  
1556 various metals bound to Selenga River sediments (Chalov et al., 2015, Pietron et al., 2018). Water shortage  
1557 decreases processes of suspended sediment retention in the delta. The seasonal hydrogeochemical patterns are  
1558 explained by wetland inundation during floods and channel erosion or Baikal wind surge during low flow  
1559 periods (Chalov et al., 2017a, 2017b).

1560

1561 *Asian water lakes*

1562

1563 The largest internal drainage basins in the world is located in Central Asia with a limited availability of both  
1564 surface and groundwater (Karthe et al., 2017a). Since the twentieth century, water resources of the region have  
1565 been over exploited and, for example, from small Mongolian headwater streams to the mighty Aral Sea, surface  
1566 waters have been partially desiccated. It seems that the implementation of the Integrated Water Resources  
1567 Management and water-food-energy nexus approaches would lead to a more environmental-friendly future  
1568 (Karthe et al., 2017). The lake-rich Qinghai-Tibet Plateau (QTP) has recently been identified as the Third Pole  
1569 of the Earth. Due to its high elevation and unique climate, QTP affects the global and local climate and played  
1570 an important role on the Central and Southern Asian water cycle (Zhang et al., 2018). The lake-atmosphere  
1571 interactions have been quantified over open-water periods, yet little is known about the lake ice  
1572 thermodynamics and heat and mass balance during the ice-covered season. A modelling study for a



1573 thermokarst lake in the QTP has been performed (Huang et al., 2019a). Strong diurnal cycles were seen for all  
1574 surface heat fluxes. The ice mass balance was dominated by growth and melt at base, but surface sublimation  
1575 was also crucial for ice loss, accounting for up to 40% of the maximum ice thickness and 41% of the lake water  
1576 loss during the ice-covered period. Strong penetration of solar radiative flux is the dominant contributor to  
1577 high value of upward sensible heat flux at ice bottom resulting a relatively thin ice cover compared with  
1578 equivalent high-latitude climate.

1579

## 1580 2.4 SOCIETY

1581

1582 The anthropogenic impact has been addressed as one of the PEEEX themes for the society system. The  
1583 discussion on the mitigation and adaptation including urban infrastructure design and risk assessment are  
1584 addressed in this context (Q10, section 3.4.1). The social transformations are discussed in terms how local  
1585 reindeer grazing interacts with the environment (Q11 section 3.4.2). The adaptive capacity of the Northern  
1586 societies depends on their environment, demographic structure and economic capacity, and the environmental  
1587 hazards and environmental health under changing climate are the key research areas in this context (Q12  
1588 section 3.4.3.).

1589

### 1590 2.4.1. Anthropogenic impact (Q10)

1591

#### 1592 *Mitigation*

1593 Arctic climate change generates a need for the long-term planning and development of a new socio-economic  
1594 infrastructure, such as dams, bridges, roads, transnational and regional energy networks. For this task, new  
1595 climate-based forecasting tools, cost estimates and operational risk and other methods and tools for the  
1596 infrastructure and urban design are needed. As an example, engineering calculations for maximal discharges  
1597 were provided for the Nadym River in Russia (Shevnina et al., 2017). Badina (2018) introduced a method for  
1598 the natural risk assessment by using indices based on the on socioeconomic potential data and spatial  
1599 distribution of natural hazards. This method has been tested and used to identify the most vulnerable  
1600 municipalities in South Siberia. Another example of new methods is a “Green Factor tool” to increase the share  
1601 and effectiveness of green areas in urban environments and cities. An ambitious target set in the tool could  
1602 encourage or force urban developers to aim higher with the planning of green areas and construction, but  
1603 existing regulations challenge its use (Juhola, 2018).

1604

1605 The energy production is of fundamental importance for the society functions, and new clean energy  
1606 technologies are needed for hindering the climate change. The potential of hydropower production under  
1607 probabilistic projections of annual runoff rate and future changes in the potential hydropower production need  
1608 to be evaluated (Shevnina et al. 2019). All the Nordic countries are vulnerable to various degrees to potential  
1609 cross-border impacts, due to their energy sectors being highly globalized and interconnected. However, cross-



1610 border impacts are not yet properly included in Nordic climate assessments or energy strategies. The EU's new  
1611 Green Deal is pivotal in this respect, as for the first time emissions along the whole supply chain (oil, gas, coal,  
1612 renewables) become under scrutiny and part of normative governance. Therefore, policy makers and energy  
1613 planners should be assisted in making comprehensive vulnerability assessments that address both domestic  
1614 and international climate risks (Groundstroem and Juhola, 2019).

1615

#### 1616 2.4.2 Environmental impact (Q11)

1617

##### 1618 *Reindeer (Rangifer tarandus L.) grazing and ground vegetation structure and biomass*

1619

1620 Reindeer (*Rangifer tarandus L.*) grazing in the North affects the ground vegetation structure and biomass and  
1621 cover of lichens. It seems that reindeers affect GHG fluxes from the forest field layer. Grazing changes affect  
1622 the vegetation composition and thereby emissions (Köster et al., 2018). Köster et al. (2017) provided detailed  
1623 information on soil CO<sub>2</sub> effluxes, which were mostly affected by the year of measurement, time of  
1624 measurement, soil temperature and also by the management, resulting in higher CO<sub>2</sub> emissions on the grazed  
1625 areas. Soil moisture content did not affect the soil CO<sub>2</sub> efflux. For example, in the Finnish Lapland the average  
1626 soil CO<sub>2</sub> efflux values were significantly higher in the year 2014 compared with 2013, mainly due to  
1627 differences in soil temperature at the beginning of the season (Köster et al., 2017). Furthermore, grazing  
1628 significantly decreased the biomass and cover of lichens and also the amount of tree regeneration. In a subarctic  
1629 mature pine forest, grazing did not affect the soil temperature or soil moisture. No statistically significant effect  
1630 of grazing on the soil CO<sub>2</sub> efflux, soil C stock or soil microbial C biomass was found. Soil microbial N biomass  
1631 was significantly lower in the grazed areas compared to the non-grazed areas. It seems that in the boreal  
1632 subarctic coniferous forests, grazing by reindeer can be considered as "C neutral" (Köster et al., 2015). There  
1633 is also indication that reindeer grazing affects the boreal forest soils e.g. their fungal community structure and  
1634 litter degradation (Santalahahti et al., 2018).

1635

#### 1636 2.4.3 Natural hazards (Q12)

1637

1638 Under this theme, the PEEX research has so far focused on environmental health issues. These include  
1639 diseases, the impact of UV radiation, and air pollution in urban environments. The spread of diseases caused  
1640 by living pathogens is basically determined by environmental conditions. Medico-geographical assessments  
1641 are usually based on identification of the links between the spread of diseases and factors of the geographical  
1642 environment.

1643

##### 1644 *Naturally-determined diseases*

1645 The climatic factor is deemed one of the main determinants for the spread of naturally-determined diseases  
1646 (Malkhazova et al., 2018). Emerging zoonotic diseases are expected to be particularly vulnerable to climate  
1647 and biodiversity disturbances. Anthrax is an archetypal zoonosis that manifests its most significant burden on



1648 vulnerable pastoralist communities. The recent findings highlight the significance of warming temperatures  
1649 for anthrax ecology in northern latitudes, and suggest potential mitigating effects of interventions targeting  
1650 megafauna biodiversity conservation in grassland ecosystems, and animal health promotion among small to  
1651 midsize livestock herds (Walsh, et al., 2018).

1652

#### 1653 *UV variations*

1654 Different geophysical parameters affecting the UV molecular number density show that especially at high  
1655 altitudes, the increased surface albedo has a significant effect on the UV growth. The new parameterization of  
1656 the on-line UV tool ([momsu.ru/uv/](https://momsu.ru/uv/)) for Northern Eurasia allows us to determine the altitude dependence of  
1657 UV and to estimate the possible effects of UV on human health considering different skin types and various  
1658 open body fraction for January and April conditions in the Alpine region (Chubarova et al., 2016b). Using UV  
1659 satellite retrievals, ERA-Interim data and the INM-RSHU chemistry-climate model, the changes in UV  
1660 irradiance and UV resources were estimated over Northern Eurasia for the 1979-2015 period, demonstrating a  
1661 significant UV increase over vast areas (Chubarova et al., 2020). Referring to long-term UV measurements  
1662 and model simulations in Moscow, a statistically significant positive trend of more than 5% per decade since  
1663 1979 was evaluated (Chubarova et al., 2018).

1664

#### 1665 *Air pollution and related health effects*

1666

1667 Street-level urban air pollution is one of the key topics of urban environments. In Norway, Bergen, the most  
1668 extreme cases of repetitive wintertime air pollution episodes, followed by increased large-scale wind speeds  
1669 above the valley, were transported by the local re-circulations to other less polluted areas with only slow  
1670 dilution. This observation is underling the need for a better described assumptions e.g. transport paths, weak  
1671 dispersion of classical air pollution dispersion models leading to better improved air quality forecasts in urban  
1672 areas. (Wolf- Grosse et al., 2017b). A link between the persistence of the flow above the Bergen valley and  
1673 the occurrence and severity of the local air pollution episodes was found. Analysis of the large-scale circulation  
1674 over the North Atlantic-European region, with respect to air pollution in Bergen, revealed that the persistence  
1675 in the meteorological conditions connected to the air pollution episodes is not necessarily caused by large-  
1676 scale anomalies of the atmospheric circulation over the Norwegian west coast. It is rather connected to  
1677 anomalies further upstream as far away as Greenland. (Wolf-Grosse et al., 2017a).

1678

1679 In Russia, especially intensive atmospheric pollution cases have severely impact the environment and human  
1680 health. Popovicheva et al (2019b) analyzed the Tver region, north of Moscow, which was considerably affected  
1681 the secondary organic aerosol (SOA) formation originated from long-lasting peat bog fires. Spectral  
1682 absorbance characteristics were similar to peat burning and traffic source emissions during fire and non-fire  
1683 related days and confirmed the effect of transported peat smoke on air quality in megacity environment  
1684 (Popovicheva et al., 2019b). Popovicheva et al. (2019b) also showed that the impact of the long-term transport  
1685 from the North-West Russia and Scandinavian on the local populations. Murmansk and Arkhangelsk are



1686 heavily altered by the emission coming from the local Cu Ni smelters. The individual loadings on population  
1687 can be up to 120 kg/person/year for the Murmansk region, but clearly less, 15 kg/person/year, in the northern  
1688 Norway, and only 5 kg/person/year in the eastern Finland. The largest loadings were observed during winter-  
1689 spring in Russia, during spring in Norway, and during autumn in Finland and Sweden.

1690

1691 Local Arctic air pollution alone can seriously affect public health and ecosystems locally, especially in  
1692 wintertime when the pollution can accumulate under inversion layers (Schmale et al., 2018a). We need more  
1693 research on the contributing emission sources and the relevant atmospheric pollution mechanisms, and more  
1694 detailed epidemiological or toxicological health impact studies in the Arctic. Socioeconomic changes  
1695 (shipping, tourism, natural resources extraction, increasing number of population) are already taking place in  
1696 the Arctic, and they will increase in the future. It is also expected that the emission types and magnitudes will  
1697 increase the number of exposed individuals (Arnold et al., 2016). There is still a large variation in the amount  
1698 of the location of emissions. Future predictions are even more difficult due to the yet unknown development  
1699 of the Arctic economic activities and their emissions (Arnold et al., 2016, Schmale et al., 2018 a,b ).

1700

### 1701 **3. SYNTHESIS AND FUTURE PROSPECTS**

1702

#### 1703 3.1 Future research needs from the system perspectives

1704

1705 For the Land ecosystem, the recent progress towards understanding of the Northern Eurasian Arctic - boreal  
1706 land ecosystems (section 3.1) are dealing with the improved methodologies relevant to land processes (Q1),  
1707 observations on permafrost thawing (Q2), and observed changes in the Northern ecosystems, especially soil  
1708 conditions (Q3).

1709

1710 Improved satellite-based methods and (validation) data together with better quantification and, especially, the  
1711 scaling of the gross primary production are enabling a better identification and quantification of Earth surface  
1712 characteristics and ecosystem carbon balance compared with the earlier capacity (Gurchenkov et al., 2017,  
1713 Rautiainen et al., 2016, Nitzbon et al., 2019, Boike et al., 2019, Terentieva et al., 2016), Zhang et al, 2018,  
1714 Pulliainen et al., 2017, Matkala et al., 2020; Bondur and Chimitdorzhiev, 2008 a,b). Intensive research has  
1715 been carried out on the quantification of the gross primary production (GPP), a key variable for biological  
1716 activity, in different conditions and at different scales (Pulliainen 2017, Kulmala et al., 2019, Matkala et al.,  
1717 2020). Further investigations are called for more detailed understanding of the seasonal dynamics of the  
1718 biological activity.

1719

1720 The Northern Eurasian ecosystems' tipping points are related to multiple simultaneous stress factors. The key  
1721 stress factors here are permafrost thawing and the factors important for ecosystem, such as prolongation of  
1722 growing season, increase in mean temperature of growing season and the forest fires (Kukkonen et al. 2020,  
1723 Biskaborn et al. 2019, Payne et al., 2016. Köster et al. 2016, Miles and Esau 2016, Miles et al., 2019). New



1724 evidence on the progress of permafrost thawing in Siberia has been introduced by Kukkonen et al. (2020) and  
1725 Biskaborn et al. (2019). The permafrost thawing is also triggering yet not clearly-known processes related to  
1726 changing fluxes, ecosystem processes and greenhouse gas sink and source dynamics (Schuur et al., 2008,  
1727 Thomson et al., 2017, Commane et al., 2017, Euskirchen et al., 2017, Dean et al., 2018, Thonat et al., 2017).  
1728 The progress affecting permafrost thawing is not yet analyzed in detail. For example, we need more  
1729 information on the dynamics how the thawing processes vary between soil types due to differences in water  
1730 movement and, in the winter time, how the snow cover affects the ground surface temperature (Bartsch et al.  
1731 2010). In addition to permafrost processes, the recent advances in observed changes in the Northern ecosystem  
1732 reveal the significant role of soil processes in biogeochemical cycles, especially the nitrogen cycle (Voigt et  
1733 al., 2016, Pärn et al., 2018). Knowledge of the soil microbiological composition and the effect of forest fires  
1734 have been improved (Köster et al., 2015, 2016, Zhang-Turpeinen et al., 2020), but further research is called  
1735 for vegetation changes influencing the below-ground microbiology, its composition and enzymatic activity  
1736 (Payne et al., 2016. Köster et al. 2016). The NDVI methods have made it possible to detect vegetation changes  
1737 (Miles and Esau 2016). A range of vegetation cover changes in Siberia have been reported, such as the Arctic  
1738 greening and browning processes, but e.g. the greening of Siberian cities remains an issue of intensive research  
1739 also in the future (Miles and Esau 2016, Miles et al., 2019).

1740 For the Atmospheric system, the recent progress in understanding the Northern Eurasian Arctic - boreal land  
1741 atmospheric system and the aspects of the megacity air quality (section 3.2) are dealing with atmospheric  
1742 composition changes (Q4), key feedbacks between climate and air quality (Q5), and synoptic scale weather  
1743 (Q6). Recent results demonstrate improved quantification of the carbon balance and CO<sub>2</sub> fluxes and  
1744 concentrations due to land use changes (Pulliainen et al., 2017, Karelin et al., 2017, Rakitin et al., 2018,  
1745 Skorokhod et al., 2017, Alekseychik et al. 2017), forest fires in Siberia, and new understanding of aerosol  
1746 sources and properties in the Arctic environment and across the Northern Eurasia. However, most of the results  
1747 deal with atmospheric aerosol chemistry and physics in boreal and Arctic environments originating from  
1748 measurements in the few flagship stations in Finland and Russia (Kerminen et al., 2018, Wiedensohler et al.,  
1749 2019, Freud et al., 2017, Paasonen et al., 2018, Östrom et al., 2017, Kalogridis et al., 2018, Bondur et al., 2016,  
1750 Bondur and Ginzburg 2016, Bondur et al., 2019 c,d, Bondur and Gordo, 2018; Mikhailov et al., 2017, Breider  
1751 et al., 2017), indicating the need for a comprehensive station network in the PEEX region. Black carbon emitted  
1752 by the Siberian forest fires and some other sources, and its long range transport to the Arctic, are also widely  
1753 discussed (Kalogridis et al., 2018, Bondur et al., 2016, Bondur and Ginzburg 2016, Mikhailov et al., 2017,  
1754 Breider et al., 2017, Shevchenko et al., 2015, Kononov et al., 2018, Marelle et al., 2018). In addition,  
1755 measurements of ozone in the troposphere and stratosphere have provided insight into atmospheric chemistry  
1756 in urban environments (Skorokhod et al., 2017), UV radiation and human health (Chubarova et al., 2019).  
1757 Environmental health, including the impacts of air quality (black carbon) and UV radiation, is foreseen as a  
1758 high momentum research topic in the PEEX domain, and further research is called for in this area.

1759

1760 The impact of air pollution was found to vary from serious effects on population health and ecosystem  
1761 processes to large-scale interactions with climate. We reported several new results on the dynamics between



1762 the haze pollution and boundary layer meteorology in enhancing air pollution in megacity environments (Zhao  
1763 et al., 2017, Ding et al., 2016a, Wang et al., 2018b, Bai et al., 2018a, Ye et al., 2017). The long-term and  
1764 comprehensive measurements carried out especially at the SORPES station in Nanjing provide valuable data  
1765 pools for such studies (Ding et al., 2016a). However, the backbone of the recent progress has been based on  
1766 improved on-line atmospheric measurements and the use of machine learning methods combined with different  
1767 methodologies, such as back trajectories together with the lidar and radiosonde data. In addition, improved  
1768 models of emission inventories together with the ECHAM-HAM and GAINS models have led to better  
1769 quantification of the aerosol number emissions. New knowledge has enabled introduction of new theoretical  
1770 arguments on the feedbacks between high aerosol concentration and the urban boundary layer (Petäjä et al.  
1771 2016). New measurements have also been obtained from Siberian cities (Elansky et al., 2016, Chubarova et  
1772 al., 2016a, Mahura et al., 2018). However, we are still in the early phase of having a holistic picture of large-  
1773 scale feedbacks due to the lack of long-term, comprehensive measurements in these regions.

1774

1775 Changes in the atmospheric dynamics in the North have potential impacts on short-term local/regional and sub  
1776 seasonal to seasonal large-scale weather predictions, and on long-term projections on biogeochemical systems.  
1777 It is therefore crucial to understand changes in boundary-layer processes as well as synoptic- and large-scale  
1778 circulation in the Arctic and Northern Eurasia. Recent results show potential, but causally arguable,  
1779 connections between the alarming sea ice decline, evaporation, cloudiness, atmospheric circulation and  
1780 moisture transport as well as Arctic and European winter temperatures (Nygård et al., 2019, Rinke et al., 2019,  
1781 McCusker et al., 2016, Mori et al., 2014, Blackport et al., 2019; Cohen et al., 2020). Further investigations are  
1782 called for atmosphere-ice-ocean interactions, coupling between small-scale processes (such as clouds and  
1783 turbulence) and synoptic-scale weather, as well as for polar prediction and extreme events. Furthermore, more  
1784 quantitative knowledge is needed on pan-Arctic energy budgets (Spengler et al., 2016). The urban heat island  
1785 (UHI) phenomena taking place in Arctic cities has received an increasing attention, and there is a special need  
1786 for improved forecasting services for Arctic cities (Miles and Esau 2017, Konstantinov et al., 2018, Varentsov  
1787 et al., 2018b).

1788

1789 For the Water system, we discussed the Arctic sea ice dynamics and thermodynamics, snow depth and sea ice  
1790 thickness, sea ice research supporting navigation, and rare elements in the snow and the ocean sediments,  
1791 especially from the perspective of improvements in the observation and modelling methods (Q7, section  
1792 3.3.1.). New evidence on atmosphere – Arctic sea ice interactions have been provided by Lei et al. (2018), and  
1793 Jakobson et al. (2019). Lei et al. (2018) analyzed how the climate warming would affect the winter growth  
1794 rate of thin and thick ice, and Jakobson et al. (2019) gave new insight into the relation between sea ice  
1795 concentration and the wind speed. Furthermore, advance has been made in understanding the thermodynamics  
1796 and metamorphosis of the snowpack on sea ice and their interactions with surface albedo changes (Dou et al.,  
1797 2019). Operational sea ice analysis is increasingly important for the Arctic shipping and navigation (Lei et al.,  
1798 2015, Karvonen et al., 2017). New results on rare elements, mineral composition and CO<sub>2</sub> and methane fluxes  
1799 associated with ocean sediments have been attained (Maslov, et al., 2018, Yasunaka et al., 2018). This serves



1800 as important information for mitigation plans, as well as for new estimates on the river runoff and discharge  
1801 in Russian rivers into the Arctic seas (Grigoriev and Frolova 2018, Agafonova et al., 2017).

1802

1803 The marine Arctic ecosystems are under a progressive increase of anthropogenic impacts, the main issues  
1804 calling for better understanding are the integrated effect of Arctic warming, and ice and snow melt, ocean  
1805 freshening, air quality and acidification of the Arctic marine ecosystems, primary production and carbon cycle  
1806 (Q8, section 3.3.2). Quantitative information about the CO<sub>2</sub> accumulation into the ocean is having a high  
1807 momentum. Marine organisms, such as coccolithophrip algae, are influencing the CO<sub>2</sub> flux exchange (Kondrik,  
1808 et al., 2018b, Pozdnyakov et al., 2017). In addition to changing marine environments, the Arctic – boreal lakes  
1809 and rivers may undergo changes in flooding, increasing the amount of fresh water and allochthonous materials  
1810 (Q9, section 3.3.3). In addition to the Arctic Ocean, the ice and snow conditions of Northern lakes are under  
1811 pressure. Lake Kilpisjärvi (Finland) (Arvola et al., 2017, Leppäranta et al., 2017) and Lake Ladoga (Russia)  
1812 (Karetnikov et al., 2017) have been under intensive research, and the recent results demonstrate changes in  
1813 heat fluxes, ice cover periods and stratification. The browning of lakes and lake sediments were discussed, and  
1814 new results were attained from the Selenga River of the Baikal Lake. Dramatically changes will be expected  
1815 in the water runoff and amount of dissolved modes of metals, also having serious impact on the environmental  
1816 health (Chalov et al., 2015, 2016, 2017 a, 2017b, Karthe et al., 2017 a, 2017b). As a comparison to the Northern  
1817 high latitudes, we also discussed freezing lakes in Central Asia, where the climate is cold and arid. There the  
1818 ice is typically snow-free or possesses only a thin snow cover, allowing penetration of sunlight into the water  
1819 body (Huang et al., 2019).

1820

1821 For the Societal system, the anthropogenic impact has been addressed as one of the main themes (Q10). The  
1822 discussion on the mitigation and adaptation, including the urban infrastructure design (Juhola 2018) and risk  
1823 assessment, were addressed in this context (section 3.4.1). In social transformations, a special attention was  
1824 given to one of the most important local livelihoods in Lapland: reindeer grazing and how it interacts with the  
1825 environment (Q11 section 3.4.2). The adaptive capacity of the Northern societies rest on their environment,  
1826 demographic structure and economic activities (Q12). Referring to the earlier statement about the future  
1827 research needs for the Atmospheric system with respect to environmental health, here again we would like to  
1828 put an increasing attention to environmental health under changing climate, including the spread of diseases  
1829 and air pollution and their combined effects (section 3.4.3.).

1830

1831 3.2 Feedback mechanisms under changing climate, cryosphere conditions and urbanization

1832

1833 During the recent years, Kulmala et al. (2004, 2020) have focused on the quantification of the Continental  
1834 Biosphere-Aerosol-Cloud-Climate (COBACC) feedback loop relevant to Northern Eurasia boreal region.  
1835 Previous results on the COBACC feedback loop are addressing the role of BVOC emission dynamics (Arneth  
1836 et al., 2016). Both higher temperatures and increased CO<sub>2</sub> concentrations are (separately) expected to increase  
1837 emissions of biogenic volatile organic compounds (BVOCs). It also seems that the GPP is controlled by the



1838 BVOC effects on the clouds. Sporre et al. (2019) used an Earth System model to estimate aerosol scattering  
1839 due to enhanced BVOC emissions and estimated the associated negative direct radiative effect ( $-0.06 \text{ W m}^{-2}$ ).  
1840 The total global radiative effect associated with this feedback was estimated to be  $-0.49 \text{ W m}^{-2}$  (Sporre et al.,  
1841 2019), indicating that it has the potential to offset about 13 % of the forcing associated with a doubling of  $\text{CO}_2$ .  
1842 The direct effect of aerosol on GPP due to an increase in the fraction of diffuse radiation was estimated between  
1843 6 and 14% increase in GPP at maximum observed aerosol loading compared to low aerosol loading in Northern  
1844 Eurasia forests (Ezhova et al., 2018b).

1845  
1846 The results from the Tibetan plateau demonstrate notable feedbacks between vegetation, BVOC emissions and  
1847 aerosols. Historical wetting of the TP region has increased the vegetation cover, allowing for feedback  
1848 processes via biogenic aerosol formation and aerosol-cloud-precipitation interactions. A significant wetting  
1849 trend since the early 1980s in Tibetan Plateau is most conspicuous in central and eastern Asia. Fang et al.  
1850 (2019) hypothesized that the current warming may enhance emissions of biogenic volatile organic compounds  
1851 (BVOC), which can increase secondary organic aerosols concentrations, contributing to the precipitation  
1852 increase. The wetting trend can increase the vegetation cover and has a positive feedback on the BVOC  
1853 emissions. The simulations suggest a significant contribution of increased BVOC emissions to the regional  
1854 organic aerosol mass and the simulated increase in BVOC emissions is significantly correlated with the wetting  
1855 trend in Tibetan Plateau.

1856  
1857 To estimate the net effects of various feedback mechanisms on land cover changes, photosynthetic activity,  
1858 GHG exchange, BVOC emissions, formation of aerosols and clouds, and radiative forcing (Q14) calls for  
1859 intensive collaboration and integration between the Arctic Ocean sciences and terrestrial sciences across the  
1860 Pan-Arctic domain and across the Arctic and high-latitude domain. The Arctic greening and browning (section  
1861 3.1.3.) call for a multi-disciplinary scientific approach, improved modelling tools and new data to deeply  
1862 understand the biosphere-atmosphere-anthroposphere interactions and feedbacks. Petäjä et al. (2020a, 2020b)  
1863 discussed the complexity of feedbacks, especially at the Arctic context, and the interplay between the  
1864 temperature, GHG, permafrost, land cover and water bodies and between photosynthetic activity, aerosols,  
1865 clouds and radiation budget. The current downturn of the arctic cryosphere (*section 3.1.2*), together with the  
1866 changes in sea ice dynamics and glaciers and the permafrost thawing, affects the marine and terrestrial carbon  
1867 cycles in interconnected ways (section 3.3.1). Parmentier et al. (2017) discussed the changing arctic cryosphere  
1868 and how the processes in the ocean and on land are too often studied as separate systems, although the sea ice  
1869 decline connects the rapid warming of the Arctic, Arctic Ocean marine processes and air–sea exchange of  $\text{CO}_2$ .  
1870 Thus, the future priorities would be on the development of our modelling tools towards all-scales modelling  
1871 approach to cover the feedbacks, processes and interactions at the land–ocean interface and also in urban  
1872 environments in the Arctic region. We also need to support the further development of the ground-based  
1873 observation networks.

1874



1875 3.3 Climate scenarios for the Arctic-boreal region

1876

1877 Climate scenarios set the urgency for the mitigation and adaptation actions for the Northern Eurasian region.  
1878 The Arctic-boreal region combines an area of both amplified climate change (Arctic amplification) and large  
1879 diversity in the model predictions (Collins et al., 2013, Hoegh-Guldberg et al., 2018). Under the “low-to-  
1880 medium” RCP4.5 forcing scenario (van Vuuren et al., 2011), the CMIP5 multi-model mean temperature  
1881 changes during the 21<sup>st</sup> century indicate the strongest winter-time warming of >5 °C in the Arctic Ocean,  
1882 whereas the majority of the terrestrial region will warm by 2–4 °C (Fig. 12). Even during summertime, the  
1883 continental warming over the region will generally exceed 2 °C. It is important to note that the diversity of  
1884 model projections is accentuated over the Arctic and Northern Eurasian domain: the mechanisms behind the  
1885 Arctic amplification are implemented in varying details in the distinct models, and the associated interactions  
1886 and feedback processes provide a diverse picture of the future in the Arctic-boreal regions.

1887

1888 In addition to considerable trends in atmospheric temperatures, the models further indicate prominent changes  
1889 in precipitation (Collins et al., 2013, Hoegh-Guldberg et al., 2018). For the Arctic boreal region, this is largely  
1890 depicted as an increasing rainfall during both winter and summer, extending to 15-25% over most of the  
1891 terrestrial domain over the winter and somewhat less during summer (Fig. 10). Contemporary warm Arctic  
1892 temperatures and large sea ice deficits (75% volume loss) demonstrate climate states outside our previous  
1893 experience. The modeled changes in the Arctic cryosphere demonstrate that even limiting the global  
1894 temperature increase to 2 °C will leave the Arctic a much different environment by mid-century, with less  
1895 snow and sea ice, melted permafrost, altered ecosystems, and a projected annual mean Arctic temperature  
1896 increase of +4 °C. Even under ambitious emission reduction scenarios, high-latitude land ice melt, including  
1897 Greenland, are foreseen to continue due to internal lags, leading to accelerating global sea level rise throughout  
1898 the century (Overland et al., 2019).

1899

1900 **4. CONCLUDING REMARKS**

1901

1902 Only the integration of different observing networks and programs into an inter-operable and integrated  
1903 observation system can provide data needed for understanding the mechanisms of the Arctic-boreal system.  
1904 There is a fundamental need for an integrated, comprehensive network of the-state-of-the art *in situ* stations  
1905 measuring Earth surface – atmosphere interactions (Kulmala et al., 2016a, 2018; Uttal et al., 2016; Hari et al.,  
1906 2016; Alekseychik et al., 2016; Vihma et al. 2019). The results obtained in the Pan Eurasian Experiment  
1907 (PEEX) programme in Russian and China introduced in this paper are based on a combination of long-term  
1908 observations and campaign data. In addition, the Arctic marine region require comprehensive observations and  
1909 subsequent synthesis, as these regions are under a lot of environmental stress. Therefore, we need more *in situ*  
1910 observations of the Arctic system covering the marine atmosphere, sea ice and ocean. However, there are  
1911 pronounced technological and logistical challenges to setup such continuous, marine *in situ* observations (e.g.  
1912 Vihma et al. 2019). Furthermore, improved monitoring is needed for river discharge and associated fluxes of



1913 greenhouse gases and other key compounds and more research on the understanding of coastal processes and  
1914 atmospheric transport and specific regional socioeconomic issues and their interactions with changing  
1915 environment (Vihma et al., 2019; Petäjä et al., 2020).

1916

1917 The international organizations and bodies like the Arctic Council (SAON's Roadmap for Arctic Observing  
1918 and Data Systems, ROADS), EU Horizon2020 (Blue Growth INTAROS and APPLICATE projects), GEO-  
1919 CRI (high Mountains and cold regions), the Belmont Forum COPERNICUS and WMO are coordinating  
1920 development of the Arctic data and services. New data products are expected from the large-scale MOSAiC  
1921 campaign and projects like ERA-PLANET iCUPE (Petäjä et al. 2020b) or ArcticFLUX to monitor interface  
1922 between the marine Arctic - Eurasian continent. Also, national-based Arctic observations and research  
1923 programs like AC<sup>3</sup> by German institutes play a significant role. Russia conducts extensive research in the  
1924 Arctic region, notably on the manned drifting ice stations. These Arctic observation activities are coordinated  
1925 and carried out by Roshydromet, universities and Russian Academy of Sciences' institutes.

1926

1927 Concerning global energy markets, the Arctic region holds 25 % or more of the world's undiscovered oil and  
1928 gas (Arctic Oil & Gas, 2008). The plans of China and Russia to build 'Ice Silk Road' along Northern Sea  
1929 linking the China and Russia to Europe is highlighting the polar region's growing economic and strategic  
1930 importance, and the increasing pressure on the Arctic environment and local communities. In addition, wide  
1931 regions of the high latitudes and Arctic regions are under the pressure of the changing economic activities of  
1932 the Arctic and are also under a high pressure of the changing environment and climate. A comprehensive  
1933 observation network providing in-situ data in close coordination with satellite observations and ground-based  
1934 remote sensing is required to monitor the environmental impacts of the envisioned operations.

1935

1936 Over the last few years, Earth system sciences is driven by the need to understand the scientific processes of  
1937 climate change and air quality, their interrelations with Earth system and their societal impacts. The interplay  
1938 between science, politics and business, and the analysis of the existing policies and strategies help us to  
1939 recognize and analyze new and emerging trends of Arctic governance (e.g. protection and resilience vis-a-vis  
1940 economic activities), geopolitics (e.g. state sovereignty vis-a-vis internationalization), geo-economics (e.g.  
1941 tourism vis-à-vis reindeer herding), and science (e.g. climate change). The intensive work towards the new  
1942 Arctic observations and data systems, together with the intensive observations on the land –atmosphere  
1943 interactions taking place at the high latitudes, will provide the baseline for cross disciplinary research era.  
1944 PEEX is aimed for these directions.

1945

#### 1946 **ACKNOWLEDGEMENTS**

1947

1948 We thank the following funding agencies and projects: Academy of Finland contracts: No 280700, 294600,  
1949 296302 (Novel Assessment of Black Carbon in the Eurasian Arctic: From Historical Concentrations and  
1950 Sources to Future Climate Impacts (NABCEA), 307331 (FCoE Atmospheric Sciences), 311932, 314798/99,



1951 315203, 317999, 337549 (Atmosphere and Climate Competence Center (ACCC), Jane and Aatos Erkko  
1952 Foundation, Russian Foundation for Basic Research (RFBR) projects No. 17-29-05027 (Selenga-Baikal river  
1953 system), 17-29-05102, 18-05-00306, 18-05-60037, 18-05-60219 (Arctic river), 18-35-20031, 18-44-860017,  
1954 18-45-700015, 18-05-60083 (Storm activity in the Barents Sea), 18-60084 (Dangerous impacts of large - scale  
1955 industrial emissions on aerosol pollution and Arctic ecosystem), 19-05-50088, 19-05-00352, 19-55-80021  
1956 (MOST and DST studies), the IAO SB RAS supported by RFBR project No. 19-05-50024, Russian Science  
1957 Foundation (RSF) projects No.17-17-01117, 18-17-00076 (Long-term measurement of aerosol chemical  
1958 composition in Central Siberia, 19-77-20109, 19-77-30004 (Moscow environment), 19-77-300-12  
1959 (Measurement networks and field sites in Kola Peninsula), Yugra State University grant No.13-01-20/39,  
1960 Ministry of Science and Higher Education of Russia - Agreement No.13.1902.21.0003, State assignment No.  
1961 0148-2019-0006, European Research Council (ERC) projects No. 742206 (ATM-GTP), No. 850614  
1962 (CHAPAs), EU Horizon 2020 projects No. 727890 (Integrated Arctic Observing System, INTAROS), 689443  
1963 (Integrative and Comprehensive Understanding on Polar Environments, iCUPE), 654109 (Aerosol Clouds and  
1964 Trace Gases Research Infrastructure, ACTRIS-2), EU7 FP MarcoPolo Grant No. 606953, Erasmus+ 561975-  
1965 EPP-1-2015-1-FI-EPPKA2-CBHE-JP, Norwegian Research Council and the Belmont Forum project SERUS,  
1966 No. 311986, National Natural Science Foundation of China Grant No. 41275137, ESA-MOST China Dragon  
1967 Cooperation projects No. 10663 and 32771 (Dragon 3 and 4).

1968

1969 Our special thanks also to Mrs. Alla Borisova, INAR, University of Helsinki, for the technical editing of the  
1970 manuscript.

1971

## 1972 REFERENCES

1973 Andreae, M. O., Andreae, T. W., and Ditas, F.: How frequent is new particle formation in the boundary layer  
1974 over the remote temperate/boreal forest?, AGU Fall Meeting, San Francisco, USA,  
1975 doi:10.1002/essoar.10501148.1, 2019.

1976 Aalto, J., Porcar-Castell, A., Atherton, J., Kolari, P., Pohja, T., Hari, P., Nikinmaa, E., Petäjä, T., and Bäck,  
1977 J.: Onset of photosynthesis in spring speeds up monoterpene synthesis and leads to emission bursts, *Plant,  
1978 Cell and Environment.*, 38, 2299-2312, 2015.

1979 Agafonova, S. A., Frolova, N. L., Surkova, G. V., and Koltermann, K., P.: Modern characteristics of the ice  
1980 regime of Russian Arctic rivers and their possible changes in the 21st century, *Geogr. Environ. Sustain.*,  
1981 10(4), 4-15, doi:10.24057/2071-9388-2017-10-4-4-15, 2017.

1982 Alekseychik, P., Lappalainen, H.K., Petäjä, T., Zaitseva, N., Heimann, M., Laurila, T., Lihavainen, H., Asmi,  
1983 E., Arshinov, M., Shevchenko, V., Makshtas, A., Dubtsov, S., Mikhailov, E., Lapshina, E., Kirpotin, S.,  
1984 Kurbatova, Y., Ding, A., Guo, H., Park, S., Lavric, J.V., Reum, F., Panov, A., Prokushkin, A., and Kulmala,  
1985 M.: Ground-based station network in Arctic and Subarctic Eurasia: An overview, *Geogr. Environ. Sustain.*,  
1986 9(2), 75-88, doi:10.24057/2071-9388-2016-9-2-19-35, 2016.



- 1987 Alekseychik, P., Mammarella, I., Karpov, D., Dengel, S., Terentieva, I., Sabrekov, A., Glagolev, M., and  
1988 Lapshina, E.: Net ecosystem exchange and energy fluxes measured with the eddy covariance technique in a  
1989 western Siberian bog, *Atmos. Chem. Phys.*, 17, 9333–9345, doi:10.5194/acp-17-9333-2017, 2017.
- 1990 AMAP, 2017: Arctic Pollution 2017. Arctic Monitoring and Assessment Programme (AMAP), Oslo,  
1991 Norway.
- 1992 Andreae, M. O.: Emission of trace gases and aerosols from biomass burning – an updated assessment,  
1993 *Atmos. Chem. Phys.*, 19, 8523-8546, doi:10.5194/acp-19-8523-2019, 2019.
- 1994 Arneth, A., Harrison, S., Zaehle, S., Tsigaridis, K., Menon, S., Bartlein, P. J., Feichter, J., Korhola, A.,  
1995 Kulmala, M., O'Donnell, D., Schurgers, G., Sorvari, S., and Vesala, T.: Terrestrial biogeochemical feedbacks  
1996 in the climate system. *Nature Geosci.*, 3, 525–532, <https://doi.org/10.1038/ngeo905>, 2010.
- 1997 Arneth, A., Makkonen, R., Olin, S., Paasonen, P., Holst, T., Kajos, M. K., Kulmala, M., Maximov, T.,  
1998 Miller, P. A., and Schurgers, G.: Future vegetation–climate interactions in Eastern Siberia: an assessment of  
1999 the competing effects of CO<sub>2</sub> and secondary organic aerosols, *Atmos. Chem. Phys.*, 16, 5243–5262,  
2000 doi:10.5194/acp-16-5243-2016, 2016.
- 2001 Arnold, S. R., Law, K. S., Brock, C. A., Thomas, J. L., Starkweather, S. M., von Salzen, K., Stohl, A.,  
2002 Sharma S., Lund, M. T., Flanner, M. G., Petaja, T., Tanimoto, H., Gamble, J., Dibb J. E., Melamed M.,  
2003 Johnson, N., Fidel, M., Tynkkynen, V.-P., Baklanov, A., Eckhardt, S., Monks, S. A., Browse, J., and Bozem,  
2004 H.: Arctic air pollution: Challenges and opportunities for the next decade, *Elementa: Science of the*  
2005 *Anthropocene*, 4:000104, <https://dx.doi.org/10.12952/journal.elementa.00010>. 2016.
- 2006 Arvola, L., Leppäranta, M., and Äijälä, C.: CDOM variations in Finnish lakes and rivers between 1913 and  
2007 2014, *Sci. Total Environ.*, 601, 1638-1648, doi:10.1016/j.scitotenv.2017.06.034, 2017.
- 2008 Arvola, L., Äijälä, C., and Leppäranta, M.: CDOM concentrations of large Finnish lakes relative to their  
2009 landscape properties, *Hydrobiologia*, 780(1), 37-46, doi:10.1007/s10750-016-2906-4, 2016.
- 2010 Asmi, E., Kondratyev, V., Brus, D., Laurila, T., Lihavainen, H., Backman, J., Vakkari, V., Aurela, M.,  
2011 Hatakka, J., Viisanen, Y., Uttal, T., Ivakhov, V., and Makshtas, A.: Aerosol size distribution seasonal  
2012 characteristics measured in Tiksi, Russian Arctic, *Atmos. Chem. Phys.*, 16, 1271–1287, doi:10.5194/acp-16-  
2013 1271-2016, 2016.
- 2014 Backman, J., Schmeisser, L., Virkkula, A., Ogren, J. A., Asmi, E., Starkweather, S., Sharma, S.,  
2015 Eleftheriadis, K., Uttal, T., Jefferson, A., Bergin, M., Makshtas, A., Tunved, P., and Fiebig, M.: On  
2016 Aethalometer measurement uncertainties and an instrument correction factor for the Arctic, *Atmos. Meas.*  
2017 *Tech.*, 10, 5039–5062, doi:10.5194/amt-10-5039-2017, 2017.
- 2018 Badina, S. V.: Socio-economic potential of municipalities in the context of natural risk (case study –  
2019 Southern Siberian regions), *IOP Conference Series: Earth and Environmental Science*, 190,  
2020 doi:10.1088/1755-1315/190/1/012001, 2018.



- 2021 Bai, J.H.: Estimation of the isoprene emission from the Inner Mongolia grassland, *Atmospheric Pollution*  
2022 *Research*, 6, 406-414, doi: 10.5094/APR.2015.045, 2015.
- 2023 Bai, J. H.: UV extinction in the atmosphere and its spatial variation in North China, *Atmos. Environ.*, 154,  
2024 318-330, doi:10.1016/j.atmosenv.2017.02.002, 2017a.
- 2025 Bai, J. H., Guenther, A., Turnipseed, A., Duhl, T., Greenberg J.: Seasonal and interannual variations in  
2026 whole-ecosystem BVOC emissions from a subtropical plantation in China. *Atmospheric Environment*, 161,  
2027 176-190. <http://dx.doi.org/10.1016/j.atmosenv.2017.05.002>, 2017b.
- 2028 Bai, J. H., de Leeuw, G., van der Ronald, A., De Smedt, I., Theys, N., Van Roozendael, M., Sogacheva, L.,  
2029 and Chai, W. H.: Variations and photochemical transformations of atmospheric constituents in North China,  
2030 *Atmos. Environ.*, 189, 213-226, doi:10.1016/j.atmosenv.2018.07.004, 2018a.
- 2031 Bai, Y., Zhang, J., Zhang, S., Yao, F., and Magliulo, V.: A remote sensing-based two-leaf canopy  
2032 conductance model: Global optimization and applications in modeling gross primary productivity and  
2033 evapotranspiration of crops, *Remote Sensing of Environment*, 215, 411-437, doi:10.1016/j.rse.2018.06.005,  
2034 2018b.
- 2035 Bai, J. H.: A calibration method of solar radiometers, *Atmos. Pollut. Res.*, 10(4), 1365-1373,  
2036 doi:10.1016/j.apr.2019.03.011, 2019.
- 2037 Baklanov, A., Mahura, A., Nazarenko, L., Tausnev, N., Kuchin, A., and Rigina, O.: *Atmospheric Pollution*  
2038 *and Climate Change in Northern Latitudes*, Russ. Acad. Sci., Apatity, Russia, 2012.
- 2039 Baklanov, A. A., Penenko, V. V., Mahura, A. G., Vinogradova, A. A., Elansky, N. F., Tsvetova, E. A.,  
2040 Rigina, O. Y., Maksimenkov, L. O., Nuterman, R. B., Pogarskii, F. A., and Zakey, A.: Aspects of  
2041 *Atmospheric Pollution in Siberia*, in *Regional Environmental Changes in Siberia and Their Global*  
2042 *Consequences*, edited by: Groisman P. Y., and Gutman, G., 303-346, Springer, Dordrecht, Netherlands,  
2043 2013.
- 2044 Baklanov, A., Molina, L.T., and Gauss, M.: Megacities, air quality and climate, *Atmospheric Environment*,  
2045 126, 235-249, <https://doi.org/10.1016/j.atmosenv.2015.11.059>, 2016.
- 2046 Baklanov, A., Smith Korsholm, U., Nuterman, R., Mahura, A., Nielsen, K. P., Sass, B. H., Rasmussen, A.,  
2047 Zakey, A., Kaas, E., Kurganskiy, A., Sørensen, B., and González-Aparicio, I.: Enviro-HIRLAM online  
2048 integrated meteorology-chemistry modelling system: strategy, methodology, developments and applications  
2049 (v7.2), *Geosci. Model Dev.*, 10, 2971-2999, <https://doi.org/10.5194/gmd-10-2971-2017>, 2017.
- 2050 Baklanov, A., Brunner, D., Carmichael, G., Flemming, J., Freitas, S., Gauss, M., Hov, O., R. Mathur, R.,  
2051 Schlünzen, K., Seigneur, C., and Vogel, B.: Key issues for seamless integrated chemistry-meteorology  
2052 modeling, *Bull. Amer. Meteor. Soc.*, doi:10.1175/BAMS-D-15-00166.1., 2018.



- 2053 Balch, W. M., Bates, N. R., Lam, P. J., Twining, B. S., Rosengard, S. Z., Bowler, B. C., and Rauschenberg,  
2054 S.: Factors regulating the Great Calcite Belt in the Southern Ocean, and its biogeochemical significance,  
2055 *Global Biogeochem. Cycles*, 30(8), 1124–1144, doi:10.1002/2016GB005414, 2016.
- 2056 Balch, W. M.: The ecology, biogeochemistry, and optical properties of coccolithophores, *Ann. Rev. Mar.*  
2057 *Sci.*, 109, 71–98, doi:10.1146/annurev-marine-121916-063319, 2018.
- 2058 Bartsch, A., Kumpula, T., Forbes, B.C. and Stammer F.: Detection of snow surface thawing and refreezing  
2059 in the Eurasian Arctic with QuikSCAT: implications for reindeer herding, *Ecol Appl.*, 20, 2346–58., doi:  
2060 10.1890/09-1927.1., 2010.
- 2061 Barreira, L. M. F., Duporté, G., Rönkkö, T., Parshintsev, J., Hartonen, K., Hyrsky, L., Heikkinen, E.,  
2062 Kulmala, M., and Riekkola, M.-L.: Field measurements of biogenic volatile organic compounds in the  
2063 atmosphere using solid-phase microextraction Arrow, *Atmos. Meas. Tech.*, 11, 881–893, 2018.
- 2064 Bashmachnikov, I.L., Yurova, A.Y., Bobylev, L.P., and Vesman, A. V.: Seasonal and Interannual Variations  
2065 of Heat Fluxes in the Barents Sea Region, *Izv., Atmos. Ocean. Phys.*, 54, 213–222,  
2066 doi:10.1134/S0001433818020032, 2018a.
- 2067 Bashmachnikov, I. L., Yurova, A.Y., Bobylev, L. P., Vesman, A.V.: Seasonal and interannual variations of  
2068 the heat fluxes in the Barents Sea region, *Izv. Atmos. Ocean. Phys.*, 54(2), 239–249,  
2069 doi:10.7868/S0003351518020149, 2018b.
- 2070 Beer, C., Reichstein, M., Tomelleri, E., Ciais, P., Jung, M., Carvalhais, N., Rödenbeck, C., Altaf Arain,  
2071 A., Baldocchi, D., Bonan, G.B., Bondeau, A., Cescatti, A., Lasslop, G., Lindroth, A., Lomas, M.,  
2072 Luysaert, S., Margolis, H., Oleson, K.W., Rouspard, O., Veenendaal, E., Viovy, N., Williams, C., F Ian  
2073 Woodward, F.I., and Papale, D.: Terrestrial gross carbon dioxide uptake: global distribution and covariation  
2074 with climate. *Science*, 329, 834–838, doi: 10.1126/science.1184984, 2010.
- 2075 Belikov, D., Arshinov, M., Belan, B., Davydov, D., Fofonov, A., Sasakawa, M., Machida, T.: Analysis of the  
2076 Diurnal, Weekly, and Seasonal Cycles and Annual Trends in Atmospheric CO<sub>2</sub> and CH<sub>4</sub> at Tower Network  
2077 in Siberia from 2005 to 2016, *Atmosphere*, 10 (11), 689, doi: 10.3390/atmos10110689, 2019.
- 2078 Berchet, A., Bousquet, P., Pison, I., Locatelli, R., Chevallier, F., Paris, J.-D., Dlugokencky, E. J., Laurila, T.,  
2079 Hatakka, J., Viisanen, Y., Worthy, D. E. J., Nisbet, E., Fisher, R., France, J., Lowry, D., Ivakhov, V., and  
2080 Hermansen, O.: Atmospheric constraints on the methane emissions from the East Siberian Shelf, *Atmos.*  
2081 *Chem. Phys.*, 16, 4147–4157, doi:10.5194/acp-16-4147-2016, 2016.
- 2082 Berezina, E., Moiseenko, K., Skorokhod, A., Elansky, N., Belikov, I., and Pankratova, N.: Isoprene and  
2083 monoterpenes over Russia and their impacts in tropospheric ozone formation, *Geogr., Environ., Sustain.*,  
2084 12(1), 63–74, doi:10.24057/2071-9388-2017-24, 2019.
- 2085 Bezuglaya, E. Y., Ed.: Air quality in largest cities of Russia for 10 years (1988–1997), Hydrometeoizdat, St.  
2086 Petersburg, Russia, 1999.



- 2087 Biskaborn, B. K., Smith, S. L., Noetzli, J., Matthes, H., Vieira, G., Streletskiy, D. A., Schoeneich, P.,  
2088 Romanovsky, V. E., Lewkowicz, A. G., Abramov, A., Allard, M., Boike, J., Cable, W. L., Christiansen, H.  
2089 H., Delaloye, R., Diekmann, B., Drozdov, D., Etzelmüller, B., Grosse, G., ... and Lantuit, H.: Permafrost is  
2090 warming at a global scale, *Nat. Commun.*, 10(1), 264, doi: 10.1038/s41467-018-08240-4, 2019.
- 2091 Blackport, R., Screen, J. A., van der Wiel, K., and Bintanja, R.: Minimal influence of reduced Arctic sea ice  
2092 on coincident cold winters in mid-latitudes, *Nat. Clim. Change*, 9, 697–704, doi: 10.1038/s41558-019-0551-  
2093 4, 2019.
- 2094 Bobylev, S.N., Chereshnya, O.Y., Kulmala, M., Lappalainen, H. K., Petäjä, T., Solov'eva, S.V., Tikunov,  
2095 V.S., and Tynkkynen, V.-P.: Indicators for digitalization of sustainable development goals in PEEEX  
2096 program, *J. Geogr. Sust.*, 11, 145-156, 2018.
- 2097 Boike, J., Nitzbon, J., Anders, K., Grigoriev, M., Bolshiyarov, D., Langer, M., Lange, S., Bornemann, N.,  
2098 Morgenstern, A., Schreiber, P., Wille, C., Chadburn, S., Gouttevin, I., Burke, E., and Kutzbach, L.: A 16-  
2099 year record (2002–2017) of permafrost, active-layer, and meteorological conditions at the Samoylov Island  
2100 Arctic permafrost research site, Lena River delta, northern Siberia: an opportunity to validate remote-sensing  
2101 data and land surface, snow, and permafrost models, *Earth Syst. Sci. Data*, 11, 261–299,  
2102 <https://doi.org/10.5194/essd-11-261-2019>, 2019.  
2103
- 2104 Bondur, G., and Vorobev, V. E.: Satellite Monitoring of Impact Arctic Regions, *Izv. Atmos. Ocean. Phys.*,  
2105 51, 949–968, doi: 10.1134/S0001433815090054, 2015.
- 2106 Bondur, V. G., and Ginzburg, A. S.: Emission of carbon-bearing gases and aerosols from natural fires on the  
2107 territory of Russia based on space monitoring, *Dokl. Earth Sci.*, 466(2), 148-152,  
2108 doi:10.1134/s1028334x16020045, 2016.
- 2109 Bondur, V. G.: Satellite monitoring of trace gas and aerosol emissions during wildfires in Russia. *Izv.*  
2110 *Atmos. Ocean. Phys.*, 52(9), 1078-1091, doi:10.1134/s0001433816090103, 2016.
- 2111 Bondur, V. G., Gordo, K. A., and Kladoy, V. L.: Spacetime distributions of wildfire areas and emissions of  
2112 carbon-containing gases and aerosols in northern eurasia according to satellite-Monitoring Data, *Izv. Atmos.*  
2113 *Ocean. Phys.*, 53(9), 859-874, doi:10.1134/s0001433817090055, 2017.
- 2114 Bondur, V. G. and Gordo, K. A.: Satellite Monitoring of Burned out Areas and Emissions of Harmful  
2115 Contaminants due to Forest and other Wildfires in Russia, *Izv., Atmos. Ocean. Phys.*, 54 (9),955–965, doi:  
2116 10.1134/S0001433818090104, 2018.
- 2117 Bondur V. G., Chimitdorzhiev T. N., Dmitriev A. V., and Dagurov P. N.: Otsenka prostranstvennoy  
2118 anizotropii neodnorodnostey lesnoy rastitelnosti pri razlichnykh azimutalnykh uglakh radarnogo  
2119 polyarimetricheskogo zondirovaniya (Spatial anisotropy assessment of the forest vegetation heterogeneity at



- 2120 various azimuth angles of the radar polarimetric sensing), *Issledovanie Zemli iz kosmosa*, Russia, 3, 92-103,  
2121 doi:10.31857/S0205-96142019392-103, 2019a.
- 2122 Bondur, V. G., Chimitdorzhiev, T. N., Dmitriev, A. V., Dagurov, P. N., Zakharov, A. I., and Zakharova, L.  
2123 N.: Metody radarnoj polyarimetrii dlya issledovaniya izmenenij mekhanizmov obratnogo rasseyaniya v  
2124 zonah opolznej na primere obrusheniya sklona berega reki Bureya (Using radar polarimetry to monitor  
2125 changes in backscattering mechanisms in landslide zones for the case study of the Bureya river bank  
2126 collapse), *Issledovanie Zemli iz kosmosa.*, Russia, 4, 3-17, doi:10.31857/S0205-9614201943-17, 2019b.
- 2127 Bondur, V. G., Tsidilina, M. N., and Cherepanova, E.V.: Satellite Monitoring of Wildfire Impacts on The  
2128 Conditions of Various Types of Vegetation Cover in The Federal Districts of the Russian Federation, *Izv.*  
2129 *Atmos. Ocean. Phys.*, 55 (9), 1238–1253, doi:10.1134/s000143381909010X, 2019 (c).
- 2130 Bondur, V. G., Tsidilina, M. N., Kladov, V. L., and Gordo, K. A.: Irregular Variability of Spatiotemporal  
2131 Distributions of Wildfires and Emissions of Harmful Trace Gases in Europe Based on Satellite Monitoring  
2132 Data // *Doklady Earth Sciences*, Vol. 485, Part 2, pp. 461–464, doi: 10.1134/S1028334X19040202, 2019(d).
- 2133 Bondur, V. G., Zakharova, L. N., and Zakharov, A. I.: Monitoring of the landslide area state on Bureya river  
2134 in 2018-2019 according to radar and optical satellite images, *Issledovanie Zemli iz kosmosa*, Russia, No. 6,  
2135 26-35, doi:10.31857/S0205-96142019626-35, 2019(e).
- 2136 Bondur, V. G., Zakharova, L. N., Zakharov, A. I., Chimitdorzhiev, T. N., Dmitriev, A. V., and Dagurov,  
2137 P.N.: Monitoring of landslide processes by means of L-band radar interferometric observations: Bureya river  
2138 bank caving case // *Issledovanie Zemli iz kosmosa*, Russia, No. 5, 3-14, DOI:  
2139 <https://doi.org/10.31857/S0205-9614201953-14>. 2019 (f).
- 2140 Bondur, V. G., Tsidilina, M. N., and Kladov, V. L.: Irregular Variability of Spatiotemporal Distributions of  
2141 Wildfires and Emissions of Harmful Trace Gases in Europe Based on Satellite Monitoring Data, *Dokl. Earth*  
2142 *Sc.*, 485, 461–464, <https://doi.org/10.1134/S1028334X19040202>, 2019.
- 2143 Bondur, V. G., Mokhov, I. I., Voronova, O. S., and Sitnov, S. A.: Satellite Monitoring of Siberian Wildfires  
2144 and Their Effects: Features of 2019 Anomalies and Trends of 20-Year Changes, *Doklady Earth Sciences*,  
2145 492, 1, 370–375. doi: 10.1134/S1028334X20050049, 2020.
- 2146 Bormann, K. J., Brown, R. D., Derksen, C., and Painter, T. H.: Estimating snow-cover trends from space,  
2147 *Nat. Clim. Chang.*, 8, 924-928, 2018.
- 2148 Boy, M., Thomson, E. S., Acosta Navarro, J.-C., Arnalds, O., Batchvarova, E., Bäck, J., Berninger, F., Bilde,  
2149 M., Brasseur, Z., Dagsson-Waldhauserova, P., Castarède, D., Dalirian, M., de Leeuw, G., Dragosics, M.,  
2150 Duplissy, E.-M., Duplissy, J., Ekman, A. M. L., Fang, K., Gallet, J.-C., Glasius, M., Gryning, S.-E., Grythe,  
2151 H., Hansson, H.-C., Hansson, M., Isaksson, E., Iversen, T., Jonsdottir, I., Kasurinen, V., Kirkevåg, A.,  
2152 Korhola, A., Krejci, R., Kristjansson, J. E., Lappalainen, H. K., Lauri, A., Leppäranta, M., Lihavainen, H.,  
2153 Makkonen, R., Massling, A., Meinander, O., Nilsson, E. D., Olafsson, H., Pettersson, J. B. C., Prisle, N. L.,



- 2154 Riipinen, I., Roldin, P., Ruppel, M., Salter, M., Sand, M., Seland, Ø., Seppä, H., Skov, H., Soares, J., Stohl,  
2155 A., Ström, J., Svensson, J., Swietlicki, E., Tabakova, K., Thorsteinsson, T., Virkkula, A., Weyhenmeyer, G.  
2156 A., Wu, Y., Zieger, P., and Kulmala, M.: Interactions between the atmosphere, cryosphere, and ecosystems  
2157 at northern high latitudes, *Atmos. Chem. Phys.*, 19, 2015–2061, <https://doi.org/10.5194/acp-19-2015-2019>,  
2158 2019.
- 2159 Breider, T.J., Mickley, L.J., Jacob, D.J., Ge, C., Wang, J., Sulprizio, M.P., Croft, B., Ridley, D.A.,  
2160 McConnell, J.R., Sharma, S., Husain, L., Dutkiewicz, V. A., Eleftheriadis, K., Skov, H., and Hopke, P. K.:  
2161 Multidecadal trends in aerosol radiative forcing over the Arctic: Contribution of changes in anthropogenic  
2162 aerosol to Arctic warming since 1980, *J. Geophys. Res.: Atmos.*, 122, 3573-3594,  
2163 <https://doi.org/10.1002/2016JD025321>, 2017.
- 2164 Burkhard, B., Kroll, F., Müller, F., and Windhorst, W. F., Landscapes' Capacities to Provide Ecosystem  
2165 Services – a Concept for Land-Cover Based Assessments, *Landscape Online* 15(1), 1-12, DOI:  
2166 10.3097/LO.200915, 2009.
- 2167 Chalov, S. R., Jarsjo, J., Kasimov, N. S., Romanchenko, A. O., Pietron, J., Thorslund, J., and Promakhova,  
2168 E. V.: Spatio-temporal variation of sediment transport in the Selenga River Basin, Mongolia and Russia,  
2169 *Environ. Earth Sci.*, 73(2), 663-680, doi:10.1007/s12665-014-3106-z, 2015.
- 2170 Chalov, S. R., Bazilova, V. O., and Tarasov, M. K.: Modelling suspended sediment distribution in the  
2171 Selenga River Delta using LandSat data, in *Integrating Monitoring and Modelling for Understanding,  
2172 Predicting and Managing Sediment Dynamics*, edited by: Collins, A., Stone, M., Horowitz, A., and Foster, I.,  
2173 Copernicus Gesellschaft, Gottingen, Germany, 375, 19-22, 2017a.
- 2174 Chalov, S., Thorslund, J., Kasimov, N., Aybultatov, D., Ilyicheva, E., Karthe, D., Kositsky, A., Lychagin,  
2175 M., Nittrouer, J., Pavlov, M., Pietron, J., Shinkareva, G., Tarasov, M., Garmayev, E., Akhtman, Y., and Jarsjö,  
2176 J.: The Selenga River delta: a geochemical barrier protecting Lake Baikal waters, *Regional Environ. Change*,  
2177 17, 2039-2053, doi: 10.1007/s10113-016-0996-1, 2017b.
- 2178 Chalov, S. R., Millionshchikova, T. D., and Moreido, V. M.: Multi-Model Approach to Quantify Future  
2179 Sediment and Pollutant Loads and Ecosystem Change in Selenga River System, *Water Resour.*, 45, S22-S34,  
2180 doi:10.1134/s0097807818060210, 2018.
- 2181 Che, Y., Xue, Y., Mei, L., Guang, J., She, L., Guo, J., Hu, Y., Xu, H., He, X., Di, A., and Fan, C.: Technical  
2182 note: Intercomparison of three AATSR Level 2 (L2) AOD products over China, *Atmos. Chem. Phys.*, 16,  
2183 9655–9674, <https://doi.org/10.5194/acp-16-9655-2016>, 2016.
- 2184 Cheng, Y., Cheng, B., Zheng, F., Vihma, T., Kontu, A., Yang, Q. and Liao, Z.: Air/snow, snow/ice and  
2185 ice/water interfaces detection from high-resolution vertical temperature profiles measured by ice mass-  
2186 balance buoys on an Arctic lake. *Annals of Glaciology*, accepted (2020).



- 2187 Chernokulsky, A. V., Esau, I., Bulygina, O. N., Davy, R., Mokhov, II, Outten, S., and Semenov, V. A.:  
2188 Climatology and interannual variability of cloudiness in the Atlantic Arctic from surface observations since  
2189 the late nineteenth century, *J. Clim.*, 30(6), 2103-2120, doi:10.1175/jcli-d-16-0329.1, 2017.
- 2190 Chernokulsky, A., and Esau, I.: Cloud cover and cloud types in the Eurasian Arctic in 1936–2012. *Int. J.*  
2191 *Climatol.*, 39(15), 5771–5790, <https://doi.org/10.1002/joc.6187>, 2019
- 2192 Chu, B., Kerminen, V.-M., Bianchi, F., Yan, C., Petäjä, T. and Kulmala, M.: Atmospheric new particle  
2193 formation in China, *Atmos. Chem. Phys.*, 19, 115-138, 2019.
- 2194 Chubarova, N. Y., Poliukhov, A. A., and Gorlova, I. D.: Long-term variability of aerosol optical thickness in  
2195 Eastern Europe over 2001–2014 according to the measurements at the Moscow MSU MO AERONET site  
2196 with additional cloud and NO<sub>2</sub> correction, *Atmos. Meas. Tech.*, 9, 313–334, [https://doi.org/10.5194/amt-9-](https://doi.org/10.5194/amt-9-313-2016)  
2197 313-2016, 2016a.
- 2198 Chubarova, N., Zhdanova, Y., and Nezval, Y.: A new parameterization of the UV irradiance altitude  
2199 dependence for clear-sky conditions and its application in the on-line UV tool over Northern Eurasia, *Atmos.*  
2200 *Chem. Phys.*, 16, 11867–11881, <https://doi.org/10.5194/acp-16-11867-2016>, 2016b.
- 2201 Chubarova, N. E., Pastukhova, A. S., and Galin, V. Y.: Long-Term Variability of UV Irradiance in the  
2202 Moscow Region according to Measurement and Modeling Data, *Izv. Atmos. Ocean. Phys.*, 54, 139–146,  
2203 <https://doi.org/10.1134/S0001433818020056>, 2018.
- 2204 Chubarova, N. E., Androsova, E. E., Kirsanov, A. A., Vogel, B., Vogel, H., Popovicheva, O. B., and Rivin,  
2205 G. S.: Aerosol and Its Radiative Effects during the Aeroradcity 2018 Moscow Experiment, *Geography,*  
2206 *Environment, Sustainability*, 12, 114-131, <https://doi.org/10.24057/2071-9388-2019-72> 2019a.
- 2207 Chubarova, N. E., Timofeev, Y. M., Virolainen, Y. A., and Polyakov, A. V.: Estimates of UV indices during  
2208 the periods of reduced ozone content over Siberia in Winter-Spring 2016, *Atmos. Oceanic Opt.*, 32, 177-179,  
2209 doi:10.1134/s1024856019020040, 2019b.
- 2210 Chubarova, N. E., Pastukhova, A.S., Zhdanova, E.Y., Volpert, E.V., Smyshlyaev and S.P., and Galin, V.Y.:  
2211 Effects of Ozone and Clouds on Temporal Variability of Surface UV Radiation and UV Resources over  
2212 Northern Eurasia Derived from Measurements and Modeling., *Atmosphere*, 11, 59, 2020.
- 2213 Cohen, J., X. Zhang, T., Jung, R. Kwok, J., Overland, T., Ballinger, U.S., Bhatt, H. W., Chen, D., Coumou,  
2214 S., Feldstein, H., Gu, D., Handorf, G., Henderson, M., Ionita, M., Kretschmer, F., Laliberte, S., Lee, H. W.,  
2215 Linderholm, W., Maslowski, Y., Peings, K., Pfeiffer, I., Rigor, T., Semmler, J., Stroeve, P.C., Taylor, S.,  
2216 Vavrus, T., Vihma, S., Wang, M., Wendisch, Y., Wu, and Yoon, J.: Divergent consensus on Arctic  
2217 amplification influence on midlatitude severe winter weather. *Nature Climate Change*, 10, 20-29,  
2218 doi:10.1038/s41558-019-0662-y, 2020.
- 2219 Collins, M., Knutti, R., Arblaster, J., Dufresne, J.-L., Fichefet, T., Friedlingstein, P., Gao, X., Gutowski,  
2220 W.J., Johns, T., Krinner, G., Shongwe, M., Tebaldi, C., Weaver, A.J., and Wehner, M.: Long-term climate



- 2221 change: Projections, commitments and irreversibility, in *Climate Change 2013: The Physical Science Basis.*  
2222 *Contribution of Working Group I to the Fifth Assessment Report of the Intergovernmental Panel on Climate*  
2223 *Change*, edited by: Stocker, T.F., Quin, D., Plattner, G.-K., Tignor, M., Allen, S.K., Doschung, J., Nauels,  
2224 A., Xia, Y., Bex, V., and Midgley, P.M., Cambridge University Press, Cambridge, United-Kingdom, 1029-  
2225 1136, doi:10.1017/CBO9781107415324.024, 2013.
- 2226 Commane, R., Lindaas, J., Benmergui, J., Luus K. A., Chang, R. Y.-W., Daube, B. C., Euskirchen, E. S.,  
2227 Henderson, J. M., Karion, A., Miller, J. B., Miller, S. M., Parazoo, N. C., Randerson, J. T., Sweeney, C.,  
2228 Tans, P., Thoning, K., Veraverbeke, S., Miller, C. E., and Wofsy, S. C.: Carbon dioxide sources from Alaska  
2229 driven by increasing early winter respiration from Arctic tundra, *PNAS*, 114(21), 5361-5366, 2017.
- 2230 Coumou, C., Petoukhov, V., Rahmstorf, S., Petri, S., and Schellnhuber, H.-J.: Quasi-resonant circulation  
2231 regimes and hemispheric synchronization of extreme weather in boreal summer, *Proc. Natl. Acad. Sci.*, 111,  
2232 12 331–12336, <https://doi.org/10.1073/pnas.1412797111>, 2014.
- 2233 Dada, L., Paasonen, P., Nieminen, T., Buenrostro Mazon, S., Kontkanen, J., Peräkylä, O., Lehtipalo, K.,  
2234 Hussein, T., Petäjä, T., Kerminen, V.-M., Bäck, J. and Kulmala, M.: Long-term analysis of clear-sky new  
2235 particle formation events and nonevents in Hyytiälä, *Atmos. Chem. Phys.*, 17, 6227-6241, 2017.
- 2236 Dada, L., Chellapermal, R., Buenrostro Mazon, S., Paasonen, P., Lampilahti, J., Manninen, H. E., Junninen,  
2237 H., Petäjä, T., Kerminen, V.-M., and Kulmala, M.: Refined classification and characterization of atmospheric  
2238 new-particle formation events using air ions, *Atmos. Chem. Phys.*, 18, 17883–17893,  
2239 <https://doi.org/10.5194/acp-18-17883-2018>, 2018.
- 2240 Dagsson-Waldhauserova, P., Meinander, O.: Atmosphere-cryosphere interaction in the Arctic, at high  
2241 latitudes and mountains with focus on transport, deposition and effects of dust, black carbon, and other  
2242 aerosols., *Front. Earth Sci.*, 7, 337, <https://www.frontiersin.org/articles/10.3389/feart.2019.00337/full>, 2019.
- 2243 Davy, R., and Esau, I.: Differences in the efficacy of climate forcings explained by variations in atmospheric  
2244 boundary layer depth, *Nat. Commun.*, 7, 8, doi:10.1038/ncomms11690, 2016.
- 2245 Davy, R., Esau, I., Chernokulsky, A., Outten, S., and Zilitinkevich, S.: Diurnal asymmetry to the observed  
2246 global warming, *Int. J. Climatol.*, 37, 79-93, doi:10.1002/joc.4688, 2017.
- 2247 Dean, J. F., Middelburg, J. J., Röckmann, T., Aerts, R., Blauw, L. G., Egger, M., Jetten, M. S. M., de Jong,  
2248 A. E. E., Meisel, O. H., Rasigraf, O., Slomp, C. P., in't Zandt, M. H., and Dolman, A. J.: Methane feedbacks  
2249 to the global climate system in a warmer world, *Rev. Geophys.*, 56(1), 207-250,  
2250 <https://doi.org/10.1002/2017RG00055>, 2018.
- 2251 Derksen, C., and Brown, R.: Spring snow cover extent reductions in the 2008-2012 period exceeding climate  
2252 model predictions, *Geophys. Res. Lett.*, 39, L19504, 2012.



- 2253 Derome, J., and Lukina, N.: Interaction between environmental pollution and land-cover/land-use change in  
2254 Arctic areas, in: Eurasian Arctic Land Cover and Land Use in a Changing Climate, edited by: Gutman, G.,  
2255 and Reissell, A., 6, 269–290, Springer, Amsterdam, Netherlands, 2011.
- 2256 Ding, A. J., Huang, X., Nie, W., Sun, J. N., Kerminen, V.-M., Petäjä, T., Su, H., Chen, Y. F., Yang, X.-Q.,  
2257 Wang, M. H., Chi, X. G., Wang, J. P., Virkkula, A., Guo, W. D., Yuan, J., Wang, S. Y., Zhang, R. J., Wu, Y.  
2258 F., Song, Y. Zhu, T., Zilitinkevich, S., Kulmala, M., and Fu, C. B.: Enhanced haze pollution by black carbon  
2259 in megacities in China, *Geophys. Res. Lett.*, 43, 2873–2879, doi:10.1002/2016GL067745, 2016a.
- 2260 Ding, A. J., Nie, W., Huang, X., Chi, X., Sun, J., Kerminen, V.-M., Xu, Z., Guo, W., Petäjä, T., Yang, X.,  
2261 Kulmala, M., and Fu, G.: Long-term observation of pollution-weather/climate interactions at the SORPES  
2262 station: a review and outlook, *Front. Environ. Sci. Eng.*, 10, doi:10.1007/s11783-016-0877-3, 2016b.
- 2263 Dou, T., Xiao, C., Liu, J., Han, W., Du, Z., Mahoney, A. R., Jones, J., and Eicken, H.: A key factor initiating  
2264 surface ablation of Arctic sea ice: earlier and increasing liquid precipitation, *The Cryosphere*, 13, 1233–  
2265 1246, <https://doi.org/10.5194/tc-13-1233-2019>, 2019.
- 2266 Dragosics, M., Meinander, O., Jonsdottir, T., Durig, T., De Leeuw, G., Palsson, F., Dagsson-Waldhauserová,  
2267 P., and Thorsteinsson, T.: Insulation effects of Icelandic dust and volcanic ash on snow and ice, *Arab. J.*  
2268 *Geosci.*, 9, 126, DOI:10.1007/s12517-015-2224-6, 2016.
- 2269 Duporte, G., Parshintsev, J., Barreira, L. M. F., Hartonen, K., Kulmala, M., and Riekkola, M. L.: Nitrogen-  
2270 containing low volatile compounds from pinonaldehyde-dimethylamine reaction in the atmosphere: a  
2271 laboratory and field study, *Environ. Sci. Technol.*, 50(9), 4693–4700, doi:10.1021/acs.est.6b00270, 2016.
- 2272 Durairaj, P., Sarangi, R., Ramalingam, S., Thirunavukarassu, T., and Chauhan, P.: Seasonal nitrate  
2273 algorithms for nitrate retrieval using OCEANSAT-2 and MODIS-AQUA satellite data, *Environ. Monit.*  
2274 *Assess.*, 187, 176–189, doi: 10.1007/s10661-015-4340-x, 2015.
- 2275 Dyukarev, E.A., Godovnikov, E.A., Karpov, D.V., Kurakov, S.A., Lapshina, E.D., Filippov, I.V., Filippova,  
2276 N.V., and Zarov, E.A.: Net ecosystem exchange, gross primary production and ecosystem respiration in  
2277 ridge-hollow complex at Mukhrino Bog, *Geography, Environment, Sustainability*, 12(2), 227–244,  
2278 doi.10.24057/2071-9388-2018-77, 2019.
- 2279 Elansky, N. F., Lavrova, O. V., Skorokhod, A. I., and Belikov, I. B.: Trace gases in the atmosphere over  
2280 Russian cities, *Atmos. Environ.*, 143, 108–119, doi:10.1016/j.atmosenv.2016.08.046, 2016.
- 2281 Esau, I., Miles, V. V., Davy, R., Miles, M. W., and Kurchatova, A.: Trends in normalized difference  
2282 vegetation index (NDVI) associated with urban development in northern West Siberia, *Atmos. Chem. Phys.*,  
2283 16, 9563–9577, <https://doi.org/10.5194/acp-16-9563-2016>, 2016.
- 2284 Esau, I., Varentsov, M., Laruelle, M., Miles, M. W., Konstantinov, P., Soromotin, A., Baklanov, A. A., and  
2285 Miles, V. V.: Warmer Climate of Arctic Cities, Chapter 3 in the monography “The Arctic: Current Issues and



- 2286 Challenges”, Edited by: Pokrovsky, O., NOVA Publishers, ISBN: 978-1-53617-306-2,  
2287 <https://novapublishers.com/shop/the-arctic-current-issues-and-challenges/>, 2020.
- 2288 Euskirchen, E. S., Bret-Harte, M. S., Shaver, G. R., Edgar, C. W., and Romanovsky, V. E.: Long-term  
2289 release of carbon dioxide from arctic tundra ecosystems in northern Alaska, *Ecosystems*, 1–15, 2017.
- 2290 Evangeliou, N., Shevchenko, V. P., Yttri, K. E., Eckhardt, S., Sollum, E., Pokrovsky, O. S., Kobelev, V. O.,  
2291 Korobov, V. B., Lobanov, A. A., Starodymova, D. P., Vorobiev, S. N., Thompson, R. L., and Stohl, A.:  
2292 Origin of elemental carbon in snow from western Siberia and northwestern European Russia during winter–  
2293 spring 2014, 2015 and 2016, *Atmos. Chem. Phys.*, 18, 963–977, <https://doi.org/10.5194/acp-18-963-2018>,  
2294 2018.
- 2295 Ezhova, E., Kerminen, V.-M., Lehtinen, K. E. J., and Kulmala, M.: A simple model for the time evolution of  
2296 the condensation sink in the atmosphere for intermediate Knudsen numbers, *Atmos. Chem. Phys.*, 18, 2431–  
2297 2442, <https://doi.org/10.5194/acp-18-2431-2018>, 2018a.
- 2298 Ezhova, E., Ylivinkka, I., Kuusk, J., Komsaare, K., Vana, M., Krasnova, A., Noe, S., Arshinov, M., Belan,  
2299 B., Park, S.-B., Lavrič, J. V., Heimann, M., Petäjä, T., Vesala, T., Mammarella, I., Kolari, P., Bäck, J.,  
2300 Rannik, Ü., Kerminen, V.-M., and Kulmala, M.: Direct effect of aerosols on solar radiation and gross  
2301 primary production in boreal and hemiboreal forests, *Atmos. Chem. Phys.*, 18, 17863–17881,  
2302 <https://doi.org/10.5194/acp-18-17863-2018>, 2018b.
- 2303 Fang, K., Makkonen, R., Guo, Z., and Seppä, H.: An increase in the biogenic aerosol concentration as a  
2304 contributing factor to the recent wetting trend in Tibetan Plateau. *Sci Rep* 5, 14628,  
2305 <https://doi.org/10.1038/srep14628>, 2015.
- 2306 Fang, Y., Changyou, L., Leppäranta, M., Xiaonghong, S., Shengnan, Z., and Chengfu, Z.: Notable increases  
2307 in nutrient concentrations in a shallow lake during seasonal ice growth, *Water Science and Technology*,  
2308 74(12), 2773–2783, 2016.
- 2309 Fang, K., Makkonen, R., Guo, Z., Zhao, Y., and Seppä, H.: An increase in the biogenic aerosol  
2310 concentration as a contributing factor to the recent wetting trend in Tibetan Plateau, *Scientific Reports*, 5,  
2311 14628, DOI: 10.1038/srep14628, 2015.
- 2312 Fletcher, S. E. M., and Schaefer, H.: Rising methane: a new climate challenge, *Science*, 364, 932–933, 2019.
- 2313 Franz, D., Mammarella, I., Boike, J., Kirillin, G., Vesala, T., Bornemann, N., Larmanou, E., Langer, M., and  
2314 Sachs, T.: Lake-Atmosphere Heat Flux Dynamics of a Thermokarst Lake in Arctic Siberia, *J. Geophys. Res.:*  
2315 *Atmos.*, 123(10), 5222–5239, doi:10.1029/2017jd027751, 2018.
- 2316 Freud, E., Krejci, R., Tunved, P., Leaitch, R., Nguyen, Q. T., Massling, A., Skov, H., and Barrie, L.: Pan-  
2317 Arctic aerosol number size distributions: seasonality and transport patterns, *Atmos. Chem. Phys.*, 17, 8101–  
2318 8128, <https://doi.org/10.5194/acp-17-8101-2017>, 2017.



- 2319 Frolova, N.L., Belyakova, P.A., Grigoriev, V.Y. *et al.* : Runoff fluctuations in the Selenga River Basin, Reg  
2320 Environ Change, 17, 1965–1976, [doi.org/10.1007/s10113-017-1199-0](https://doi.org/10.1007/s10113-017-1199-0), 2017.
- 2321
- 2322 Fu, B. J., and Forsius, M.: Ecosystem services modeling in contrasting landscapes, Landscape Ecol., 30(3),  
2323 375-379, doi:10.1007/s10980-015-0176-6, 2015.
- 2324 Garmaev, E. Z., Kulikov, A. I., Tsydypov, B. Z., Sodnomov, B. V., and Ayurzhanayev, A. A.: Environmental  
2325 Conditions Of Zakamensk Town (Dzhida River Basin Hotspot), Geography, Environment,  
2326 Sustainability, 12(3), 224-239, <https://doi.org/10.24057/2071-9388-2019-32>, 2019.
- 2327 Georgiadi, A. G., Koronkevich, N. I., Milyukova, I. P., and Barabanova, E. A.: Integrated projection for  
2328 runoff changes in large Russian river basins in the XXI Century, Geography, Environment, Sustainability,  
2329 9(2), 38-46, 2016.
- 2330 GGO: Air quality in cities of Russia during the year 2015, St. Petersburg, Voeikov Main Geophysical  
2331 Observatory, RosHydroMet, 2016.
- 2332 Giamarelou, M., Eleftheriadis, K., Nyeki, S., Tunved, P., Torseth, K., and Biskos, G.: Indirect evidence of  
2333 the composition of nucleation mode atmospheric particles in the high Arctic, J. Geophys. Res.: Atmos.,  
2334 121(2), 965-975, doi:10.1002/2015jd023646, 2016.
- 2335 Gil, J., Pérez, T., Boering, K., Martikainen, P. J., and Biasi, C.: Mechanisms responsible for high N<sub>2</sub>O  
2336 emissions from subarctic permafrost peatlands studied via stable isotope techniques, Global Biogeochem.  
2337 Cycles, 31(1), 172, doi:10.1002/2015GB005370, 2017.
- 2338 Glagolev, M.V., Ilyasov, D. V. I., Terentjeva, E., Sabrekov, A. F., Yu Mochenov, S., and Maksutov, S. S.:  
2339 Methane and carbon dioxide fluxes in the waterlogged forests of south and middle taiga of Western Siberia,  
2340 IOP Conf. Ser.: Earth Environ. Sci., 138 012005, 2018.
- 2341 Gnatiuk, N., Radchenko, I., Davy, R., Morozov E., and Bobylev, L.: Simulation of factors affecting  
2342 *Emiliana huxleyi* blooms in Arctic and sub-Arctic seas by CMIP5 climate models: model validation and  
2343 selection, Biogeosciences, 17, 1199–1212. doi: 10.5194/bg-17-1199-2020, 2020.
- 2344 Godrijan, J., Drapeau, D., and Balch, W. M.: Mixotrophic uptake of organic compounds by coccolithophores,  
2345 Limnol. Ocean., Early bird publication, <https://doi.org/10.1002/lno.11396>, 2020.
- 2346 Gordov, E.P., Okladnikov, I.G., Titov, A.G., Voropay N.N., Ryazanova A.A., and Lykosov V.N.:  
2347 Development of Information-computational Infrastructure for Modern Climatology, Russ. Meteorol. Hydrol.,  
2348 43, 722–728, <https://doi.org/10.3103/S106837391811002X>, 2018.
- 2349 Granath, G., Rydin, H., Baltzer, J. L., Bengtsson, F., Boncek, N., Bragazza, L., Bu, Z.-J., Caporn, S. J. M.,  
2350 Dorrepaal, E., Galanina, O., Gałka, M., Ganeva, A., Gillikin, D. P., Goia, I., Goncharova, N., Hájek, M.,  
2351 Haraguchi, A., Harris, L. I., Humphreys, E., Jiroušek, M., Kajukało, K., Karofeld, E., Koronatova, N. G.,



- 2352 Kosykh, N. P., Lamentowicz, M., Lapshina, E., Limpens, J., Linkosalmi, M., Ma, J.-Z., Mauritz, M., Munir,  
2353 T. M., Natali, S. M., Natcheva, R., Noskova, M., Payne, R. J., Pilkington, K., Robinson, S., Robroek, B. J.  
2354 M., Rochefort, L., Singer, D., Stenøien, H. K., Tuittila, E.-S., Vellak, K., Verheyden, A., Waddington, J. M.,  
2355 and Rice, S. K.: Environmental and taxonomic controls of carbon and oxygen stable isotope composition in  
2356 Sphagnum across broad climatic and geographic ranges, *Biogeosciences*, 15, 5189–5202,  
2357 <https://doi.org/10.5194/bg-15-5189-2018>, 2018.
- 2358 Grigoriev, V. Y., and Frolova, N. L.: Terrestrial water storage change of European Russia and its impact on  
2359 water balance, *Geography, Environment, Sustainability*, 11(1), 38-50. [https://doi.org/10.24057/2071-9388-](https://doi.org/10.24057/2071-9388-2018-11-1-38-50)  
2360 [2018-11-1-38-50](https://doi.org/10.24057/2071-9388-2018-11-1-38-50), 2018.
- 2361 Groundstroem, F., and Juhola, S.: A framework for identifying cross-border impacts of climate change on  
2362 the energy sector, *Environment Systems and Decisions*, 39(1), 3-15, doi:10.1007/s10669-018-9697-2, 2019.
- 2363 Gunchin, G., Manousakas, M., Osan, J., Karydas, A. G., Eleftheriadis, K., Lodoysamba, S., Shagjjamba, D.,  
2364 Migliori, A., Padilla-Alvarez, R., Strelia, C., and Darby, I.: Three-year long source apportionment study of  
2365 airborne particles in Ulaanbaatar using x-ray fluorescence and positive matrix factorization, *Aerosol and Air*  
2366 *Quality Research*, 19(5), 1056-1067, doi:10.4209/aaqr.2018.09.0351, 2019.
- 2367 Guo, Y., Yan, C., Li, C., Feng, Z., Zhou, Y., Lin, Z., Dada, L., Stolzenburg, D., Yin, R., Kontkanen, J.,  
2368 Daellenbach, K. R., Kangasluoma, J., Yao, L., Chu, B., Wang, Y., Cai, R., Bianchi, F., Liu, Y., and Kulmala,  
2369 M.: Formation of Nighttime Sulfuric Acid from the Ozonolysis of Alkenes in Beijing, *Atmos. Chem. Phys.*  
2370 *Discuss.*, <https://doi.org/10.5194/acp-2019-1111>, in review, 2020.
- 2371 Gurchenkov, A. A., Murynin, A. B., Trekin, A. N., and Ignatyev, V. Y.: Object-oriented classification of  
2372 substrate surface objects in Arctic impact regions aerospace monitoring, *Herald of the Bauman Moscow*  
2373 *State Technical University*, 135-146. doi:10.18698/1812-3368-2017-3-135-146, 2017.
- 2374 Göckede, M., Kittler, F., Kwon, M. J., Burjack, I., Heimann, M., Kolle, O., Zimov, N., and Zimov, S.:  
2375 Shifted energy fluxes, increased Bowen ratios, and reduced thaw depths linked with drainage-induced  
2376 changes in permafrost ecosystem structure, *The Cryosphere*, 11, 2975–2996, [https://doi.org/10.5194/tc-11-](https://doi.org/10.5194/tc-11-2975-2017)  
2377 [2975-2017](https://doi.org/10.5194/tc-11-2975-2017), 2017.
- 2378 Göckede, M., Kwon, M. J., Kittler, F., Heimann, M., Zimov, N., and Zimov, S.: Negative feedback processes  
2379 following drainage slow down permafrost degradation, *Glob. Change Biol.*, 25, 3254–3266,  
2380 <https://doi.org/10.1111/gcb.14744>, 2019.
- 2381 Hao, L., Garmash, O., Ehn, M., Miettinen, P., Massoli, P., Mikkonen, S., Jokinen, T., Roldin, P., Aalto, P.,  
2382 Yli-Juuti, T., Joutsensaari, J., Petäjä, T., Kulmala, M., Lehtinen, K. E. J., Worsnop, D. R., and Virtanen, A.:  
2383 Combined effects of boundary layer dynamics and atmospheric chemistry on aerosol composition during  
2384 new particle formation periods, *Atmospheric Chemistry and Physics*, 18(23), 17705-17716. doi:10.5194/acp-  
2385 18-17705-2018, 2018.



- 2386 Hari, P. & Kulmala, M.: Station for Measuring Ecosystem–Atmosphere Relations (SMEAR II). *Boreal Env.*  
2387 *Res.* 10: 315–322, 2005.
- 2388
- 2389 Hari, P., Andreae M., Kabat P., and Kulmala M.: A comprehensive network of measuring stations to monitor  
2390 climate change. *Boreal Env. Res.* 14: 442–446, 2009.
- 2391
- 2392 Hari, P., Petäjä, T., Bäck, J., Kerminen, V.-M., Lappalainen, H. K., Vihma, T., Laurila, T., Viisanen, Y.,  
2393 Vesala, T., and Kulmala, M.: Conceptual design of a measurement network of the global change, *Atmos.*  
2394 *Chem. Phys.*, 16, 1017–1028, doi:10.5194/acp-16-1017-2016, 2016.
- 2395 Hari, P., Kerminen, V.-M., Kulmala, L., Kulmala, M., Noe, S., Petäjä, T., Vanhatalo, A., and Bäck, J.:  
2396 Annual cycle of Scots pine photosynthesis, *Atmos. Chem. Phys.*, 17, 15045–15053, doi:10.5194/acp-17-  
2397 15045-2017, 2017.
- 2398 Heikkilä, A., Makelä, J. S., Lakkala, K., Meinander, O., Kaurola, J., Koskela, T., Karhu, J. M., Karppinen,  
2399 T., Kyro, E., and De Leeuw, G.: In search of traceability: two decades of calibrated Brewer UV  
2400 measurements in Sodankyla and Jokioinen, *Geoscientific Instrumentation, Methods and Data Systems*, 5(2),  
2401 531–540, doi:10.5194/gi-5-531-2016, 2016.
- 2402 Heintzenberg, J., Tunved, P., Galí, M., and Leck, C.: New particle formation in the Svalbard region 2006–  
2403 2015, *Atmos. Chem. Phys.*, 17, 6153–6175, doi:10.5194/acp-17-6153-2017, 2017.
- 2404 Helin, A., Sietiö, O.-M., Heinonsalo, J., Bäck, J., Riekkola, M.-L., and Parshintsev, J.: Characterization of  
2405 free amino acids, bacteria and fungi in size-segregated atmospheric aerosols in boreal forest: seasonal  
2406 patterns, abundances and size distributions, *Atmos. Chem. Phys.*, 17, 13089–13101, doi.org/10.5194/acp-17-  
2407 13089-2017, 2017.
- 2408 Hellén, H., Praplan, A. P., Tykkä, T., Ylivinkka, I., Vakkari, V., Bäck, J., Petäjä, T., Kulmala, M., and  
2409 Hakola, H.: Long-term measurements of volatile organic compounds highlight the importance of  
2410 sesquiterpenes for the atmospheric chemistry of a boreal forest, *Atmos. Chem. Phys.*, 18, 13839–13863,  
2411 <https://doi.org/10.5194/acp-18-13839-2018>, 2018.
- 2412 Hinzman, L.D., Bettez, N.D., Bolton, W.R. et al. :Evidence and Implications of Recent Climate Change in  
2413 Northern Alaska and Other Arctic Regions, *Climatic Change*, 72, 251–298, [doi.org/10.1007/s10584-005-](https://doi.org/10.1007/s10584-005-5352-2)  
2414 [5352-2](https://doi.org/10.1007/s10584-005-5352-2), 2005.
- 2415 Hoegh-Guldberg, O., Jacob, D., Taylor, M., Bindi, M., Brown, S., Camilloni, I., Diedhiou, A.,  
2416 Djalante, R., Ebi, K. L., Engelbrecht, F., Guiot, J., Hijjoka, Y., Mehrotra, S., Payne, A., Seneviratne, S. I.,  
2417 Thomas, A., Warren, R., and Zhou, G.: Impacts of 1.5°C Global Warming on Natural and Human Systems,  
2418 in: *Global Warming of 1.5°C: An IPCC Special Report on the impacts of global warming of 1.5°C above*  
2419 *pre-industrial levels and related global greenhouse gas emission pathways, in the context of*  
2420 *strengthening the global response to the threat of climate change, sustainable development, and efforts to*



- 2421 eradicate poverty, edited by: Masson-Delmotte, V., Zhai, P., Pörtner, H.-O., Roberts, D., Skea, J., Shukla, P.  
2422 R., Pirani, A., Moufouma-Okia, W., Péan, C., Pidcock, R., Connors, S., Matthews, J. B. R., Chen, Y., Zhou,  
2423 X., Gomis, M. I., Lonnoy, E., Maycock, T., Tignor, M., and Waterfield, T., WMO, Geneva, Switzerland,  
2424 2018.
- 2425 Hong, J., Kim, J., Nieminen, T., Duplissy, J., Ehn, M., Äijälä, M., Hao, L. Q., Nie, W., Sarnela, N., Prisle, N.  
2426 L., Kulmala, M., Virtanen, A., Petäjä, T., and Kerminen, V.-M.: Relating the hygroscopic properties of  
2427 submicron aerosol to both gas- and particle-phase chemical composition in a boreal forest environment,  
2428 *Atmos. Chem. Phys.*, 15, 11999–12009, <https://doi.org/10.5194/acp-15-11999-2015>, 2015.
- 2429 Huang, W., Cheng, B., Zhang, J., Zhang, Z., Vihma, T., Li, Z., and Niu, F.: Modeling experiments on  
2430 seasonal lake ice mass and energy balance in the Qinghai–Tibet Plateau: a case study, *Hydrol. Earth Syst.*  
2431 *Sci.*, 23, 2173-2186, 2019a.
- 2432 Huang, W., Zhang, J., Leppäranta, M., Li, Z., Cheng, B. and Lin, Z. 2019b. Thermal structure and water-ice  
2433 heat transfer in a shallow ice-covered thermokarst lake in central Qinghai-Tibet Plateau, *Journal of*  
2434 *Hydrology*, 578, [124122], 2019b.
- 2435 Hölttä, T., Lintunen, A., Chan, T., Mäkelä, A., and Nikinmaa, E.: A steady state stomatal model of balanced  
2436 leaf gas exchange, hydraulics and maximal source-sink flux, *Tree Physiology*, 37, 851-868, doi:  
2437 10.1093/treephys/tpx011, 2017.
- 2438 IPCC: Special Report on the Ocean and Cryosphere in a Changing Climate, edited by Pörtner, H.-O.,  
2439 Roberts, D.C., Masson-Delmotte, V., Zhai, P., Tignor, M., Poloczanska, E., Mintenbeck, K., Alegría, A.,  
2440 Nicolai, M., Okem, A., Petzold, J., Rama, B., and Weyer, N. M., 2019.
- 2441 Ivakhov, V. M., Paramonova, N. N., Privalov, V. I., Zinchenko, A. V., Loskutova, M. A., Makshtas, A. P.,  
2442 Kustov, V. Y., Laurila, T., Aurela, M., and Asmi, E.: Atmospheric Concentration of Carbon Dioxide at Tiksi  
2443 and Cape Baranov Stations in 2010-2017, *Russ. Meteorol. Hydrol.*, 44, 291–299,  
2444 doi:10.3103/s1068373919040095, 2019.
- 2445 Jaffe, D., Bertschi, I., Jaegle, L., Novelli, P., Reid, J. S., Tanimoto, H., Vingarzan, R. and Westphal, D. L.:  
2446 Long-range transport of Siberian biomass burning emissions and impact on surface ozone in western North  
2447 America, *Geophys. Res. Lett.*, 31(16), L16106, doi:10.1029/2004GL020093, 2004.
- 2448 Jakobson, L., T. Vihma, and E. Jakobson,: Relationships between Sea Ice Concentration and Wind Speed  
2449 over the Arctic Ocean during 1979–2015., *J. Climate*, 32, 7783–7796, [https://doi.org/10.1175/JCLI-D-19-](https://doi.org/10.1175/JCLI-D-19-0271.1)  
2450 0271.1, 2019.
- 2451 Juhola, S.: Planning for a green city: The Green Factor tool, *Urban Forestry and Urban Greening*, 34, 254-  
2452 258, doi:10.1016/j.ufug.2018.07.019, 2018.
- 2453 Juutinen, S., Virtanen, T., Kondratyev, V., Laurila, T., Linkosalmi, M., Mikola, J., Nyman, J., Räsänen, A.,  
2454 Tuovinen, J.-P., and Aurela, M.: Spatial variation and seasonal dynamics of leaf-area index in the arctic



- 2455 tundra-implications for linking ground observations and satellite images, *Environ. Res. Lett.*, 12(9), 10,  
2456 doi:10.1088/1748-9326/aa7f85, 2017.
- 2457 Kalogridis, A.C., Popovicheva, O.B., Engling, G., Diapouli, E., Kawamura, K., Tachibana, E., Ono, K.,  
2458 Kozlov, V.S., and Eleftheriadis, K.: Smoke aerosol chemistry and aging of Siberian biomass burning  
2459 emissions in a large aerosol chamber, *Atmos. Environ.*, 185,15-28, 2018.
- 2460 Kangasluoma, J., Ahonen, L. R., Laurila, T., Cai, R., Enroth, J., Mazon, S., Korhonen, F., Aalto, P.,  
2461 Kulmala, M., Attoui, M. and Petäjä, T.: Laboratory verification of a new high flow differential mobility  
2462 particle sizer, and field measurements in Hyytiälä, *J Aerosol Sci*, 124, 1-9, 2018.
- 2463 Karelin, D. V., Goryachkin, S. V., Zamolodchikov, D. G., Dolgikh, A. V., Zazovskaya, E. P., Shishkov, V.  
2464 A., and Kraev, G. N.: Human footprints on greenhouse gas fluxes in cryogenic ecosystems, *Dokl. Earth Sc.*,  
2465 477, 1467–1469, doi:10.1134/S1028334X17120133, 2017.
- 2466 Karetnikov, S., Leppäranta, M., and Montonen, A.: A time series of over 100 years of ice seasons on Lake  
2467 Ladoga, *Journal of Great Lakes Research*, 43(6), 979-988, doi:10.1016/j.jglr.2017.08.010, 2017.
- 2468 Karthe, D., Abdullaev, I., Boldgiv, B., Borchardt, D., Chalov, S., Jarsjö, J., Li, L., and Nittrouer, J.A.: Water  
2469 in Central Asia: an integrated assessment for science-based management, *Environmental Earth Sciences*,  
2470 76(20), 15, doi:10.1007/s12665-017-6994-x, 2017a.
- 2471 Karthe, D., Chalov, S., Moreido, V., Pashkina, M., Romanchenko, A., Batbayar, G., Kalugin, A., Westphal,  
2472 K., Malsy, M., and Flörke, M.: Assessment of runoff, water and sediment quality in the Selenga River basin  
2473 aided by a web-based geoservice, *Water Resources*, 44(3), 399-416, 2017b.
- 2474 Karthe D., Chalov S., Gradel A., and Kusbach A.: Special issue: Environment change on the Mongolian  
2475 plateau: atmosphere, forests, soils and water, *Geography, Environment, Sustainability*, 12(3), 60-65,  
2476 doi:10.24057/2071-9388-2019-1411, 2019.
- 2477 Karvonen, J., Shi, L., Cheng, B., Similä, M., Mäkynen, M., and Vihma, T.: Bohai Sea ice parameter  
2478 estimation based on thermodynamic ice model and Earth observation data, *Remote Sensing*, 9, 234,  
2479 doi:10.3390/rs9030234, 2017.
- 2480 Kasimov, N., Karthe, D., and Chalov, S.: Environmental change in the Selenga River—Lake Baikal Basin,  
2481 *Reg. Environ. Chang.*, 17, 1945–1949, 2017a.
- 2482 Kasimov, N. S., Kosheleva, N. E., Nikiforova, E. M., and Vlasov, D. V.: Benzo a pyrene in urban  
2483 environments of eastern Moscow: pollution levels and critical loads, *Atmos. Chem. Phys.*, 17(3), 2217-2227,  
2484 doi:10.5194/acp-17-2217-2017, 2017b.
- 2485 Kasimov, N., Shinkareva, G., Lychagin, M., Kosheleva, N., Chalov, S., Pashkina, M., Thorslund, J., and  
2486 Jarsjö, J.: River water quality of the selenga-baikal basin: Part i—spatio-temporal patterns of dissolved and  
2487 suspended metals, *Water*, 12(8), 2137, 2020a.
- 2488



- 2489 Kasimov, N., Shinkareva, G., Lychagin, M., Chalov, S., Pashkina, M., Thorslund, J., and Jarsjö, J.: River water  
2490 quality of the selenga-baikal basin: part ii — metal partitioning under different hydroclimatic conditions,  
2491 *Water*, 12(9), 2392, 2020b.
- 2492
- 2493 Kaus, A., Schäffer, M., Karthe, D., Büttner, O., von Tümpling, W., and Borchardt, D.: Regional patterns of  
2494 heavy metal exposure and contamination in the fish fauna of the Kharaa River basin, Mongolia, *Reg.*  
2495 *Environ. Change*, 17, 2023–2037, doi: 10.1007/s10113-016-0969-4, 2017.
- 2496 Kazakov, E., Kondrik, D., and Pozdnyakov, D.: A synthetic satellite dataset of the spatio-temporal  
2497 distributions of *Emiliana huxleyi* blooms and their impacts on Arctic and sub-Arctic marine environments  
2498 (1998–2016), *Earth Systems Science Data*, 11, 119–128, doi: 10.5194/essd-11-119-2019, 2019.
- 2499 Kecorius, S., Vogl, T., Paasonen, P., Lampilahti, J., Rothenberg, D., Wex, H., Zeppenfeld, S., van Pinxteren,  
2500 M., Hartmann, M., Henning, S., Gong, X., Welti, A., Kulmala, M., Stratmann, F., Herrmann, H., and  
2501 Wiedensohler, A.: New particle formation and its effect on cloud condensation nuclei abundance in the  
2502 summer Arctic: a case study in the Fram Strait and Barents Sea, *Atmos. Chem. Phys.*, 19, 14339–14364, doi:  
2503 10.5194/acp-19-14339-2019, 2019.
- 2504 Kerminen, V.-M., Chen, X., Vakkari, V., Petäjä, T., Kulmala, M., and Bianchi, F.: Atmospheric new particle  
2505 formation and growth: review of field observations, *Environ. Res. Lett.*, 13, 103003, doi: 10.1088/1748-  
2506 9326/aadf3c, 2018.
- 2507 Kim, J., Kim, H. M., Cho, C.-H., Boo, K.-O., Jacobson, A. R., Sasakawa, M., Machida, T., Arshinov, M.,  
2508 and Fedoseev, N.: Impact of Siberian observations on the optimization of surface CO<sub>2</sub> flux, *Atmos. Chem.*  
2509 *Phys.*, 17, 2881–2899, <https://doi.org/10.5194/acp-17-2881-2017>, 2017.
- 2510 Kirillin, G., Leppäranta, M., Terzhevik, A., Bernhardt, J., Engelhardt, C., Granin, N., Golosov, S., Efremova,  
2511 T., Palshin, N., Sherstyankin, P., Zdorovenova, G., and Zdorovenov, R.: Physics of seasonally ice-covered  
2512 lakes: major drivers and temporal/spatial scales, *Aquatic Ecol.*, 74, 659–682, 2012.
- 2513 Kirillin, G., Aslamov, I., Leppäranta, M., and Lindgren, E.: Turbulent mixing and heat fluxes under lake ice:  
2514 the role of seiche oscillations, *Hydrology of Earth System Sciences*, 22(12), 6493–6504, doi:10.5194/hess-  
2515 22-6493-2018, 2018.
- 2516 Kirschke, S., Bousquet, P., Ciais, P., Saunio, M., Canadell, J. G., Dlugokencky, E. J., Bergamaschi, P.,  
2517 Bergmann, D., Blake, D. R., Bruhwiler, L., Cameron-Smith, P., Castaldi, S., Chevallier, F., Feng, L., Fraser,  
2518 A., Heimann, M., Hodson, E. L., Houweling, S., Josse, B., Fraser, P. J., Krummel, P. B., Lamarque, J.-F.,  
2519 Langenfelds, R. L., Le Quere, C., Naik, V., O’Doherty, S., Palmer, P. I., Pison, I., Plummer, D., Poulter, B.,  
2520 Prinn, R. G., Rigby, M., Ringeval, B., Santini, M., Schmidt, M., Shindell, D. T., Simpson, I. J., Spahni, R.,  
2521 Steele, L. P., Strode, S. A., Sudo, K., Szopa, S., van der Werf, G.R., Voulgarakis, A., van Weele, M., Weiss,  
2522 R. F., Williams, J. E., and Zeng, G.: Three decades of global methane sources and sinks, *Nature Geoscience*,  
2523 6(10), 813–823, doi: 10.1038/ngeo1955, 2013.



- 2524 Kiselev, M. V., Voropay, N. N., and Cherkashina, A. A.: influence of anthropogenic activities on the  
2525 temperature regime of soils of the South-Western Baikal region, *IOP Conf. Ser.: Earth Environ. Sci.*, 381,  
2526 012043, doi: 10.1088/1755-1315/381/1/012043, 2019.
- 2527 Kittler, F., Heimann, M., Kolle, O., Zimov, N., Zimov, S., and Göckede, M.: Long-term drainage reduces  
2528 CO<sub>2</sub> uptake and CH<sub>4</sub> emissions in a Siberian permafrost ecosystem, *Global Biogeochemical Cycles*, 31,  
2529 1704–1717. doi: 10.1002/2017GB005774, 2017.
- 2530 Kiuru, P., Ojala, A., Mammarella, I., Heiskanen, J., Kämäräinen, M., Vesala, T. and Huttula, T.: Effects of  
2531 Climate Change on CO<sub>2</sub> Concentration and Efflux in a Humic Boreal Lake: A Modeling Study, *Journal of*  
2532 *Geophysical Research, Biogeosciences*, 123, 7, 2212–2233, 2018.
- 2533 Kondrik, D., Pozdnyakov, D., and Pettersson, L.: Particulate inorganic carbon production within *E. huxleyi*  
2534 blooms in subpolar and polar seas: a satellite time series study (1998–2013), *International Journal of Remote*  
2535 *Sensing*, 38:22, 6179–6205, doi: 10.1080/01431161.2017.1350304, 2017.
- 2536 Kondrik, D. V., Pozdnyakov, D. V., and Johannessen, O. M.: Satellite evidence that *E. huxleyi*  
2537 phytoplankton blooms weaken marine carbon sinks, *Geophys. Res. Lett.*, 5, 846–854. doi:  
2538 10.1002/2017GL076240, 2018a.
- 2539 Kondrik, D. V., Pozdnyakov, D. V., and Pettersson, L. H.: Tendencies in Coccolithophorid Blooms in Some  
2540 Marine Environments of the Northern Hemisphere according to the Data of Satellite Observations in 1998–  
2541 2013. *Izv. Atmos. Ocean. Phys.*, 53, 955–964, doi: 10.1134/S000143381709016X, 2018b.
- 2542 Kondrik, D. V., Kazakov, E. E., Pozdnyakov, D. V., and Johannessen, O. M.: Satellite evidence for  
2543 enhancement of the column mixing ratio of atmospheric CO<sub>2</sub> over *E. huxleyi* blooms, *Transactions of the*  
2544 *Karelian Research Centre of the Russian Academy of Sciences, Limnologoia i Oceanologia series*, 9, 1–11,  
2545 doi: 10/17076/lim1107, 2019.
- 2546 Konovalov, I. B., Lvova, D. A., Beekmann, M., Jethva, H., Mikhailov, E. F., Paris, J.-D., Belan, B. D.,  
2547 Kozlov, V. S., Ciaï, P., and Andreae, M. O.: Estimation of black carbon emissions from Siberian fires using  
2548 satellite observations of absorption and extinction optical depths, *Atmos. Chem. Phys.*, 18, 14889–14924,  
2549 doi: 10.5194/acp-18-14889-2018, 2018.
- 2550 Konovalov V., Rets E., and Pimankina N.: Interrelation between glacier summer mass balance and runoff in  
2551 mountain river basins, *Geography, Environment, Sustainability*, 12(1), 23–33, doi: 10.24057/2071-9388-  
2552 2018-26, 2019.
- 2553 Konstantinov, P. I., Grishchenko, M. Y., and Varentsov, M. I.: Mapping urban heat islands of arctic cities  
2554 using combined data on field measurements and satellite images based on the example of the city of Apatity  
2555 (Murmansk Oblast), *Izv. Atmos. Ocean. Phys.*, 51(9), 992–998, doi:10.1134/s000143381509011x, 2015.
- 2556 Konstantinov, P., Varentsov, M., and Esau, I.: A high density urban temperature network deployed in several  
2557 cities of Eurasian Arctic, *Environ. Res. Lett.*, 13(7), 12, doi:10.1088/1748-9326/aacb84, 2018.



- 2558 Kontkanen, J., Paasonen, P., Aalto, J., Back, J., Rantala, P., Petäjä, T., and Kulmala, M.: Simple proxies for  
2559 estimating the concentrations of monoterpenes and their oxidation products at a boreal forest site, *Atmos.*  
2560 *Chem. Phys.*, 16(20), 13291-13307, doi:10.5194/acp-16-13291-2016, 2016.
- 2561 Kooijmans, L. M. J., Sun, W., Aalto, J., Erkkilä, K.M., Maseyk, K., Seibt, U., Vesala, T., Mammarella, I.,  
2562 and Chen, H.: Influences of light and humidity on carbonyl sulfide-based estimates of photosynthesis,  
2563 *Proceedings of the National Academy of Sciences*, 116 (7), 2470-2475, doi:10.1073/pnas.1807600116, 2019.
- 2564 Korneykova, M. V., and Evdokimova, G. A.: Microbiota of the ground air layers in natural and industrial  
2565 zones of the Kola Arctic, *J Environ. Sci. Health A*, 53(3), 271-277, doi:10.1080/10934529.2017.1397444,  
2566 2018a.
- 2567 Korneikova, M. V., Redkina, V. V., and Shalygina, R. R.: Algological and mycological characterization of  
2568 soils under pine and birch forests in the Pasvik Reserve, *Eurasian Soil Science*, 51(2), 211-220,  
2569 doi:10.1134/s1064229318020047, 2018b.
- 2570 Koronatova, N. G., & Milyaeva, E. V.: Plant community succession in post-mined quarries in the northern-  
2571 taiga zone of West Siberia. *Contemporary Problems of Ecology*, 4(5), 513–518, 2011.
- 2572 Kukkonen, I., Ezhova, E., Suhonen, E. A. J., Lappalainen, H. K., Gennadinik, V., Ponomareva, O., Gravis,  
2573 A., Miles, V., Kulmala, M., Melnikov, V., and Drozdov, D.: Observations and modelling of ground  
2574 temperature evolution in the discontinuous permafrost zone in Nadym, North-West Siberia, *Permafrost and*  
2575 *Periglacial Processes*, 1– 17, doi:10.1002/ppp.2040, 2020.
- 2576 Kulmala, M., Vehkamäki, H., Petäjä, T., Dal Maso, M., Lauri, A., Kerminen, V.-M., Birmili, W., and  
2577 McMurry, P.H.: Formation and growth rates of ultrafine atmospheric particles: a review of observations,  
2578 *Journal of Aerosol Science*, 35, 143-176, doi:10.1134/S1995425511050, 2004.
- 2579 Kulmala, M.: Atmospheric chemistry: China's choking cocktail, *Nature*, 526, 497-499,  
2580 doi:10.1038/526497a, 2015a.
- 2581 Kulmala, M., Lappalainen, H. K., Petäjä, T., Kurten, T., Kerminen, V.-M., Viisanen, Y., Hari, P., Sorvari, S.,  
2582 Bäck, J., Bondur, V., Kasimov, N., Kotlyakov, V., Matvienko, G., Baklanov, A., Guo, H. D., Ding, A.,  
2583 Hansson, H.-C., and Zilitinkevich, S.: Introduction: The Pan-Eurasian Experiment (PEEX) –  
2584 multidisciplinary, multiscale and multicomponent research and capacity-building initiative, *Atmos. Chem.*  
2585 *Phys.*, 15, 13085-13096, doi:10.5194/acp-15-13085-2015, 2015b.
- 2586 Kulmala, M., Lappalainen, H. K., Petäjä, T., Kerminen, V.-M., Viisanen, Y., Matvienko, G., Melnikov, V.,  
2587 Baklanov, A., Bondur, V., Kasimov, N., and Zilitinkevich, S.: Pan-Eurasian Experiment (PEEX) Program:  
2588 Grant Challenges in the Arctic-boreal context, *J. Geography Environment Sustainability*, 2, 5–18, 2016a.
- 2589 Kulmala, M., Petäjä, T., Kerminen, V. M., Kujansuu, J., Ruuskanen, T., Ding, A., Nie, W., Hu, M., Wang,  
2590 Z., Wu, Z., and Wang, L.: On secondary new particle formation in China, *Front. Environ. Sci. Eng.*, 10, 8,  
2591 doi:10.1007/s11783-016-0850-1, 2016b.



- 2592 Kulmala, M., Kerminen, V.-M., Petäjä, T., Ding, A. J., and Wang L.: Atmospheric gas-to-particle  
2593 conversion: why NPF events are observed in megacities?, *Faraday Discuss.*, 200, 271-288,  
2594 doi:10.1039/c6fd00257a, 2017.
- 2595 Kulmala, M.: Build a global Earth observatory, *Nature*, 553, 21-23, doi: 10.1038/d41586-017-08967-y, 2018.
- 2596 Kulmala, L., Pumpanen, J., Kolari, P., Dengel, S., Berninger, F., Köster, K., Matkala, L., Vanhatalo, A.,  
2597 Vesala, T., and Bäck, J.: Inter- and intra-annual dynamics of photosynthesis differ between forest floor  
2598 vegetation and tree canopy in a subarctic Scots pine stand, *Agricultural and Forest Meteorology*, 271, 1-11,  
2599 doi: 10.1016/j.agrformet.2019.02.029, 2019.
- 2600 Kulmala, M., Dada, L., Daellenbach, K. R., Yan, C., Stolzenburg, D., Kontkanen, J., Ezhova, E., Hakala, S.,  
2601 Tuovinen, S., Kokkonen, T. V., Kurppa, M., Cai, R., Zhou, Y., Yin, R., Baalbaki, R., Chan, T., Chu, B.,  
2602 Deng, C., Fu, Y., Ge, M., He, H., Heikkinen, L., Junninen, H., Liu, Y., Lu, Y., Nie, W., Rusanen, A.,  
2603 Vakkari, V., Wang, V., Yang, G., Yao, L., Zheng, J., Kujansuu, J., Kangasluoma, J., Petäjä, T., Paasonen, P.,  
2604 Järvi, L., Worsnop, D., Ding, A., Liu, Y., Wang, L., Jiang, J., Bianchi, F., and Kerminen, V.-M.: Is reducing  
2605 new particle formation a plausible solution to mitigate particulate air pollution in Beijing and other Chinese  
2606 megacities?, *Faraday Discussions*, doi: 10.1039/D0FD00078G.2021.
- 2607 Kwon, M. J., Beulig, F., Ilie, I., Wildner, M., Küsel, K., Merbold, L., Mahecha, M. D., Zimov, N., Zimov, S.  
2608 A., Heimann, M., Schuur, E. A. G., Kostka, J. E., Kolle, O., Hilke, I. and Göckede, M.: Plants,  
2609 microorganisms, and soil temperatures contribute to a decrease in methane fluxes on a drained Arctic  
2610 floodplain, *Glob. Change Biol.*, 23, 2396-2412, doi:10.1111/gcb.13558, 2017.
- 2611 Kwon, M. J., Natali, S. M., Hicks Pries, C. E., Schuur, E. A., Steinhof, A., Crummer, K. G., Zimov, N.,  
2612 Zimov, S. A., Heimann, M., Kolle, O., and Göckede, M.: Drainage enhances modern soil carbon contribution  
2613 but reduces old soil carbon contribution to ecosystem respiration in tundra ecosystems, *Glob. Change Biol.*,  
2614 25, 1315– 1325, doi: 10.1111/gcb.14578, 2019.
- 2615 Kühn, T., Kupiainen, K., Miinalainen, T., Kokkola, H., Paunu, V.-V., Laakso, A., Tonttila, J., Van  
2616 Dingenen, R., Kulovesi, K., Karvosenoja, N., and Lehtinen, K. E. J.: Effects of black carbon mitigation on  
2617 Arctic climate, *Atmos. Chem. Phys.*, 20, 5527–5546, doi: 10.5194/acp-20-5527-2020, 2020.
- 2618 Köster, E., Köster, K., Berninger, F., and Pumpanen, J.: Carbon dioxide, methane and nitrous oxide fluxes  
2619 from podzols of a fire chronosequence in the boreal forests in Värriö, Finnish Lapland, *Geoderma Regional*,  
2620 5, 181-187, doi:10.1016/j.geodrs.2015.07.001, 2015.
- 2621 Köster, E., Köster, K., Berninger, F., Prokushkin, A., Aaltonen, H., Zhou, X., and Pumpanen, J.: Changes in  
2622 fluxes of carbon dioxide and methane caused by fire in Siberian boreal forest with continuous permafrost,  
2623 *Journal of Environmental Management*, 228, 405-415, doi:10.1016/j.jenvman.2018.09.051, 2018.



- 2624 Köster, K., Berninger, F., Koster, E., and Pumpanen, J.: Influences of reindeer grazing on above- and  
2625 belowground biomass and soil carbon dynamics, *Arctic Antarctic and Alpine Res.*, 47(3), 495-503,  
2626 doi:10.1657/aaar0014-062, 2015.
- 2627 Köster, K., Berninger, F., Heinonsalo, J., Lindén, A., Köster, E., Ilvesniemi, H., and Pumpanen J.: The long-  
2628 term impact of low-intensity surface fires on litter decomposition and enzyme activities in boreal coniferous  
2629 forests, *Int. J Wildland Fire*, 25(2), 213-223, doi:10.1071/wf14217\_co, 2016.
- 2630 Köster, K., Koster, E., Berninger, F., Heinonsalo, J., and Pumpanen, J.: Contrasting effects of reindeer  
2631 grazing on CO<sub>2</sub>, CH<sub>4</sub>, and N<sub>2</sub>O fluxes originating from the northern boreal forest floor. *Land Degradation  
2632 and Development*, 29(2), 374-381, doi:10.1002/ldr.2868, 2018.
- 2633 Köster, K., Koster, E., Kulmala, L., Berninger, F., and Pumpanen, J.: Are the climatic factors combined with  
2634 reindeer grazing affecting the soil CO<sub>2</sub> emissions in subarctic boreal pine forest? *Catena*, 149, 616-622,  
2635 doi:10.1016/j.catena.2016.06.011, 2017.
- 2636 Lan, H., Holopainen, J., Hartonen, K., Jussila, M., Ritala, M. and Riekkola, M.-L.: Fully automated online  
2637 dynamic in-tube extraction for continuous sampling of volatile organic compounds in air, *Anal. Chem.*, 91,  
2638 8507, 2019.
- 2639 Lappalainen, H.K., Kulmala, M. and Zilitinkevich, S. (Eds.): *Pan Eurasian Experiment (PEEX) Science Plan*,  
2640 web: [www.atm.helsinki.fi/peex](http://www.atm.helsinki.fi/peex), ISBN 978-951-51-0587-5 (printed), ISBN 978-951-51-0588-2 (online),  
2641 2015.
- 2642 Lappalainen H.K., Petäjä T., Kujansuu J., Kerminen V., Shvidenko A., Bäck J., Vesala T., Vihma T., De  
2643 Leeuw G., Lauri A., Ruuskanen T., Lapshin V.B., Zaitseva N., Glezer O., Arshinov M., Spracklen D.V.,  
2644 Arnold S.R., Juhola S., Lihavainen H., Viisanen Y., Chubarova N., Chalov S., Filatov N., Skorokhod A.,  
2645 Elansky N., Dyukarev E., Esau I., Hari P., Kotlyakov V., Kasimov N., Bondur V., Matvienko G., Baklanov  
2646 A., Mareev E., Troitskaya Y., Ding A., Guo H., Zilitinkevich S., and Kulmala M.: Pan-Eurasian Experiment  
2647 (PEEX) – a research initiative meeting the grand challenges of the changing environment of the northern Pan-  
2648 Eurasian arctic-boreal areas, *J. Geography Environment Sustainability*, 2(7), 13-48, doi:10.24057/2071-  
2649 9388-2014-7-2-13-48, 2014.
- 2650 Lappalainen, H. K., Kerminen, V.-M., Petäjä, T., Kurten, T., Baklanov, A., Shvidenko, A., Bäck, J., Vihma,  
2651 T., Alekseychik, P., Andreae, M. O., Arnold, S. R., Arshinov, M., Asmi, E., Belan, B., Bobylev, L., Chalov,  
2652 S., Cheng, Y., Chubarova, N., de Leeuw, G., Ding, A., Dobrolyubov, S., Dubtsov, S., Dyukarev, E., Elansky,  
2653 N., Eleftheriadis, K., Esau, I., Filatov, N., Flint, M., Fu, C., Glezer, O., Gliko, A., Heimann, M., Holtslag, A.  
2654 A. M., Hörrak, U., Janhunen, J., Juhola, S., Järvi, L., Järvinen, H., Kanukhina, A., Konstantinov, P.,  
2655 Kotlyakov, V., Kieloaho, A.-J., Komarov, A. S., Kujansuu, J., Kukkonen, I., Duplissy, E.-M., Laaksonen, A.,  
2656 Laurila, T., Lihavainen, H., Lisitzin, A., Mahura, A., Makshtas, A., Mareev, E., Mazon, S., Matishov, D.,  
2657 Melnikov, V., Mikhailov, E., Moisseev, D., Nigmatulin, R., Noe, S. M., Ojala, A., Pihlatie, M., Popovicheva,  
2658 O., Pumpanen, J., Regerand, T., Repina, I., Shcherbinin, A., Shevchenko, V., Sipilä, M., Skorokhod, A.,



- 2659 Spracklen, D. V., Su, H., Subetto, D. A., Sun, J., Terzhevik, A. Y., Timofeyev, Y., Troitskaya, Y.,  
2660 Tynkkynen, V.-P., Kharuk, V. I., Zaytseva, N., Zhang, J., Viisanen, Y., Vesala, T., Hari, P., Hansson, H. C.,  
2661 Matvienko, G. G., Kasimov, N. S., Guo, H., Bondur, V., Zilitinkevich, S., and Kulmala, M.: Pan-Eurasian  
2662 Experiment (PEEX): towards a holistic understanding of the feedbacks and interactions in the land–  
2663 atmosphere–ocean–society continuum in the northern Eurasian region, *Atmos. Chem. Phys.*, 16, 14421–  
2664 14461, <https://doi.org/10.5194/acp-16-14421-2016>, 2016.
- 2665 Lappalainen, H.K., Kulmala, M., Kujansuu, J., Petäjä, T., Mahura, A., de Leeuw, G., Zilitinkevich, S.,  
2666 Juustila, M., Kerminen, V.M., Bornstein, B. and Jiahua, Z.: The Silk Road agenda of the Pan-Eurasian  
2667 Experiment (PEEX) program, *Big Earth Data*, 2(1), 8-35, doi:10.1080/20964471.2018.1437704, 2018.
- 2668 Lei, R. B., Xie, H. J., Wang, J., Leppäranta, M., Jonsdottir, I., and Zhang, Z. H.: Changes in sea ice  
2669 conditions along the Arctic Northeast Passage from 1979 to 2012, *Cold Regions Science and Technology*,  
2670 119, 132-144. doi:10.1016/j.coldregions.2015.08.004, 2015.
- 2671 Lei, R., Tian-Kunze, X., Leppäranta, M., Wang, J., Kaleschke, L., and Zhang, Z.: Changes in summer sea  
2672 ice, albedo, and partitioning of surface solar radiation in the Pacific sector of Arctic Ocean during 1982-2009,  
2673 *J. Geophys. Res.: Oceans*, 121(8), 5470-5486, doi:10.1002/2016jc011831, 2016.
- 2674 Lei, R. B., Cheng, B., Heil, P., Vihma, T., Wang, J., Ji, Q., and Zhang, Z. H.: Seasonal and interannual  
2675 variations of sea ice mass balance from the Central Arctic to the Greenland Sea, *J. Geophys. Res.: Oceans*,  
2676 123(4), 2422-2439, doi:10.1002/2017jc013548, 2018.
- 2677 Leino, K., Nieminen, T., Manninen, H. E., Petäjä, T., Kerminen, V.-M., and Kulmala, M.: Intermediate ions  
2678 as a strong indicator of new particle formation bursts in a boreal forest, *Boreal Environ. Res.*, 21(3-4), 274-  
2679 286, 2016.
- 2680 Leppäranta, M.: Structure and properties of lake ice. *Freezing of Lakes and the Evolution of their Ice Cover*,  
2681 Springer, Berlin/Heidelberg, Germany, 51–90. doi: 10.1007/978-3-642-29081-7\_3, 2015.
- 2682 Leppäranta, M., Lindgren, E., and Shirasawa, K.: The heat budget of Lake Kilpisjärvi in the Arctic tundra,  
2683 *Hydrol. Res.*, 48(4), 969-980, doi:10.2166/nh.2016.171, 2017.
- 2684 Leppäranta, M., Lewis, J. E., Heini, A., and Arvola, L.: Spatial statistics of hydrography and water chemistry  
2685 in a eutrophic boreal lake based on sounding and water samples, *Environ. Monit. Assess.*, 190(7), 378,  
2686 doi:10.1007/s10661-018-6742-z, 2018.
- 2687 Leppäranta, M., Lindgren, E., Wen, L. and Kirillin, G.: Ice cover decay and heat balance in Lake Kilpisjärvi  
2688 in Arctic tundra, *Journal of Limnology*, 78(2). doi: 10.4081/jlimnol.2019.1879, 2019.
- 2689 Leppäranta, M., Meleshko, V., Uotila, P., and Pavlova, T.: Sea ice modelling, 315-387, *Sea Ice in the Arctic*  
2690 (Springer, Cham), 2020.



- 2691 Li, H., Väiliranta, M., Mäki, M., Kohl, L., Sannel, B., Pumpanen, J., Koskinen, M., Bäck, J. and Bianchi, F.:  
2692 Overlooked organic vapor emissions from thawing Arctic permafrost, *Environmental Research Letters* 15,  
2693 Issue 10, id.104097, 12 pp., 2020a.
- 2694 Li, M., Wang, L., Liu, J., Gao, W., Song, T., Sun, Y., Li, L., Li, X., Wang, Y., Liu, L. and Daellenbach,  
2695 K.R., Paasonen, P.J., Kerminen, V.-M., Kulmala, M., and Wang Y.: Exploring the regional pollution  
2696 characteristics and meteorological formation mechanism of PM<sub>2.5</sub> in North China during 2013–2017,  
2697 *Environment international*, 134, 105283, 2020b.
- 2698 Liao, Z., Cheng, B., Zhao, J., Vihma, T., Jackson, K., Yang, Q., Yang, Y., Zhang, L., Li, Z., Qiu, Y., and  
2699 Cheng, X.: Snow depth and ice thickness derived from SIMBA ice mass balance buoy data using an  
2700 automated algorithm, *Int. J. Digital Earth*, 12(8), 962-979, doi:10.1080/17538947.2018.1545877, 2018.
- 2701 Lin, X., Rogers, B. M., Sweeney, C., Chevallier, F., Arshinov, M., Dlugokencky, E., Machida, T., Motoki  
2702 Sasakawa, Tans, P., Keppel-Aleks, G.: Siberian and temperate ecosystems shape Northern Hemisphere  
2703 atmospheric CO<sub>2</sub> seasonal amplification, *PNAS*, 117 (35), 21079-21087, doi:10.1073/pnas.1914135117,  
2704 2020.
- 2705 Lintunen, A., Paljakka, T., Salmon, Y., Dewar, R., Riikonen, A. and Hölttä, T.: The influence of soil  
2706 temperature and water content on belowground hydraulic conductance and leaf gas exchange in mature trees  
2707 of three boreal species, *Plant, Cell and Environment*, 43, 532-547, doi: 10.1111/pce.13709, 2020.
- 2708 Liu, J., Wang, L., Li, M., Liao, Z., Sun, Y., Song, T., Gao, W., Wang, Y., Li, Y., Ji, D., Hu, B., Kerminen,  
2709 V.-M., Wang, Y., and Kulmala, M.: Quantifying the impact of synoptic circulation patterns on ozone  
2710 variability in northern China from April to October 2013–2017, *Atmos. Chem. Phys.*, 19, 14477–14492,  
2711 doi:10.5194/acp-19-14477-2019, 2019 a.
- 2712 Liu, W., Atherton, J., Möttus, M., Gastellu-Etchegorry, J.P., Malenovsky, Z., Raunonen, P., Åkerblom, M.,  
2713 Mäkipää, R. and Porcar-Castell, A.: Simulating solar-induced chlorophyll fluorescence in a boreal forest  
2714 stand reconstructed from terrestrial laser scanning measurements, *Remote Sensing of Environment*, 232,  
2715 111274, 2019b.
- 2716 Liu, Y., de Leeuw, G., Kerminen, V.-M., Zhang, J., Zhou, P., Nie, W., Qi, X., Hong, J., Wang, Y., Ding, A.,  
2717 Guo, H., Krüger, O., Kulmala, M., and Petäjä, T.: Analysis of aerosol effects on warm clouds over the  
2718 Yangtze River Delta from multi-sensor satellite observations, *Atmos. Chem. Phys.*, 17, 5623–5641,  
2719 doi:10.5194/acp-17-5623-2017, 2017.
- 2720 Liu, Y., Zhang, J., Zhou, P., Lin, T., Hong, J., Shi, L., Yao, F., Wu, J., Guo, H., and de Leeuw, G.: Satellite-  
2721 based estimate of the variability of warm cloud properties associated with aerosol and meteorological  
2722 conditions, *Atmos. Chem. Phys.*, 18, 18187–18202, doi:10.5194/acp-18-18187-2018, 2018.



- 2723 López-Blanco, E., Exbrayat, J.-F., Lund, M., Christensen, T. R., Tamstorf, M. P., Slevin, D., Hugelius, G.,  
2724 Bloom, A. A., and Williams, M.: Evaluation of terrestrial pan-Arctic carbon cycling using a data-  
2725 assimilation system, *Earth Syst. Dynam.*, 10, 233–255, doi:10.5194/esd-10-233-2019, 2019.
- 2726 Lu, P., Leppäranta, M., Cheng, B., and Li, Z.: Influence of melt-pond depth and ice thickness on Arctic sea-  
2727 ice albedo and light transmittance, *Cold Regions Science and Technology*, 124, 1-10,  
2728 doi:10.1016/j.coldregions.2015.12.010, 2016.
- 2729 Lu, P., Cheng, B., Leppäranta, M., and Li, Z. J.: Partitioning of solar radiation in Arctic sea ice during melt  
2730 season, *Oceanologia*, 60(4), 464-477, doi:10.1016/j.oceano.2018.03.002, 2018a.
- 2731 Lu, P., Leppäranta, M., Cheng, B., Li, Z., Istomina, L., and Heygster, G.: The color of melt ponds on Arctic  
2732 sea ice, *The Cryosphere*, 12, 1331–1345, doi:10.5194/tc-12-1331-2018, 2018b.
- 2733 Luoma, K., Virkkula, A., Aalto, P.P., Petäjä, T., and Kulmala, M.: Over a 10-year record of aerosol optical  
2734 properties at SMEAR II, *Atmos. Chem. Phys.*, 19, 11363–11382, doi:10.5194/acp-19-11363-2019, 2019.
- 2735 Lychagin, M., Chalov, S., Kasimov, N., Shinkareva, G., Jarsjo, J., and Thorslund, J.: Surface water pathways  
2736 and fluxes of metals under changing environmental conditions and human interventions in the Selenga River  
2737 system, *Environ. Earth Sci.*, 76(1), 14, doi:10.1007/s12665-016-6304-z, 2017.
- 2738 Ma, J., Yan, X., Dong, W. et al.: Gross primary production of global forest ecosystems has been  
2739 overestimated, *Sci Rep* 5, 10820, doi:10.1038/srep10820, 2015.
- 2740 Magritsky, D. V., Frolova, N. L., Evstigneev, V. M., Povalishnikova, E. S., Kireeva, M. B., and  
2741 Pakhomova, O. M.: Long-term changes of river water inflow into the seas of the Russian Arctic sector,  
2742 *Polarforschung*, 87(2), 177-194, doi: 10.2312/polarforschung.87.2.177, 2018.
- 2743 Mahura A., Baklanov A., Sørensen, J. H., Svetlov, A., and Koshkin, V.: Assessment of Long-Range  
2744 Transport and Deposition from Cu-Ni Smelters of Russian North. In "Air, Water and Soil Quality Modelling  
2745 for Risk and Impact Assessment", Security Through Science, Series C - Environmental Security. Eds. A.  
2746 Ebel, T. Davitashvili, Springer Elsevier Publishers, pp. 115-124, 2007.
- 2747 Mahura, A., Gonzalez-Aparacio, I., Nuterman, R., and Baklanov, A.: Seasonal Impact Analysis on  
2748 Population due to Continuous Sulphur Emissions from Severonikel Smelters of the Kola Peninsula.  
2749 *Geography, Environment, Sustainability*, 11(1), 130-144, doi:10.24057/2071-9388-2018-11-1-130-144,  
2750 2018.
- 2751 Malkhazova, S. M., Mironova, V. A., Orlov, D. S., and Adishcheva, O. S.: Influence of climatic factor on  
2752 naturally determined diseases in a regional context, *Geography, Environment, Sustainability*, 11(1), 157-170,  
2753 doi:10.24057/2071-9388-2018-11-1-157-170, 2018.
- 2754 Malsy, M., Flörke, M., and Borchardt, D.: What drives the water quality changes in the Selenga basin:  
2755 climate change or socio-economic development?, *Reg Environ Chang.*, 17, 1977–1989 doi:10.1007/s10113-  
2756 016-1005-4, 2017.



- 2757 Mammarella, I., Nordbo, A., Rannik, Ü., Haapanala, S., Levula, J., Laakso, H., Ojala, A., Peltola, O.,  
2758 Heiskanen, J., Pumpanen, J. and Vesala, T.: Carbon dioxide and energy fluxes over a small boreal lake in  
2759 Southern Finland, *J. Geophys. Res.: Biogeosciences*, 120(7), 1296-1314, doi:10.1002/2014jg002873, 2015.
- 2760 Manasypov, R. M., Vorobyev, S. N., Loiko, S. V., Krivtsov, I. V., Shirokova, L. S., Shevchenko, V. P.,  
2761 Kirpotin, S. N., Kulizhsky, S. P., Kolesnichenko, L. G., Zemtsov, V. A. and Sinkinov, V. V.: Seasonal  
2762 dynamics of thermokarst lake chemical composition in discontinuous permafrost zone of Western Siberia,  
2763 *Biogeosciences*, 12, 3009-3028, 2015.
- 2764 Marelle, L., Raut, J. C., Law, K. S., and Duclaux, O.: Current and future arctic aerosols and ozone from  
2765 remote emissions and emerging local sources-modeled source contributions and radiative effects, *J.*  
2766 *Geophys. Res.: Atmos.*, 123(22), 12942-12963, doi:10.1029/2018jd028863, 2018.
- 2767 Maslov, A. V., Shevchenko, V. P., Bobrov, V. A., Belogub, E. V., Ershova, V. B., Vereshchagin, O. S., and  
2768 Khvorov, P. V.: Mineralogical-geochemical features of ice-rafted sediments in some arctic regions,  
2769 *Lithology and Mineral Resources*, 53(2), 110-129, doi:10.1134/s0024490218020037, 2018a.
- 2770 Maslov, A. V., Shevchenko, V. P., Kuznetsov, A. B., and Stein, R.: Geochemical and Sr-Nd-Pb-isotope  
2771 characteristics of ice-rafted sediments of the Arctic Ocean, *Geochem. Int.*, 56(8), 751-765,  
2772 doi:10.1134/s0016702918080050, 2018b.
- 2773 Matkala, L., Kulmala, L., Kolari, P., Aurela, M., and Bäck, J.: Resilience of carbon dioxide and water  
2774 exchange to extreme weather events in subarctic Scots pine and Norway spruce stands, *Agricultural and*  
2775 *Forest Meteorology*, 296, 108239, 2020.
- 2776 McCusker, K., Fyfe, J., and Sigmond, M.: Twenty-five winters of unexpected Eurasian cooling unlikely due  
2777 to Arctic sea-ice loss, *Nature Geoscience* 9, 838–842, doi:10.1038/ngeo2820, 2016.
- 2778 Meinander, O., Heikkinen, E., Aurela, M., and Hyvärinen, A.: Sampling, Filtering, and Analysis Protocols to  
2779 Detect Black Carbon, Organic Carbon, and Total Carbon in Seasonal Surface Snow in an Urban Background  
2780 and Arctic Finland (>60° N), *Atmosphere*, 11, 923. doi:10.3390/atmos11090923, 2020a.
- 2781 Meinander, O., Kontu, A., Kouznetsov, R., Sofiev, M.: Snow Samples Combined with Long-Range  
2782 Transport Modeling to Reveal the Origin and Temporal Variability of Black Carbon in Seasonal Snow in  
2783 Sodankylä (67° N), *Front. Earth Sci.*, 8, 13,  
2784 <https://www.frontiersin.org/articles/10.3389/feart.2020.00153/full>, 2020b.
- 2785 Merkouriadi, I., Cheng, B., Graham, R. M., Rösel, A., and Granskog, M. A.: Critical role of snow on sea ice  
2786 growth in the Atlantic sector of the Arctic Ocean. *Geophysical Research Letters*, 44,  
2787 doi:10.1002/2017GL075494, 2017
- 2788 Merkouriadi, I., Cheng, B., Graham, R. M., Rösel, A., and Granskog, M. A.: Critical role of snow on sea ice  
2789 growth in the Atlantic sector of the Arctic Ocean, *Geophys. Res. Lett.*, 44, doi: 10.1002/2017GL075494,  
2790 2018.



- 2791 Mikhailov, E. F., Mironova, S. Y., Makarova, M. V., Vlasenko, S. S., Ryshkevich, T. I., Panov, A. V., and  
2792 Andreae, M. O.: Studying seasonal variations in carbonaceous aerosol particles in the atmosphere over  
2793 central Siberia, *Izv. Atmos. Oceanic Phys.*, 51(4), 423–430, doi:10.1134/s000143381504009x, 2015a.
- 2794 Mikhailov, E. F., Mironov, G. N., Pöhlker, C., Chi, X., Krüger, M. L., Shiraiwa, M., Förster, J.-D., Pöschl,  
2795 U., Vlasenko, S. S., Ryshkevich, T. I., Weigand, M., Kilcoyne, A. L. D., and Andreae, M. O.: Chemical  
2796 composition, microstructure, and hygroscopic properties of aerosol particles at the Zotino Tall Tower  
2797 Observatory (ZOTTO), Siberia, during a summer campaign, *Atmos. Chem. Phys.*, 15, 8847–8869,  
2798 doi:10.5194/acp-15-8847-2015, 2015b.
- 2799 Mikhailov, E. F., Mironova, S., Mironov, G., Vlasenko, S., Panov, A., Chi, X., Walter, D., Carbone, S.,  
2800 Artaxo, P., Heimann, M., Lavric, J., Pöschl, U., and Andreae, M. O.: Long-term measurements (2010–2014)  
2801 of carbonaceous aerosol and carbon monoxide at the Zotino Tall Tower Observatory (ZOTTO) in central  
2802 Siberia, *Atmos. Chem. Phys.*, 17, 14365–14392, doi:10.5194/acp-17-14365-2017, 2017.
- 2803 Mikola, J., Virtanen, T., Linkosalmi, M., Vähä, E., Nyman, J., Postanogova, O., Räsänen, A., Kotze, D. J.,  
2804 Laurila, T., Juutinen, S., Kondratyev, V., and Aurela, M.: Spatial variation and linkages of soil and  
2805 vegetation in the Siberian Arctic tundra – coupling field observations with remote sensing data,  
2806 *Biogeosciences*, 15, 2781–2801, doi:10.5194/bg-15-2781-2018, 2018.
- 2807 Miles, V. V., and Esau, I.: Spatial heterogeneity of greening and browning between and within bioclimatic  
2808 zones in northern West Siberia, *Environ. Res. Lett.*, 11(11), 12, doi:10.1088/1748-9326/11/11/115002, 2016.
- 2809 Miles, V., and Esau, I.: Seasonal and Spatial Characteristics of Urban Heat Islands (UHIs) in Northern West  
2810 Siberian Cities., *Remote Sens.*, 9, 989, 2017.
- 2811 Miles, M. W., Miles, V., and Esau, I.: Varying climate response across the tundra, forest–tundra and boreal  
2812 forest biomes in northern West Siberia, *Environ. Res. Lett.*, 14, 075008, doi:10.1088/1748-9326/ab2364,  
2813 2019.
- 2814 Miles, V., and Esau, I.: Surface urban heat islands in 57 cities across different climates in northern  
2815 Fennoscandia, *Urban Climate*, 31, 10.1016/j.uclim.2019.100575, 2020.
- 2816 Miles, V.: [Arctic surface Urban Heat Island \(UHI\), MODIS Land Surface Temperature \(LST\) data, 2000-  
2817 2016](#). Arctic Data Center. doi:10.18739/A2TB0XW4T, 2020.
- 2818 Mori, M., Watanabe, M., Shiogama, H., Inoue, J., and Kimoton, M.: Robust Arctic sea-ice influence on the  
2819 frequent Eurasian cold winters in past decades, *Nat. Geosci.*, 7, 869–873, doi:10.1038/ngeo2277, 2014.
- 2820 Mori, M., Kosaka, Y., Watanabe, M., Nakamura, H., and Kimoto, M.: A reconciled estimate of the influence  
2821 of Arctic sea-ice loss on recent Eurasian cooling, *Nat. Clim. Change*, 9, 123–129, doi: 10.1038/s41558-018-  
2822 0379-3, 2019.
- 2823 Morozov, E. A., Kondrik, D. V., Chepikova, S. S., and Pozdnyakov, D. V.: Atmospheric columnar CO<sub>2</sub>  
2824 enhancement over *E. huxleyi* blooms: case studies in the North Atlantic and Arctic waters. *Transactions of*



- 2825 the Karelian Research Centre of the Russian Academy of Sciences, *Limnologia i Oceanologia* series, 3, 1-6.  
2826 doi:10.17076/lim989, 2019.
- 2827 Myslenkov S., Medvedeva A., Arkhipkin V., Markina M., Surkova G., Krylov A., Dobrolyubov S.,  
2828 Zilitinkevich S., and Koltermann P.: Long-term statistics of storms in the Baltic, Barents and White Seas and  
2829 their future climate projections., *Geography, environment, sustainability*, 11, 93-112, doi:10.24057/2071-  
2830 9388-2018-11-1-93-112, 2018.
- 2831 Mäki, M., Krasnov, D., Hellén, H., Noe, S. M., and Bäck, J.: Stand type affects fluxes of volatile organic  
2832 compounds from the forest floor in hemiboreal and boreal climates, *Plant Soil*, 441, 363–381,  
2833 doi:10.1007/s11104-019-04129-3, 2019.
- 2834 Naakka, T., Nygård, T., Vihma, T., Graversen, R., and Sedlar, J.: Atmospheric moisture transport between  
2835 mid-latitudes and the Arctic: regional, seasonal and vertical distributions, *Int. J. Climatol.*, 32, 1–18,  
2836 doi:10.1002/joc.5988, 2019.
- 2837 Natali, S.M., Watts, J.D., Rogers, B.M., Potter, S., Ludwig, S. M., Selbmann, A. K., Sullivan, P.F. Abbott, B.  
2838 W., Arndt, K. A., Birch, L., Björkman, M.P., Bloom, A., Celis, G., Christensen, T. R., Christiansen, C. T.,  
2839 Commane, R., Cooper, E. J., Crill, P., Czimeczik, C., Davydov, S., Du, J., Egan, J.E., Elberling, B.,  
2840 Euskirchen, B.S., Friborg, T., Genet, H., Göckede, M., Goodrich, J.P., Grogan, P., Helbig, M., Jafarov, E.E.,  
2841 Jastrow, J. D., Kalhori, A.A.M., Kim, Y Kimball, J. S., Kutzbach, L., Lara, M. J, Larsen, K., S., Lee, B.-Y.,  
2842 Liu, Z., Loranty, M. M., Lund, M., Lupascu, M., Madani, N., Malhotra, A., Matamala, R., McFarland, J.,  
2843 McGuire, A. D., Michelsen, A., Minions, C., Oechel, W., Olefeldt, D., Parmentier, F.-J., Pirk, N., Poulter,  
2844 B., Quinton, W., Rezanezhad, F., Risk, D., Sachs, T., Schaefer, K., Schmidt, N. M., Schuur, E., Semenchuk,  
2845 P. R., Shaver, G., Sonnentag, O., Starr, G., Treat, C. C., Waldrop, M. P., Wang, Y., Welker, J., Wille, C., Xu,  
2846 X., Zhang, Z., Zhuang, Q., and Zona, D.: Large loss of CO<sub>2</sub> in winter observed across the northern  
2847 permafrost region, *Nat. Clim. Chang.*, 9, 852–857, doi:10.1038/s41558-019-0592-8, 2019.
- 2848 Nikandrova, A., Tabakova, K., Manninen, A., Väänänen, R., Petäjä, T., Kulmala, M., Kerminen, V.-M., and  
2849 O'Connor, E.: Combining airborne in situ and ground-based lidar measurements for attribution of aerosol  
2850 layers, *Atmos. Chem. Phys.*, 18, 10575–10591, doi:10.5194/acp-18-10575-2018, 2018.
- 2851 NILU, 2013: Sandanger, T.M., Anda, E., Berglen, T.F., Evenset, A., Christensen, G., and Heimstad, E.S.:  
2852 Health and environmental impacts in the Norwegian border area related to local Russian industrial emissions.  
2853 Knowledge status, 40/2013, 2013.
- 2854 Nissen, C., Munnich, M., Grube, M., and Haumann, N.: Factors controlling coccolithophore biogeography in  
2855 the Southern Ocean, *Biogeosciences*, 15(22), 6997-7024, doi:10.5194/bg-15-6997-2018, 2018.
- 2856 Nitzbon, J., Langer, M., Westermann, S., Martina, L., Aas, K. S., and Boike, J.: Pathways of ice-wedge  
2857 degradation in polygonal tundra under different hydrological conditions, *Cryosphere*, 13(4), 1089-1123,  
2858 doi:10.5194/tc-13-1089-2019, 2019.



- 2859 Nygård, T., Graversen, R. G., Uotila, P., Naakka, T., and Vihma, T.: Strong dependence of wintertime Arctic  
2860 moisture and cloud distributions on atmospheric large-scale circulation, *J. Climate*, 32, 8771-8790, doi:  
2861 10.1175/JCLI-D-19-0242.1, 2019.
- 2862 Overland, J., Dunlea, E., Box, J. E., Corell, R., Forsius, M., Kattsov, V., Olsen, M. S., Pawlak, J., Reiersen,  
2863 L. O., and Wang, M.: The urgency of Arctic change, *Polar Science*, 21, 6-13,  
2864 doi:10.1016/j.polar.2018.11.008, 2019.
- 2865 Paasonen, P., Peltola, M., Kontkanen, J., Junninen, H., Kerminen, V.-M., and Kulmala, M.: Comprehensive  
2866 analysis of particle growth rates from nucleation mode to cloud condensation nuclei in boreal forest, *Atmos.*  
2867 *Chem. Phys.*, 18, 12085–12103, doi:10.5194/acp-18-12085-2018, 2018.
- 2868 Palo, T., Vihma, T., Jaagus, J., and Jakobson, E.: Observations on temperature inversion over central Arctic  
2869 sea ice in summer, *Q. J. R. Meteorol. Soc.*, 143(708), 2741-2754, doi:10.1002/qj.3123, 2017.
- 2870 Panov, A. V., Prokushkin, A. S., Bryukhanov, A. V., Korets, M. A., Ponomarev, E. I., Sidenko, N. V.,  
2871 Zrazhevskaya, G. K., Timokhina, A. V., and Andreae, M. O.: A complex approach for the estimation of  
2872 carbonaceous emissions from wildfires in Siberia, *Russian Meteorol. Hydrol.*, 43(5), 295-301, 2018.
- 2873 Parmentier, F. W., Christensen, T. R., Rysgaard, S. Bendtsen, J., Glud, R. N., Else, B., van Huissteden, J.,  
2874 Sachs, T., Vonk, J. E., and Sejr, M. K.: A synthesis of the arctic terrestrial and marine carbon cycles under  
2875 pressure from a dwindling cryosphere, *Ambio*, 46, 53–69, doi:10.1007/s13280-016-0872-8, 2017.
- 2876 Parshintsev, J., Vaikkinen, A., Lipponen, K., Vrkoslav, V., Cvačka, J., et al. : Desorption atmospheric  
2877 pressure photoionization high-resolution mass spectrometry: a complementary approach for the chemical  
2878 analysis of atmospheric aerosols, *Rapid Commun. Mass Spectrom.*, 29, 1233–1241, 2015.
- 2879 Passananti, M., Zapadinsky, E., Zanca, T., Kangasluoma, J., Myllys, N., Rissanen, M.P., Kurtén, T., Ehn, M.,  
2880 Attoui, M., and Vehkamäki, H.: How well can we predict cluster fragmentation inside a mass spectrometer?  
2881 *Chem. Commun.*, 55, 5946-5949, 2019.
- 2882 Payne, R. J., Creevy, A., Malysheva, E., Ratcliffe, J., Andersen, R., Tsyganov, A. N., Rowson, J., Marcisz,  
2883 K., Zielinska, M., Lamentowicz, M., Lapshina, E. D., and Mazei, Y.: Tree encroachment may lead to  
2884 functionally-significant changes in peatland testate amoeba communities. *Soil Biology & Biochemistry*, 98,  
2885 18-21. doi:10.1016/j.soilbio.2016.04.002, 2016.
- 2886 Peltola, O., Vesala, T., Gao, Y.; Rätty, O. et al. : Monthly gridded data product of northern wetland methane  
2887 emissions based on upscaling eddy covariance observations, *Earth System Science Data*, 11, 1263-1289,  
2888 doi:10.5194/essd-11-1263-2019, 2019.
- 2889 Peltoniemi, J. I., Gritsevich, M., Hakala, T., Dagsson-Waldhauserová, P., Arnalds, Ó., Anttila, K., Hannula,  
2890 H.-R., Kivekäs, N., Lihavainen, H., Meinander, O., Svensson, J., Virkkula, A., and de Leeuw, G.: Soot on



- 2891 Snow experiment: bidirectional reflectance factor measurements of contaminated snow, *The Cryosphere*, 9,  
2892 2323–2337, doi:10.5194/tc-9-2323-2015, 2015.
- 2893 Peterson, B. J., Holmes, R. M., McClelland, J. W., Vörösmarty, C. J., Lammers, R. B., Shiklomanov, A. I.,  
2894 Shiklomanov, I. A., and Rahmstorf, S.: Increasing river discharge to the Arctic Ocean, *Science*, 80, 298,  
2895 2171–2173, doi: 10.1126/science.1077445, 2002.
- 2896 Petäjä, T., Järvi, L., Kerminen, V.-M., Ding, A. J., Sun, J. N., Nie, W., Kujansuu, J., Virkkula, A., Yang, X.-  
2897 Q., Fu, C. B., Zilitinkevich, S., and Kulmala M.: Enhanced air pollution via aerosol-boundary layer feedback  
2898 in China, *Scientific Reports*, 6, 18998, doi:10.1038/srep18998, 2016.
- 2899 Petäjä, T., Duplissy, E.-M., Tabakova, K., Schmale, J., Altstädter, B., Ancellet, G., Arshinov, M., Balin, Y.,  
2900 Baltensperger, U., Bange, J., Beamish, A., Belan, B., Berchet, A., Bossi, R., Cairns, W. R. L., Ebinghaus, R.,  
2901 El Haddad, I., Ferreira-Araujo, B., Franck, A., Huang, L., Hyvärinen, A., Humbert, A., Kalogridis, A.-C.,  
2902 Konstantinov, P., Lampert, A., MacLeod, M., Magand, O., Mahura, A., Marelle, L., Masloboev, V.,  
2903 Moiseev, D., Moschos, V., Neckel, N., Onishi, T., Osterwalder, S., Ovaska, A., Paasonen, P., Panchenko,  
2904 M., Pankratov, F., Pernov, J. B., Platis, A., Popovicheva, O., Raut, J.-C., Riandet, A., Sachs, T., Salvatori, R.,  
2905 Salzano, R., Schröder, L., Schön, M., Shevchenko, V., Skov, H., Sonke, J. E., Spolaor, A., Stathopoulos, V.,  
2906 K., Strahlendorff, M., Thomas, J. L., Vitale, V., Vratolis, S., Barbante, C., Chabrillat, S., Dommergue, A.,  
2907 Eleftheriadis, K., Heilimo, J., Law, K. S., Massling, A., Noe, S. M., Paris, J.-D., Prévôt, A. S. H., Riipinen,  
2908 I., Wehner, B., Xie, Z., and Lappalainen, H. K.: Overview: Integrative and Comprehensive Understanding on  
2909 Polar Environments (iCUPE) – concept and initial results, *Atmos. Chem. Phys.*, 20, 8551–8592,  
2910 doi:10.5194/acp-20-8551-2020, 2020a.
- 2911 Petäjä, T., Ganzei, K. S., Lappalainen, H. K., Tabakova, K., Makkonen, R., Räisänen, J., Chalov, S.,  
2912 Kulmala, M., Zilitinkevich, S. S., Baklanov, P., Shakirov, R. B., Mishina, N.V., Egidarev, E.G., and  
2913 Kondrat'ev, I. I.: Research agenda for the Russian Far East and utilization of multi-platform comprehensive  
2914 environmental observations, *J. Big Data*, submitted, 2020b.
- 2915 Pietron, J., Jarsjo, J., Romanchenko, A. O., and Chalov, S. R.: Model analyses of the contribution of in-  
2916 channel processes to sediment concentration hysteresis loops, *Journal of Hydrology*, 527, 576-589.  
2917 doi:10.1016/j.jhydrol.2015.05.009, 2015.
- 2918 Pietron, J., Nittrouer, J. A., Chalov, S. R., Dong, T. Y., Kasimov, N., Shinkareva, G., and Jarsjö, J.:  
2919 Sedimentation patterns in the Selenga River delta under changing hydroclimatic conditions, *Hydrological  
2920 Processes*, 32(2), 278-292, doi:10.1002/hyp.11414, 2018.
- 2921 Pirazzini, R., Leppanen, L., Picard, G., Lopez-Moreno, J. I., Marty, C., Macelloni, G., Kontu, A., Von  
2922 Lerber, A., Tanis, C.M., Schneebeli, M., De Rosnay, P., Arslan, A. N.: European in-situ snow measurements:  
2923 practices and purposes, *Sensors*, 18(7), 51, doi:10.3390/s18072016, 2018.
- 2924 Pisso, I., Myhre, C. L., Platt, S. M., Eckhardt, S., Hermansen, O., Schmidbauer, N., Mienert, J.,  
2925 Vadakkepuliambatta, S., Bauguitte, S., Pitt, J., Allen, G., Bower, K. N., O'Shea, S., Gallagher, M. W.,



- 2926 Percival, C. J., Pyle, J., Cain, M., and Stohl, A.: Constraints on oceanic methane emissions west of Svalbard  
2927 from atmospheric in situ measurements and Lagrangian transport modeling, *J. Geophys. Res. Atmos.*,  
2928 121(23), 14188-14200, doi:10.1002/2016jd025590, 2016.
- 2929 Platt, S. M., Eckhardt, S., Ferré, B., Fisher, R. E., Hermansen, O., Jansson, P., Lowry, D., Nisbet, E. G.,  
2930 Pisso, I., Schmidbauer, N., Silyakova, A., Stohl, A., Svendby, T. M., Vadakkepuliambatta, S., Mienert, J.,  
2931 and Lund Myhre, C.: Methane at Svalbard and over the European Arctic Ocean, *Atmos. Chem. Phys.*, 18,  
2932 17207–17224, doi:10.5194/acp-18-17207-2018, 2018.
- 2933 Ponomarev, Evgenii I., Kharuk, Viacheslav I., and Ranson, Kenneth J.: Wildfires Dynamics in Siberian Larch  
2934 Forests, *Forests*, 7(6), 125, 2016.
- 2935 Popovicheva O., Evangeliou N., Eleftheriadis K., Kalogridis A. C., Sitnikov V. N., Eckhardt S., Stohl A.:  
2936 Black carbon sources constrained by observations and modeling in the Russian high Arctic, *Environmental*  
2937 *Science Technology*, 51(7), 3871-3879, 2017.
- 2938 Popovicheva, O., Diapouli, E., Makshatas, A., Shonija, N., Manousakas, M., Saraga, D., Uttal, T., and  
2939 Eleftheriadis, K.: East Siberian Arctic background and black carbon polluted aerosols at HMO Tiksi, *Science*  
2940 *of the Total Environment*, 655, 924-938, doi:10.1016/j.scitotenv.2018.11.165, 2019a.
- 2941 Popovicheva, O. B., Engling, G., Ku, I. T., Timofeev, M. A., and Shonija, N. K.: Aerosol emissions from  
2942 long-lasting smoldering of boreal peatlands: chemical composition, markers, and microstructure, *Aerosol*  
2943 *and Air Quality Research*, 19(3), 484-503, doi:10.4209/aaqr.2018.08.0302, 2019b.
- 2944 Popovicheva, O. B., Padoan, S., Schnelle-Kreis, J., Nguyen, D. L., Adam, T.W., Kistler, M., Steinkogler, T.,  
2945 Kasper-Giebl, A., Zimmermann, R., and Chubarova, N. E.: Spring aerosol in urban atmosphere of megacity:  
2946 analytical and statistical assessment for source impacts, *Aerosol and Air Quality Research*, 20, 702–719,  
2947 2020a.
- 2948 Popovicheva O., Ivanov A., and Vojtisek M.: Functional Factors of Biomass Burning Contribution to Spring  
2949 Aerosol Composition in a Megacity: Combined FTIR-PCA Analyses, *Atmosphere*, 11, 319-339, 2019b.
- 2950 Popovicheva, O., Volpert, E., Sitnikov, N., Chichayeva, M., and Padoan, S.: Black carbon in spring aerosols  
2951 of Moscow urban background, *Geography, Environment, Sustainability*, 13, 1, 233-243, 2020c
- 2952 Pozdnyakov D. V., Pettersson L. H., and Korosov A. A.: Exploring the Marine Ecology from Space.  
2953 Springer, Switzerland, 2017.
- 2954 Pozdnyakov, D. V., Kondrik, D.V., Kazakov, E. E., and Chepikova, S.: Environmental conditions favoring  
2955 coccolithophore blooms in subarctic and arctic seas: a 20-year satellite and multi-dimensional statistical  
2956 study, *Proc. SPIE 11150, Remote Sensing of the Ocean, Sea Ice, Coastal Waters, and Large Water Regions*,  
2957 111501W, 14 October 2019, doi: 10.1117/12.2547868, 2019.



- 2958 Pozdnyakov D., Kondrik D., and Chepikova S.: Origination of *E. huxleyi* extraordinary bloom outbursts in  
2959 the Bering Sea between the late 1990s and early 2000s, and in 2018–2019: A hypothesis, *Fisheries*  
2960 *Oceanography*, submitted, 2020.
- 2961 Preis, Y. I., Simonova, G. V., Voropay, N. N., and Dyukarev, E. A.: Estimation of the influence of  
2962 hydrothermal conditions on the carbon isotope composition in *Sphagnum* mosses of bogs of Western Siberia,  
2963 *IOP Conf. Series: Earth Environ. Sci.*, 211, doi:10.1088/1755-1315/211/1/012031, 2018.
- 2964 Pugach S. P., Pipko I. I., Shakhova, N. E., Shirshin, E. A., Perminova, I. V., Gustafsson, O., Bondur, V. G.,  
2965 Ruban, A. S., and Semiletov, I. P.: Dissolved organic matter and its optical characteristics in the Laptev and  
2966 East Siberian seas: spatial distribution and interannual variability (2003–2011), *Ocean Sci.*, 14, 87–103,  
2967 doi:10.5194/os-14-87-2018, 2018.
- 2968 Pulliainen, J., Aurela, M., Laurila, T., Aalto, T., Takala, M., Salminen, M., Kulmala, M., Barr, A., Heimann,  
2969 M., Lindroth, A., Laaksonen, A., Derksen, C., Mäkelä, A., Markkanen, T., Lemmetyinen, J., Susiluoto, J.,  
2970 Dengel, S., Mammarella, I., Tuovinen, J.-P., and Vesala, T.: Early snowmelt significantly enhances boreal  
2971 springtime carbon uptake, *PNAS*, 114(42), 11081–11086, doi:10.1073/pnas.1707889114, 2017.
- 2972 Pulliainen, J., Luojus, K., Derksen, C., Mudryk, L., Lemmetyinen, J., Salminen, M., Ikonen, J., Takala, M.,  
2973 Cohen, J., Smolander, T., and Norberg, J.: Patterns and trends of Northern Hemisphere snow mass from  
2974 1980 to 2018, *Nature* 581, 294–298, doi:10.1038/s41586-020-2258-0, 2020.
- 2975 Pärn, J., Verhoeven, J.T., Butterbach-Bahl, K., Dise, N.B., Ullah, S., Aasa, A., Egorov, S., Espenberg, M.,  
2976 Järveoja, J., Jauhiainen, J. and Kasak, K.: Nitrogen-rich organic soils under warm well-drained conditions  
2977 are global nitrous oxide emission hotspots, *Nat. Commun.*, 9, 1135, doi:10.1038/s41467-018-03540-1, 2018.
- 2978 Qi, X. M., Ding, A. J., Nie, W., Petäjä, T., Kerminen, V.-M., Herrmann, E., Xie, Y. N., Zheng, L. F.,  
2979 Manninen, H., Aalto, P., Sun, J. N., Xu, Z. N., Chi, X. G., Huang, X., Boy, M., Virkkula, A., Yang, X.-Q.,  
2980 Fu, C. B., and Kulmala, M.: Aerosol size distribution and new particle formation in the western Yangtze  
2981 River Delta of China: 2 years of measurements at the SORPES station, *Atmos. Chem. Phys.*, 15, 12445–  
2982 12464, doi:10.5194/acp-15-12445-2015, 2015.
- 2983 Rakitin, V. S., Elansky, N. F., Wang, P., Wang, G., Pankratova, N. V., Shtabkin, Y. A., Skorokhod A.I.,  
2984 Safronov A.N., Makarova M.V., and Grechko E.I.: Changes in trends of atmospheric composition over urban  
2985 and background regions of Eurasia: estimates based on spectroscopic observations, *Geography,*  
2986 *Environment, Sustainability*, 11(2), 84–96, doi:10.24057/2071-9388-2018-11-2-84-96, 2018.
- 2987 Rautiainen, K., Parkkinen, T., Lemmetyinen, J., Schwank, M., Wiesmann, A., Ikonen, J., Derksen, C.,  
2988 Davydov, S., Davydova, A., Boike, J., Langer, M., Drusch, M., and Pulliainen, J.: SMOS prototype  
2989 algorithm for detecting autumn soil freezing, *Remote Sensing of Environment*, 180, 346–360,  
2990 doi:10.1016/j.rse.2016.01.012, 2016.



- 2991 Rinke, A., Segger, B., Crewell, S., Maturilli, M., Naakka, T., Nygård, T., Vihma, T., Alshawaf, F., Dick, G.,  
2992 Wickert, J., and Keller, J.: Trends of vertically integrated water vapor over the Arctic during 1979-2016:  
2993 Consistent moistening all over?, *J. Climate*, 32, 6097–6116, doi:10.1175/JCLI-D-19-0092.1, 2019.
- 2994 Ripple, W. J., Wolf, C., Newsome, T. M., Galetti, M., Alamgir, M., Crist, E., Mahmoud, M. I., Laurance, W.  
2995 F., and 15,364 scientist signatories from 184 countries. World scientists' warning to humanity: A second  
2996 notice, *BioScience*, 67(12), 1026-1028, 2017.
- 2997 Rivero-Calle, S., Gnanadesikan, A., Del Castillo, C., Balch, W., and Guikema, S.: Multidecadal increase in  
2998 North Atlantic coccolithophores and the potential role of rising CO<sub>2</sub>, *Science*, 350 (6267), 1533-1537, doi:  
2999 10.1126/science.aaa8026, 2015.
- 3000 Romanowsky, E., Handorf, D., Jaiser, R., Wohltmann, I., Dorn, W., Ukita, J., Cohen, J., Dethloff, K., and  
3001 Rex, M.: The role of stratospheric ozone for Arctic-midlatitude linkages, *Sci. Rep.* 9, 7962,  
3002 doi:10.1038/s41598-019-43823-1, 2019.
- 3003 Romanovsky, V. E., and Osterkamp, T. E.: Effects of unfrozen water on heat and mass transport processes in  
3004 the active layer and permafrost, *Permafrost Periglac. Process*, 11, 219–39, 2000.
- 3005 Rost, B., and Riebesell, U.: Coccolithophores and the biological pump: responses to environmental changes,  
3006 in: *Coccolithophores, from molecular processes to global impact*, edited by: Thierstein, H. R., Young, J. R.,  
3007 99–125, Springer, Heidelberg, Germany, 2004.
- 3008 Ryazanova, A., and Voropay, N. N.: Droughts and Excessive Moisture Events in Southern Siberia in the  
3009 Late XXth - Early XXIst Centuries, *IOP Conf. Ser.: Earth Environ. Sci.*, 96, 012015, 2017.
- 3010 Räisänen, J.: Effect of atmospheric circulation on recent temperature changes in Finland, *Clim. Dyn.*, 53,  
3011 5675–5687, doi:10.1007/s00382-019-04890-2, 2019.
- 3012 Räisänen, J.: Effect of atmospheric circulation on surface air temperature trends in years 1979-2018, *Clim.*  
3013 *Dyn.*, *Clim. Dyn.*, in press, 2020.
- 3014 Saarela, T., Rissanen, A. J., Ojala, A. et al.: CH<sub>4</sub> oxidation in a boreal lake during the development of  
3015 hypolimnetic hypoxia, *Aquat Sci*, 82, 19, /doi.org/10.1007/s00027-019-0690-8, 2020.
- 3016 Salmon, Y., Lintunen, A., Dayet, A., Chan, T., Dewar, R., Vesala, T. and Hölttä, T.: Leaf carbon and water  
3017 status control stomatal and non-stomatal limitations of photosynthesis in trees, *New Phytologist* 226, 690-  
3018 703. doi: 10.1111/nph.16436, 2020.
- 3019 Santalahti, M., Sun, H., Sietiö, O.M., Köster, K., Berninger, F., Laurila, T., Pumpanen, J., and Heinonsalo,  
3020 J.: Reindeer grazing alter soil fungal community structure and litter decomposition related enzyme activities  
3021 in boreal coniferous forests in Finnish Lapland, *App. Soil Ecol.*, 132, 74-82,  
3022 doi:10.1016/j.apsoil.2018.08.013, 2018.



- 3023 Schallhart, S., Rantala, P., Kajos, M. K., Aalto, J., Mammarella, I., Ruuskanen, T. M., and Kulmala, M.:  
3024 Temporal variation of VOC fluxes measured with PTR-TOF above a boreal forest, *Atmospheric Chemistry*  
3025 *and Physics*, 18(2), 815-832. doi:10.5194/acp-18-815-2018, 2018.
- 3026 Schmale, J., Arnold, S. R., Law, K. S., Thorp, T., Anenberg, S., Simpson, W. R., Mao, J. and Pratt, K. A.:  
3027 Local Arctic air pollution: a neglected but serious problem, *Earths Future*, 6(10), 1385-1412,  
3028 doi:10.1029/2018ef000952, 2018a.
- 3029 Schmale, J., Henning, S., Decesari, S., Henzing, B., Keskinen, H., Sellegri, K., Ovadnevaite, J., Pöhlker, M.  
3030 L., Brito, J., Bougiatioti, A., Kristensson, A., Kalivitis, N., Stavroulas, I., Carbone, S., Jefferson, A., Park,  
3031 M., Schlag, P., Iwamoto, Y., Aalto, P., Äijälä, M., Bukowiecki, N., Ehn, M., Frank, G., Fröhlich, R.,  
3032 Frumau, A., Herrmann, E., Herrmann, H., Holzinger, R., Kos, G., Kulmala, M., Mihalopoulos, N., Nenes,  
3033 A., O'Dowd, C., Petäjä, T., Picard, D., Pöhlker, C., Pöschl, U., Poulain, L., Prévôt, A. S. H., Swietlicki, E.,  
3034 Andreae, M. O., Artaxo, P., Wiedensohler, A., Ogren, J., Matsuki, A., Yum, S. S., Stratmann, F.,  
3035 Baltensperger, U., and Gysel, M.: Long-term cloud condensation nuclei number concentration, particle  
3036 number size distribution and chemical composition measurements at regionally representative observatories,  
3037 *Atmos. Chem. Phys.*, 18, 2853–2881, doi:10.5194/acp-18-2853-2018, 2018b.
- 3038 Schmeisser, L., Backman, J., Ogren, J. A., Andrews, E., Asmi, E., Starkweather, S., Uttal, T., Fiebig, M.,  
3039 Sharma, S., Eleftheriadis, K., Vratolis, S., Bergin, M., Tunved, P., and Jefferson, A.: Seasonality of aerosol  
3040 optical properties in the Arctic, *Atmos. Chem. Phys.*, 18, 11599–11622, doi:10.5194/acp-18-11599-2018,  
3041 2018.
- 3042 Schuur, E. A. G., Bockheim, J., Canadell, J. G., Euskirchen, E., Field, C. B., Goryachkin, S. V., Hagemann,  
3043 S., Kuhry, P., Laflour, P.M., Lee, H., Mazhitova, G., Nelson, F. E., Rinke, A., Romanovsky, V. E.,  
3044 Shiklomanov, N., Tarnocai, C., Venevsky, S., Vogel, J. G., and Zimov, S. A.: Vulnerability of permafrost  
3045 carbon to climate change: implications for the global carbon cycle, *BioScience*, 58(8), 701–714,  
3046 doi:10.1641/B580807, 2008.
- 3047 Schuur, E. A. G., McGuire, A. D., Romanovsky, V., Schädel, C., and Mack, M.: Chapter 11: Arctic and  
3048 boreal carbon, in: *Second State of the Carbon Cycle Report (SOCCR2): A Sustained Assessment Report*,  
3049 edited by: Cavallaro, N., Shrestha, G., Birdsey, R., Mayes, M. A., Najjar, R. G., Reed, S. C., Romero-  
3050 Lankao, P., and Zhu, Z., U.S. Global Change Research Program, Washington, DC, USA, 428-468,  
3051 doi:10.7930/SOCCR2.2018.Ch11, 2018.
- 3052 Scott, C. E., Monks, S. A., Spracklen, D. V., Arnold, S. R., Forster, P. M., Rap, A., Äijälä, M., Artaxo, P.,  
3053 Carslaw, K. S., Chipperfield, M. P., Ehn, M., Gilardoni, S., Heikkinen, L., Kulmala, M., Petäjä, T.,  
3054 Reddington, C. L. S., Rizzo, L. V., Swietlicki, E., Vignati, E., and Wilson, C.: Impact on short-lived climate  
3055 forcers increases projected warming due to deforestation, *Nat. Commun.*, 9, 9, doi:10.1038/s41467-017-  
3056 02412-4, 2018.



- 3057 Shakhova, N., Semiletov, I., and Belcheva, N.: The great Siberian rivers as a source of methane on the  
3058 Russian Arctic shelf, *Dokl. Earth Sci.*, 415, 734–736, doi: 10.1134/S1028334X07050169, 2007.
- 3059 Shalina, E. V., and Sandven, S.: Snow depth on Arctic sea ice from historical in situ data, *Cryosphere*, 12(6),  
3060 1867-1886, doi:10.5194/tc-12-1867-2018, 2018.
- 3061 Shen, Y., Virkkula, A., Ding, A., Wang, J., Chi, X., Nie, W., Qi, X., Huang, X., Liu, Q., Zheng, L., Xu, Z.,  
3062 Petäjä, T., Aalto, P. P., Fu, C., and Kulmala, M.: Aerosol optical properties at SORPES in Nanjing, east  
3063 China, *Atmos. Chem. Phys.*, 18, 5265–5292, doi: 10.5194/acp-18-5265-2018, 2018.
- 3064 Shen, Y., Virkkula, A., Ding, A., Luoma, K., Keskinen, H., Aalto, P. P., Chi, X., Qi, X., Nie, W., Huang, X.,  
3065 Petäjä, T., Kulmala, M., and Kerminen, V.-M.: Estimating cloud condensation nuclei number concentrations  
3066 using aerosol optical properties: role of particle number size distribution and parameterization, *Atmos.*  
3067 *Chem. Phys.*, 19, 15483–15502, doi:10.5194/acp-19-15483-2019, 2019.
- 3068 Shestakova, T. A., Gutierrez, E., Valeriano, C., Lapshina, E., and Voltas, J.: Recent loss of sensitivity to  
3069 summer temperature constrains tree growth synchrony among boreal Eurasian forests, *Agr. Forest Meteorol.*,  
3070 268, 318-330, doi:10.1016/j.agrformet.2019.01.039, 2019.
- 3071 Shevchenko, V. P., Starodymova, D. P., Vinogradova, A. A., Lisitzin, A. P., Makarov, V. I., Popova, S. A.,  
3072 Sivonen, V. V., and Sivonen, V. P.: Elemental and organic carbon in atmospheric aerosols over the  
3073 northwestern coast of Kandalaksha Bay of the White Sea, *Dokl. Earth Sci.*, 461(1), 242-246,  
3074 doi:10.1134/s1028334x1503006x, 2015.
- 3075 Shevchenko, V. P., Maslov, A. V., and Stein, R.: Distribution of some rare and trace elements in ice-rafted  
3076 sediments in the Yermak Plateau area, the Arctic Ocean, *Oceanol.*, 57(6), 855-863,  
3077 doi:10.1134/s0001437017060157, 2017a.
- 3078 Shevchenko, V. P., Pokrovsky, O. S., Vorobyev, S. N., Krickov, I. V., Manasyov, R. M., Politova, N. V.,  
3079 Kopysov, S. G., Dara, O. M., Auda, Y., Shirokova, L. S., Kolesnichenko, L. G., Zemtsov, V. A., and  
3080 Kirpotin, S. N.: Impact of snow deposition on major and trace element concentrations and elementary fluxes  
3081 in surface waters of the Western Siberian Lowland across a 1700 km latitudinal gradient, *Hydrol. Earth Syst.*  
3082 *Sci.*, 21, 5725–5746, doi:10.5194/hess-21-5725-2017, 2017b.
- 3083 Shevchenko, V. P., Kopeikin, V. M., Novigatsky, A. N., and Malafeev, G. V.: Black carbon in the  
3084 atmospheric boundary layer over the North Atlantic and the Russian Arctic seas in June–September 2017,  
3085 *Oceanol.*, 59(5), doi:10.1134/S0001437019050199, 692–696, 2019.
- 3086 Shevnina, E., Kourzeneva, E., Kovalenko, V., and Vihma, T.: Assessment of extreme flood events in a  
3087 changing climate for a long-term planning of socio-economic infrastructure in the Russian Arctic, *Hydrol.*  
3088 *Earth Syst. Sci.*, 21(5), 2559-2578, doi:10.5194/hess-21-2559-2017, 2017.
- 3089 Shevnina, E., Silaev, A., and Vihma, T.: Probabilistic projections of annual runoff and potential hydropower  
3090 production in Finland, *Universal Journal of Geoscience*, 7(2), 43-55, doi:10.13189/ujg.2019.070201, 2019.



- 3091 Shiklomanov, A.I., and Lammers, R.B.: Record Russian river discharge in 2007 and the limits of analysis,  
3092 *Environ. Res. Lett.*, 4, doi: 10.1088/1748-9326/4/4/045015, 2009.
- 3093 Shinkareva G. L., Lychagin M. Y., Tarasov M. K., Pietroni J., Chichaeva M. A., and Chalov S. R.:  
3094 Biogeochemical specialization of macrophytes and their role as a biofilter in the Selenga delta, *Geography,*  
3095 *Environment, Sustainability*, 12(3), 240-263, 2019.
- 3096 Silkin, V. A., Pautova, L., Giordano, M., Chasovnikov, V., Vostokov, S., Podymov, O., Parkhomova, S., and  
3097 Moskalenko, L.: Drivers of phytoplankton blooms in the northeastern Black Sea, *Mar. Pollution Bull.*, 138,  
3098 274-284, doi:10.1016/j.marpolbul.2018.11.042, 2018.
- 3099 Sizov O. S., and Lobotrosova S. A.: Features of revegetation of drift sand sites in the northern taiga subzone  
3100 of Western Siberia. *Earth Cryosphere*, (3), 3–13, doi:10.21782/kz1560-7496-2016-3(3-13), 2016.
- 3101 Skorokhod, A. I., Berezina, E. V., Moiseenko, K. B., Elansky, N. F., and Belikov, I. B.: Benzene and toluene  
3102 in the surface air of northern Eurasia from TROICA-12 campaign along the Trans-Siberian Railway, *Atmos.*  
3103 *Chem. Phys.*, 17(8), 5501-5514, doi:10.5194/acp-17-5501-2017, 2017.
- 3104 Slukovskaya, M. V., Vasenev, V. I., Ivashchenko, K. V., Morev, D. V., Drogobuzhskaya, S. V., Ivanova, L.  
3105 A., and Kremenetskaya, I. P.: Technosols on mining wastes in the subarctic: Efficiency of remediation under  
3106 Cu-Ni atmospheric pollution, *Int. Soil Water Conserv. Res.*, 7(3), 297-307, doi:10.1016/j.iswcr.2019.04.002,  
3107 2019.
- 3108 Smith, L.: *The new north: The world in 2050*, Profile Books, London, UK, 2011.
- 3109 Song, S., Li, C., Shi, X., Zhao, S., Li, Z., Bai, Y., Cao, X., Wang, Q., Huotari, J., Tulonen, T., Uusheimo, S.,  
3110 Leppäranta, M., and Arvola, L.: Under-ice metabolism in a shallow lake (Wuliangsu Hai) in Inner Mongolia,  
3111 in cold and arid climate zone, *Freshw. Biol.*, 1–11, 2019.
- 3112 Spengler, T., Renfrew, I. A., Terpstra, A., Tjernström, M., Screen, J., Brooks, I. M., Andrew Carleton, A.,  
3113 Chechin, D., Chen, L., Doyle, J., Esau, I., Hezel, P. J., Jung, T., Kohyama, T., Lüpkes, C., McCusker, C. E.,  
3114 Nygård, T., Sergeev, D., Shupe, M. D., Sodemann, H., and Vihma, T.: High-latitude dynamics of  
3115 atmosphere–ice–ocean interactions, *Bull. Am. Meteorol. Soc.*, 97(9), ES179-ES182, doi:10.1175/bams-d-15-  
3116 00302.1, 2016.
- 3117 Sporre, M. K., Blichner, S. M., Karset, I. H. H., Makkonen, R., and Berntsen, T. K.: BVOC–aerosol–climate  
3118 feedbacks investigated using NorESM, *Atmos. Chem. Phys.*, 19, 4763–4782, doi:10.5194/acp-19-4763-  
3119 2019, 2019.
- 3120 Starodymova, D. P., Shevchenko, V. P., Sivonen, V. P., and Sivonen, V. V.: Material and elemental  
3121 composition of surface aerosols on the north-western coast of the Kandalaksha Bay of the White Sea, *Atmos.*  
3122 *Oceanic Opt.*, 29(6), 507-511, doi:10.1134/s1024856016060154, 2016.



- 3123 Sun, H., Santalahti, M., Pumpanen, J., Koster, K., Berninger, F., Raffaello, T., Asiegbu, F. O., and  
3124 Heinonsalo, J.: Bacterial community structure and function shift across a northern boreal forest fire  
3125 chronosequence, *Scientific Rep.*, 6, 12, doi:10.1038/srep32411, 2016.
- 3126 Sun, Y., Frankenberg C., Wood JD, Schimel DS., Jung, M., Guanter L., Drewry, DT., Verma, M., Porcar-  
3127 Castell, A., Griffis, TJ., Gu, L., Magney, S., Köhler P., Evans B., and Yuen, K.: OCO-2 advances  
3128 photosynthesis observation from space via solar-induced chlorophyll fluorescence, *Science* 358, 189,  
3129 doi:10.1126/science.aam5747, 2017.
- 3130 Suomi, I., Gryning, S-E. , O'Connor E.J., and Vihma, T.: Methodology for obtaining wind gusts  
3131 using Doppler lidar, *Quarterly Journal of the Royal Meteorological Society*, 143, 2061-2072,  
3132 doi.org/10.1002/qj.3059, 2016.
- 3133 Svensson, J., Virkkula, A., Meinander, O., Kivekäs, N., Hannula, H.-R., Järvinen, O., Peltoniemi, J.I.,  
3134 Gritsevich, M., Heikkilä, A., Kontu, A., Neitola, K., Brus, D., DagssonWaldhauserova, P., Anttila, K.,  
3135 Vehkamäki, M., Hienola, A., de Leeuw, G., and Lihavainen, H.: Soot-doped natural snow and its albedo —  
3136 results from field experiments, *Boreal Environment Research*, 21, 481-503, 2016.
- 3137 Svensson, J., Ström, J., Kivekäs, N., Dkhar, N. B., Tayal, S., Sharma, V. P., Jutila, A., Backman, J.,  
3138 Virkkula, A., Ruppel, M., Hyvärinen, A., Kontu, A., Hannula, H.-R., Leppäranta, M., Hooda, R. K., Korhola,  
3139 A., Asmi, E., and Lihavainen, H.: Light absorption of dust and elemental carbon in snow in the Indian  
3140 Himalayas and the Finnish Arctic, *Atmos. Meas. Tech.*, 11, 1403-1416, doi:10.5194/amt-11-1403-2018,  
3141 2018.
- 3142 Svensson, J., Ström, J., and Virkkula, A.: Multiple-scattering correction factor of quartz filters and the effect  
3143 of filtering particles mixed in water: implications for analyses of light absorption in snow samples, *Atmos.*  
3144 *Meas. Tech.*, 12, 5913-5925, doi:10.5194/amt-12-5913-2019, 2019.
- 3145 Taylor, K. E., Stouffer, R. J., and Meehl, G. A.: An overview of CMIP5 and the experiment design, *Bull.*  
3146 *Am. Meteorol. Soc.*, 93, 485-498, doi: 10.1175/BAMS-D-11-00094.1, 2012.
- 3147 Taylor, A., Brownlee, C., and Wheeler, G.: Coccolithophore cell biology: chalking up progress, *Ann. Rev.*  
3148 *Mar. Sci.*, 9, 283-310, doi:10.1146/annurev-marine-122414-034032, 2017.
- 3149 Terentieva, I. E., Glagolev, M. V., Lapshina, E. D., Sabrekov, A. F., and Maksyutov, S.: Mapping of West  
3150 Siberian taiga wetland complexes using Landsat imagery: implications for methane emissions,  
3151 *Biogeosciences*, 13, 4615–4626, doi:10.5194/bg-13-4615-2016, 2016.
- 3152 Thompson, R. L., Sasakawa, M., Machida, T., Aalto, T., Worthy, D., Lavric, J. V., Lund Myhre, C., and  
3153 Stohl, A.: Methane fluxes in the high northern latitudes for 2005–2013 estimated using a Bayesian  
3154 atmospheric inversion, *Atmos. Chem. Phys.*, 17, 3553–3572, doi:10.5194/acp-17-3553-2017, 2017.
- 3155 Thonat, T., Saunio, M., Bousquet, P., Pison, I., Tan, Z., Zhuang, Q., Crill, P. M., Thornton, B. F., Bastviken,  
3156 D., Dlugokencky, E. J., Zimov, N., Laurila, T., Hatakka, J., Hermansen, O., and Worthy, D. E. J.:



- 3157 Detectability of Arctic methane sources at six sites performing continuous atmospheric measurements,  
3158 *Atmos. Chem. Phys.*, 17, 8371–8394, doi:10.5194/acp-17-8371-2017, 2017.
- 3159 Thorslund, J., Jarsjo, J., Wallstedt, T., Morth, C. M., Lychagin, M. Y., and Chalov, S. R.: Speciation and  
3160 hydrological transport of metals in non-acidic river systems of the Lake Baikal basin: Field data and model  
3161 predictions, *Reg. Environ. Chang.*, 17(7), 2007–2021, doi:10.1007/s10113-016-0982-7, 2017.
- 3162 Tian, Z. X., Cheng, B., Zhao, J. C., Vihma, T., Zhang, W. L., Li, Z. J., and Zhang, Z. H.: Observed and  
3163 modelled snow and ice thickness in the Arctic Ocean with CHINARE buoy data, *Acta Oceanologica Sinica*,  
3164 36(8), 66–75, doi:10.1007/s13131-017-1020-4, 2017.
- 3165 Tillman, H., Yang, J. and Nielsson, E.: The Polar Silk Road: China's New Frontier of International  
3166 Cooperation, *China Quarterly of International Strategic Studies*, 4, 10.1142/S2377740018500215, 2018.
- 3167 Timokhina, A. V., Prokushkin, A. S., Onuchin, A. A., Panov, A. V., Kofman, G. B., and Heimann, M.:  
3168 Variability of ground CO<sub>2</sub> concentration in the middle taiga subzone of the Yenisei region of Siberia, *Russ.*  
3169 *J. Ecol.*, 46, 143–151, doi:10.1134/s1067413615020125, 2015a.
- 3170 Timokhina, A. V., Prokushkin, A. S., Onuchin, A. A., Panov, A. V., Kofman, G. B., Verkhovets, S. V., and  
3171 Heimann, M., Long-term trend in CO<sub>2</sub> concentration in the surface atmosphere over Central Siberia, *Russ.*  
3172 *Meteorol. Hydrol.*, 40, 186–190, 2015b.
- 3173 Tsuruta, A., Aalto, T., Backman, L., Hakkarainen, J., ... and Peters, W.: Global methane emission estimates  
3174 for 2000–2012 from CarbonTracker Europe-CH4 v1.0. *Geosci. Model Dev.*, 10, 1261–1289, 2017.
- 3175 Tuovinen, J-P., Aurela, M., Hatakka, J., Räsänen, A., ... Laurila, T.: Interpreting eddy covariance data from  
3176 heterogeneous Siberian tundra: land-cover-specific methane fluxes and spatial representativeness,  
3177 *Biogeosciences*, 16, 255–274, 2019.
- 3178 Uotila, P., Vihma, T., and Haapala, J.: Atmospheric and oceanic conditions and the extremely low Bothnian  
3179 Bay sea ice extent in 2014/2015, 42, 7740–7749, *Geophysical Research and Letters*, 2015.
- 3180 Uotila, P., Iovino, D., Vancoppenolle, M., Lensu, M., and Rousset, C., Comparing sea ice, hydrography and  
3181 circulation between NEMO3.6 LIM3 and LIM2, *Geosci. Model Dev.*, 10, 1009–1031, doi:10.5194/gmd-10-  
3182 1009-2017, 2017.
- 3183 Uotila, P., Goosse, H., Haines, K., Chevallier, M., Barthélemy, A., Bricaud, C., Carton, J., Fučkar, N.,  
3184 Garric, G., Iovino, D., Kauker, F., Korhonen, M., Lien, V. S., Marnela, M., Massonnet, F., Mignac, D.,  
3185 Peterson, K. A., Sadikni, R., Shi, L., Tietsche, S., Toyoda, T., Xie, J., and Zhang, A.: An assessment of ten  
3186 ocean reanalyses in the polar regions, *Clim Dyn* 52, 1613–1650, doi:10.1007/s00382-018-4242-z, 2019.
- 3187 Uttal, T., Starkweather, S., Drummond, J. R., Vihma, T., Makshtas, A. P., Darby, L. S., Burkhart, J. F., Cox,  
3188 C. J., Schmeisser, L. N., Haiden, T., Maturilli, M., Shupe, M. D., De Boer, G., Saha, A., Grachev, A. A.,  
3189 Crepinsek, S. M., Bruhwiler, L., Goodison, B., McArthur, B., Walden, V. P., Dlugokencky, E. J., P. Persson,  
3190 O., Lesins, G., Laurila, T., Ogren, J. A., Stone, R., Long, C. N., Sharma, S., Massling, A., Turner, D. D.,



- 3191 Stanitski, D. M., Asmi, E., Aurela, M., Skov, H., Eleftheriadis, K., Virkkula, A., Platt, A., Førlund, E. J.,  
3192 Iijima, Y., Nielsen, I. E., Bergin, M. H., Candlish, L., Zimov, N. S., Zimov, S. A., O'Neill, N. T., Fogal, P.  
3193 F., Kivi, R., Konopleva-Akish, E. A., Verlinde, J., Kustov, V. Y., Vassel, B., Ivakhov, V. M., Viisanen Y.,  
3194 and Intrieri, J. M.: International Arctic Systems for Observing the Atmosphere: An International Polar Year  
3195 Legacy Consortium, *Bull. Amer. Meteor. Soc.*, *97*, 1033–1056, doi:10.1175/BAMS-D-14-00145.1, 2016.
- 3196 Walker, X. J., Baltzer, J. L., Cumming, S. G., Day, N. J., Ebert, C., Goetz, S., Johnstone, J. F., Potter, S.,  
3197 Rogers, B. M., Schuur, E. A. G., Turetsky, M. R., and Mack, M. C., Increasing wildfires threaten historic  
3198 carbon sink of boreal forest soils, *Nature*, *572*, 520–523, doi:10.1038/s41586-019-1474-y, 2019.
- 3199 Walsh, M. G., de Smalen, A. W., and Mor, S. M.: Climatic influence on anthrax suitability in warming  
3200 northern latitudes, *Sci Rep*, *8*(1), 9269, doi:10.1038/s41598-018-27604-w, 2018.
- 3201 van Vuuren, D. P., Edmonds, J., Kainuma, M., Riahi, K., Thomson, A., Hibbard, K., Hurtt, G. C., Kram, T.,  
3202 Krey, V., Lamarque, J. F., Masui, T., Meinshausen, M., Nakicenovic, N., Smith, S. J., and Rose, S. K.: The  
3203 representative concentration pathways: an overview, *Clim. Chang.*, *109*, 5–31, doi:10.1007/s10584-011-  
3204 0148-z, 2011.
- 3205 Wang, J., Ge, X., Chen, Y., Shen, Y., Zhang, Q., Sun, Y., Xu, J., Ge, S., Yu, H., and Chen, M.: Highly time-  
3206 resolved urban aerosol characteristics during springtime in Yangtze River Delta, China: insights from soot  
3207 particle aerosol mass spectrometry, *Atmos. Chem. Phys.*, *16*, 9109–9127, doi:10.5194/acp-16-9109-2016,  
3208 2016.
- 3209 Wang, J., Zhao, B., Wang, S., Yang, F., Xing, J., Morawska, L., Ding, A., Kulmala, M., Kerminen, V.-M.,  
3210 Kujansuu, J., Wang, Z., Ding, D., Zhang, X., Wang, H., Tian, M., Petäjä, T., Jiang, J., and Hao J.: Particulate  
3211 matter pollution over China and the effects of control policies, *Sci. Total Environ.*, *584–585*, 426–447, 2017a.
- 3212 Wang, Z. B., Wu, Z. J., Yue, D. L., Shang, D. J., Guo, S., Sun, J. Y., Ding, A. J., Wang, L., Jiang, J. K., Guo,  
3213 H., Gao, J., Cheung, H. C., Morawska, L., Keywood, M., and Hu, M.: New particle formation in China:  
3214 Current knowledge and further directions, *Sci. Total Environ.*, *577*, 258–266,  
3215 doi:10.1016/j.scitotenv.2016.10.177, 2017b.
- 3216 Wang, P. C., Elansky, N. F., Timofeev, Y. M., Wang, G. C., Golitsyn, G. S., Makarova, M. V., Rakitin, V.  
3217 S., Shtabkin, Yu., Skorokhod, A. I., Grechko, E. I., Fokeeva, E. V., Safronov, A. N., Ran, L., and Wang, T.:  
3218 Long-term trends of carbon monoxide total columnar amount in urban areas and background regions:  
3219 ground- and satellite-based spectroscopic measurements, *Adv. Atmos. Sci.*, *35*(7), 785–795,  
3220 doi:10.1007/s00376-017-6327-8, 2018a.
- 3221 Wang, Y., Wang, Y., Wang, L., Petäjä, T., Zha, Q., Gong, C., Li, S., Pan, Y., Hu, B., Xin, J., and Kulmala,  
3222 M.: Increased inorganic aerosol fraction contributes to air pollution and haze in China, *Atmos. Chem. Phys.*,  
3223 *19*, 5881–5888, doi:10.5194/acp-19-5881-2019, 2019.



- 3224 Wang, Y.H., Yu, M., Wang, Y., Tang, G., Song, T., Zhou, P., Liu, Z., Hu, B., Ji, D.S., Wang, L., Zhu, X.,  
3225 Yan, C., Ehn, M., Gao, W.K., Pan, Y.P., Xin, J.Y., Sung, Y., Kerminen, V.-M., Kulmala, M. and Petäjä, T.:  
3226 Rapid formation of intense haze episode via aerosol-boundary layer feedback in Beijing, *Atmos. Chem.*  
3227 *Phys.*, 10, 45-53, 2020.
- 3228 Wang, Z., Huang, X., and Ding, A.: Dome effect of black carbon and its key influencing factors, *Atmos.*  
3229 *Chem. Phys.*, 18, 2821-2834, 2018b.
- 3230 Vanhatalo, A., Ghirardo, A., Juurola, E., Schnitzler, J.-P., Zimmer, I., Hellén, H., Hakola, H., and Bäck, J.:  
3231 Long-term dynamics of monoterpene synthase activities, monoterpene storage pools and emissions in boreal  
3232 Scots pine, *Biogeosciences*, 15, 5047–5060, doi:10.5194/bg-15-5047-2018, 2018.
- 3233 Varentsov, M., Konstantinov, P., Baklanov, A., Esau, I., Miles, V., and Davy, R.: Anthropogenic and natural  
3234 drivers of a strong winter urban heat island in a typical Arctic city, *Atmos. Chem. Phys.*, 18(23), 17573-  
3235 17587, doi:10.5194/acp-18-17573-2018, 2018a.
- 3236 Varentsov, M., Wouters, H., Platonov, V., and Konstantinov, P.: Megacity-induced mesoclimatic effects in  
3237 the lower atmosphere: a modeling study for multiple summers over Moscow, Russia, *Atmos.*, 9(2), 24,  
3238 doi:10.3390/atmos9020050, 2018b.
- 3239 Vasileva, A., Moiseenko, K., Skorokhod, A., Belikov, I., Kopeikin, V., and Lavrova, O.: Emission ratios of  
3240 trace gases and particles for Siberian forest fires on the basis of mobile ground observations, *Atmos. Chem.*  
3241 *Phys.*, 17(20), 12303-12325, doi:10.5194/acp-17-12303-2017, 2017.
- 3242 Wei, L. X., Deng, X. H., Cheng, B., Vihma, T., Hannula, H. R., Qin, T., and Pulliainen, J.: The impact of  
3243 meteorological conditions on snow and ice thickness in an Arctic lake, *Tellus A: Dyn. Meteorol. Oceanogr.*,  
3244 68, 12, doi:10.3402/tellusa.v68.31590, 2016.
- 3245 Vestenius, M., Hellén, H., Levula, J., Kuronen, P., Helminen, K. J., Nieminen, T., Kulmala, M., and Hakola,  
3246 H.: Acidic reaction products of monoterpenes and sesquiterpenes in atmospheric fine particles in a boreal  
3247 forest, *Atmos. Chem. Phys.*, 14, 7883–7893, doi:10.5194/acp-14-7883-2014, 2014.
- 3248 Wickström, S., Jonassen, M., Vihma, T., and Uotila, P.: Trends in cyclones in the high latitude North  
3249 Atlantic during 1979-2016, *Q. J. R. Meteorol. Soc.*, 146, 762– 779, doi:10.1002/qj.3707, 2020.
- 3250 Wiedensohler, A., Ma, N., Birmili, W., Heintzenberg, J., Ditas, F., Andreae, M. O., and Panov, A.:  
3251 Infrequent new particle formation over the remote boreal forest of Siberia, *Atmos. Environ.*, 200, 167-169,  
3252 doi:10.1016/j.atmosenv.2018.12.013, 2019.
- 3253 Vihma, T., Uotila, P., Sandven, S., Pozdnyakov, D., Makshtas, A., Pelyasov, A., Pirazzini, R., Danielsen, F.,  
3254 Chalov, S., Lappalainen, H. K., Ivanov, V., Frolov, I., Albin, A., Cheng, B., Dobrolyubov, S., Arkhipkin, V.,  
3255 Myslenkov, S., Petäjä, T., and Kulmala, M.: Towards an advanced observation system for the marine Arctic  
3256 in the framework of the Pan-Eurasian Experiment (PEEX), *Atmos. Chem. Phys.*, 19, 1941-1970,  
3257 doi:10.5194/acp-19-1941-2019, 2019.



- 3258 Vihma, T., Graverson, R., Chen, L., Dörthe H., Skific, N., Francis, J.A., Tyrrell, N., Hall, R., Hanna, E.,  
3259 Uotila, P., Dethloff, K., Karpechko, A. Y., Björnsson, H. and Overland, J. E.: Effects of the tropospheric  
3260 large-scale circulation on European winter temperatures during the period of amplified Arctic warming, *Int J*  
3261 *Climatol.*, 40, 509–529, doi:10.1002/joc.6225, 2020
- 3262 Wild, B., Andersson, A., Bröder, L., Vonk, J., Hugelius, G., McClelland, J.W., Song, W., Raymond, P.A.,  
3263 and Gustafsson, Ö.: Rivers across the Siberian Arctic unearth the patterns of carbon release from thawing  
3264 permafrost *Proceedings of the National Academy of Sciences*, 116 (21) 10280-10285., 2019.
- 3265 Williams, P. J., and Smith, M. W.: *The Frozen Earth: Fundamentals of Geocryology*, Cambridge University  
3266 Press, Cambridge, UK, 1989.
- 3267 Virkkula, A., Chi, X., Ding, A., Shen, Y., Nie, W., Qi, X., Zheng, L., Huang, X., Xie, Y., Wang, J., Petäjä,  
3268 T., and Kulmala, M.: On the interpretation of the loading correction of the aethalometer, *Atmos. Meas.*  
3269 *Tech.*, 8, 4415-4427, doi:10.5194/amt-8-4415-2015, 2015.
- 3270 WMO, 2019 Guidance on Integrated Urban Hydrometeorological, Climate and Environmental Services.  
3271 Volume 1: Concept and Methodology, Grimmond, S., Bouchet, S., Molina, L., Baklanov, A., Joe, P. et al.,  
3272 WMO-No. 1234, [https://library.wmo.int/doc\\_num.php?explnum\\_id=9903](https://library.wmo.int/doc_num.php?explnum_id=9903), 2019.
- 3273 Voigt, C., Marushchak, M.E., Lamprecht, R.E., et al.: Nitrous oxide emissions from thawing permafrost,  
3274 *PNAS* May 2017, 201702902; DOI: 10.1073/pnas.1702902114.
- 3275 Voigt, C., Lamprecht, R. E., Marushchak, M. E., Lind, S. E., Novakovskiy, A., Aurela, M., Martikainen, P. J.  
3276 and Biasi, C.: Warming of subarctic tundra increases emissions of all three important greenhouse gases -  
3277 carbon dioxide, methane, and nitrous oxide, *Glob. Change Biol.*, 23(8), 3121-3138, doi:10.1111/gcb.13563,  
3278 2016.
- 3279 Wolf-Grosse, T., Esau, I., and Reuder, J.: The large-scale circulation during air quality hazards in Bergen,  
3280 Norway, *Tellus A: Dyn. Meteorol. Oceanogr.*, 69, 16, doi:10.1080/16000870.2017.1406265, 2017a.
- 3281 Wolf-Grosse, T., Esau, I., and Reuder, J.: Sensitivity of local air quality to the interplay between small- and  
3282 large-scale circulations: a large-eddy simulation study, *Atmos. Chem. Phys.*, 17(11), 7261-7276,  
3283 doi:10.5194/acp-17-7261-2017, 2017b.
- 3284 Voropay N.N., Ryazanova A.A., Dyukarev E.A. Variability of vegetation index NDVI during periods of  
3285 drought in the Tomsk Region, *IOP Conf. Series: Earth Environ. Sci.*, 381, 012096, doi:10.1088/1755-  
3286 1315/381/1/012096, 2019.
- 3287 Voropay, N. N., Kichigina, N. V.: Long-term changes in the hydroclimatic characteristics in the Baikal  
3288 region, *IOP Conf. Ser.: Earth Environ. Sci.*, 107, 012042, 2018.
- 3289 Xausa, F., Paasonen, P., Makkonen, R., Arshinov, M., Ding, A., Denier Van Der Gon, H., Kerminen, V.-M.,  
3290 and Kulmala, M.: Advancing global aerosol simulations with size-segregated anthropogenic particle number  
3291 emissions, *Atmos. Chem. Phys.*, 18, 10039–10054, doi:10.5194/acp-18-10039-2018, 2018.



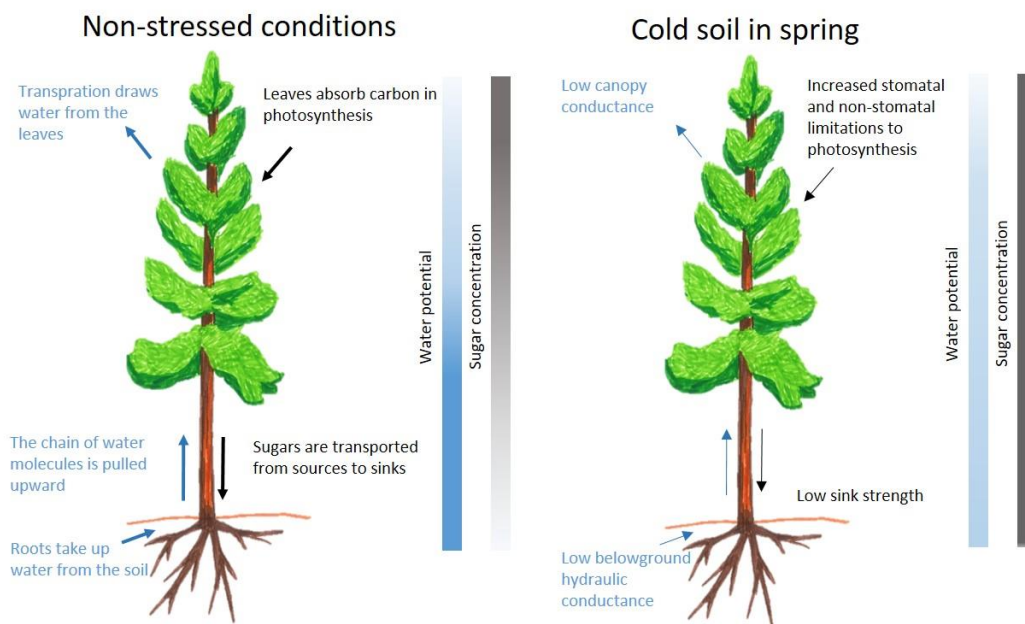
- 3292 Xiao., S., Wang, M. Y., Yao, L., Zhou, B., Yang, X., Chen, J. M., Wang, D. F., Fu, Q. Y., Worsnop, D. R.  
3293 and Wang, L.: Strong atmospheric new particle formation in winter in urban Shanghai, China, *Atmos. Chem.*  
3294 *Phys.*, 15, 1769-1781, 2015.
- 3295 Xie, Y. N., Ding, A. J., Nie, W., Mao, H. T., Qi, X. M., Huang, X., Xu, Z., Kerminen, V. K., Petäjä, T., Chi,  
3296 X., Virkkula, A., Boy, M., Xue, L., Guo, J., Sun, J., Yang, X., Kulmala, M., and Fu, C. B.: Enhanced sulfate  
3297 formation by nitrogen dioxide: Implications from in situ observations at the SORPES station, *J Geophys.*  
3298 *Res.: Atmos.*, 120(24), 12679-12694, doi:10.1002/2015jd023607, 2015.
- 3299 Yan, C., Yin, R., Lu, Y., Dada, L., Yang, D., Fu, Y., Kontkanen, J., Deng, C., Garmash, O., Ruan, J.,  
3300 Baalbaki, R., Schervish, M., Cai, R., Bloss, M., Chan, T., Chen, T., Chen, Q., Chen, X., Chen, Y., Chu, B.,  
3301 Dällenbach, K., Foreback, B., He, X., Heikkinen, L., Jokinen, T., Junninen, H., Kangasluoma, J., Kokkonen,  
3302 T., Kurppa, M., Lehtipalo, K., Li, H., Li, H., Li, X., Liu, Y. Ma, Q., Paasonen, P., Rantala, P., Pileci, R. E.,  
3303 Rusanen, A., Sarnela, N., Simonen, P., Wang, S., Wang, W., Wang, Y. Xue, M., Yang, G., Yao, L., Zhou,  
3304 Y., Kujansuu, J., Petäjä, T., Nie, W., Ma, N., Ge, M., He, H., Donahue, N. M., Worsnop, D. R., Kerminen,  
3305 V.-M., Wang, L., Liu, Y., Zheng, J., Kulmala, M., Jiang, J. and Bianchi, F. (2021) The synergistic role of  
3306 sulfuric acid, bases, and oxidized organics governing new-particle formation in Beijing. *Geophys. Res. Lett.*  
3307 (in press).
- 3308 Yang, F., Li, C., Leppäranta, M., Shi, X., Zhao, S. and Zhang, C.: Notable increases in nutrient  
3309 concentrations in a shallow lake during seasonal ice growth, *Water Sci. Technol.*, 74(12), 2773–2883, 2016.
- 3310 Yang, Y., Leppäranta, M. J., Ki, Z., Cheng, B., Zhai, M., and Demchev, D.: Model simulations of the annual  
3311 cycle of the landfast ice thickness in the East Siberian Sea, *Advances in Polar Sciences*, 26(2), 168-178,  
3312 doi:10.13679/j.advps.2015.2.00168, 2015.
- 3313 Yao, L., Garmash, O., Bianchi, F., Zheng, J., Yan, C., Kontkanen, J., Junninen, H., Mazon, S.B., Ehn, M.,  
3314 Paasonen, P., Sipilä, M., Wang, M.Y., Wang, X.K., Xiao, S., Chen, H.F., Lu, Y.Q., Zhang, B.W., Wang,  
3315 D.F., Fu, Q.Y., Geng, F.H., Li, L., Wang, H.L., Qiao, L.P., Yang, X., Chen, J.M., Kerminen, V.-M., Petäjä,  
3316 T., Worsnop, D.R., Kulmala, M. and Wang, L.: Atmospheric new particle formation from sulfuric acid and  
3317 amines in a Chinese megacity, *Science*, 361, 278-281, 2018.
- 3318 Yasunaka, S., Siswanto, E., Olsen, A., Hoppema, M., Watanabe, E., Fransson, A., Chierici, M., Murata, A.,  
3319 Lauvset, S. K., Wanninkhof, R., Takahashi, T., Kosugi, N., Omar, A. M., van Heuven, S., and Mathis, J. T.:  
3320 Arctic Ocean CO<sub>2</sub> uptake: an improved multiyear estimate of the air–sea CO<sub>2</sub> flux incorporating chlorophyll  
3321 a concentrations, *Biogeosciences*, 15, 1643–1661, doi:10.5194/bg-15-1643-2018, 2018.
- 3322 Ye, Z., Liu, J., Gu, A., Feng, F., Liu, Y., Bi, C., Xu, J., Li, L., Chen, H., Chen, Y., Dai, L., Zhou, Q., and Ge,  
3323 X.: Chemical characterization of fine particulate matter in Changzhou, China, and source apportionment with  
3324 offline aerosol mass spectrometry, *Atmos. Chem. Phys.*, 17, 2573–2592, doi:10.5194/acp-17-2573-2017,  
3325 2017.



- 3326 Ylivinkka, I., Kaupinmäki, S., Virman, M., Peltola, M., Taipale, D., Petäjä, T., Kerminen, V.-M., Kulmala,  
3327 M., and Ezhova, E.: Clouds over Hyytiälä, Finland: an algorithm to classify clouds based on solar radiation  
3328 and cloud base height measurements, *Atmos. Meas. Tech.*, 13, 5595–5619, 2020.
- 3329 He, Y., Chen, F., Jia, H., and Valery, G.: Bondur: Different Drought Legacies between Rain-fed and  
3330 Irrigated Croplands in a Typical Russian Agricultural Region, *Remote Sens.*, 12(11), 1700,  
3331 doi:10.3390/rs12111700, 2020
- 3332 Zaidan, M. A., Haapasilta, V., Relan, R., Junninen, H., Aalto, P. P., Kulmala, M., Laurson, L., and Foster, A.  
3333 S.: Predicting atmospheric particle formation days by Bayesian classification of the time series features,  
3334 *Tellus B: Chem. Phys. Meteorol.*, 70, 10, doi:10.1080/16000889.2018.1530031, 2018a.
- 3335 Zaidan, M. A., Haapasilta, V., Relan, R., Paasonen, P., Kerminen, V.-M., Junninen, H., Kulmala, M., and  
3336 Foster, A. S.: Exploring non-linear associations between atmospheric new-particle formation and ambient  
3337 variables: a mutual information approach, *Atmos. Chem. Phys.*, 18, 12699–12714, doi:10.5194/acp-18-  
3338 12699-2018, 2018b.
- 3339 Zanatta, M., Laj, P., Gysel, M., Baltensperger, U., Vratolis, S., Eleftheriadis, K., Kondo, Y., Dubuisson, P.,  
3340 Winiarek, V., Kazadzis, S., Tunved, P., and Jacobi, H.-W.: Effects of mixing state on optical and radiative  
3341 properties of black carbon in the European Arctic, *Atmos. Chem. Phys.*, 18, 14037–14057, doi:10.5194/acp-  
3342 18-14037-2018, 2018.
- 3343 Zapadinsky, E., Passananti, M., Myllys, N., Kurten, T., and Vehkamäki, H.: Modeling on Fragmentation of  
3344 Clusters inside a Mass Spectrometer, *Journal of Physical Chemistry, A* 123 (2), 611–624,  
3345 <https://doi.org/10.1021/acs.jpca.8b10744>, 2019.
- 3346 Zha, Q., Yan, C., Junninen, H., Riva, M., Sarnela, N., Aalto, J., Quéléver, L., Schallhart, S., Dada, L.,  
3347 Heikkinen, L., Peräkylä, O., Zou, J., Rose, C., Wang, Y., Mammarella, I., Katul, G., Vesala, T., Worsnop, D.  
3348 R., Kulmala, M., Petäjä, T., Bianchi, F., and Ehn, M.: Vertical characterization of highly oxygenated  
3349 molecules (HOMs) below and above a boreal forest canopy, *Atmos. Chem. Phys.*, 18, 17437–17450,  
3350 doi:10.5194/acp-18-17437-2018, 2018.
- 3351 Zhang, J., Liu, C., and Chen, H.: The modulation of Tibetan Plateau heating on the multi-scale northernmost  
3352 margin activity of East Asia summer monsoon in northern China, *Global Planet. Change*, 161, 149–161,  
3353 2018.
- 3354 Zhang, S., Zhang, J. H., Bai, Y., Koju, U. A., Igbawua, T., Chang, Q., Zhang, D., and Yao, F. M.: Evaluation  
3355 and improvement of the daily boreal ecosystem productivity simulator in simulating gross primary  
3356 productivity at 41 flux sites across Europe, *Ecol. Model.*, 368, 205–232,  
3357 doi:10.1016/j.ecolmodel.2017.11.023, 2018.
- 3358 Zhang-Turpeinen, H., Kivimäenpää, M., Aaltonen, H., Berninger, F., Köster, E., Köster, K., Menyailo, O.,  
3359 Prokushkin, A., and Pumpanen, J.: Wildfire effects on BVOC emissions from boreal forest floor on

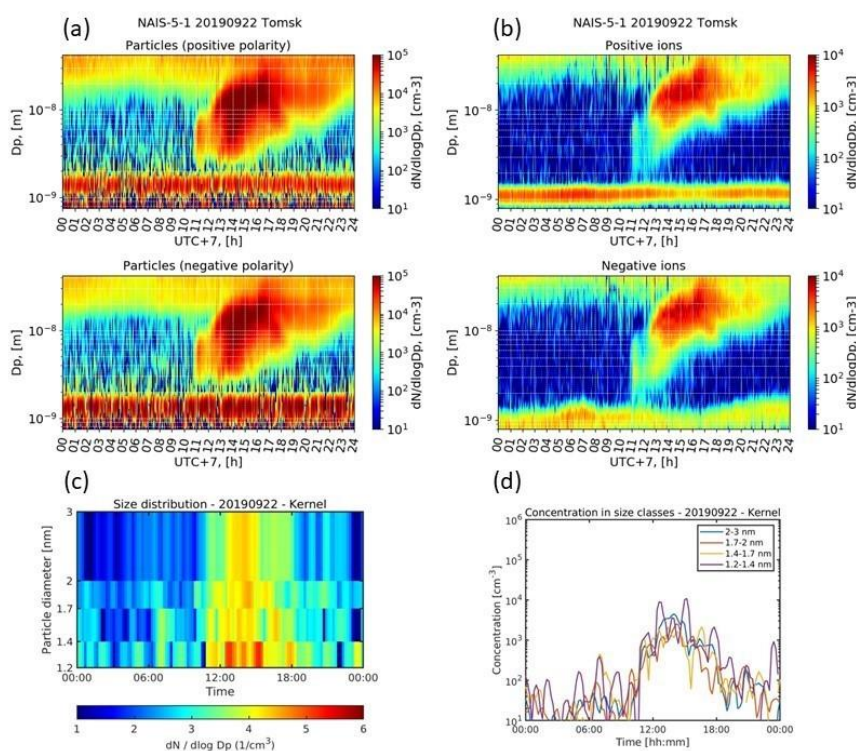


- 3360 permafrost soil in Siberia, *Science of the Total Environment*, 134851, doi:10.1016/j.scitotenv.2019.134851,  
3361 2020.
- 3362 Zhao, H., Li, X., Zhang, Q., Jiang, X., Lin, J., Peters, G. P., Li, M., Geng, G., Zheng, B., Huo, H., Zhang, L.,  
3363 Wang, H., Davis, S. J., and He, K.: Effects of atmospheric transport and trade on air pollution mortality in  
3364 China, *Atmos. Chem. Phys.*, 17, 10367–10381, doi:10.5194/acp-17-10367-2017, 2017.
- 3365 Zhdanova, E. Y., Chubarova, N. Y., and Lyapustin, A. I.: Assessment of urban aerosol pollution over the  
3366 Moscow megacity by the MAIAC aerosol product, *Atmos. Meas. Tech.*, 13, 877–891, doi:10.5194/amt-13-  
3367 877-2020, 2020.
- 3368 Zhou, Y., Dada, L., Liu, Y., Fu, Y., Kangasluoma, J., Chan, T., Yan, C., Chu, B., Daellenbach, K. R.,  
3369 Bianchi, F., Kokkonen, T. V., Liu, Y., Kujansuu, J., Kerminen, V.-M., Petäjä, T., Wang, L., Jiang, J., and  
3370 Kulmala, M.: Variation of size-segregated particle number concentrations in wintertime Beijing, *Atmos.*  
3371 *Chem. Phys.*, 20, 1201–1216, doi:10.5194/acp-20-1201-2020, 2020.
- 3372 Zilitinkevich, S., Druzhinin, O., Glazunov, A., Kadantsev, E., Mortikov, E., Repina, I., and Troitskaya, Y.:  
3373 Dissipation rate of turbulent kinetic energy in stably stratified sheared flows, *Atmos. Chem. Phys.*, 19, 2489–  
3374 2496, doi:10.5194/acp-19-2489-2019, 2019.
- 3375 Öström, E., Putian, Z., Schurgers, G., Mishurov, M., Kivekäs, N., Lihavainen, H., Ehn, M., Rissanen, M. P.,  
3376 Kurtén, T., Boy, M., Swietlicki, E., and Roldin, P.: Modeling the role of highly oxidized multifunctional  
3377 organic molecules for the growth of new particles over the boreal forest region, *Atmos. Chem. Phys.*, 17,  
3378 8887–8901, doi:10.5194/acp-17-8887-2017, 2017.
- 3379



3380  
 3381  
 3382

Figure 1.

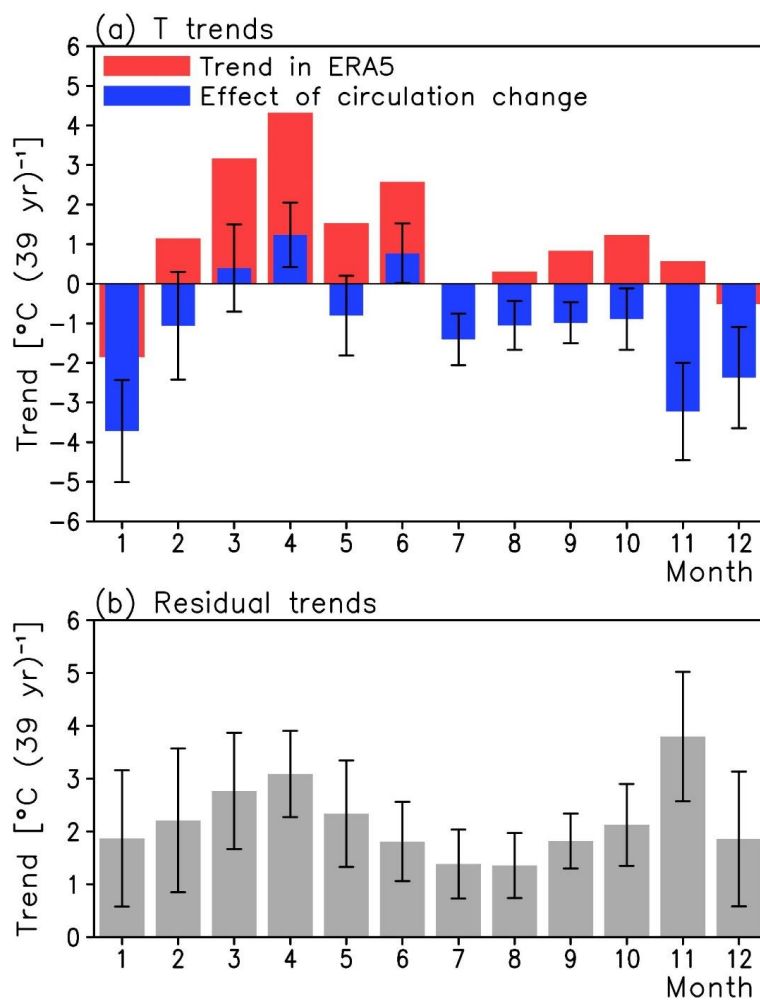


3383



3384 Figure 2.

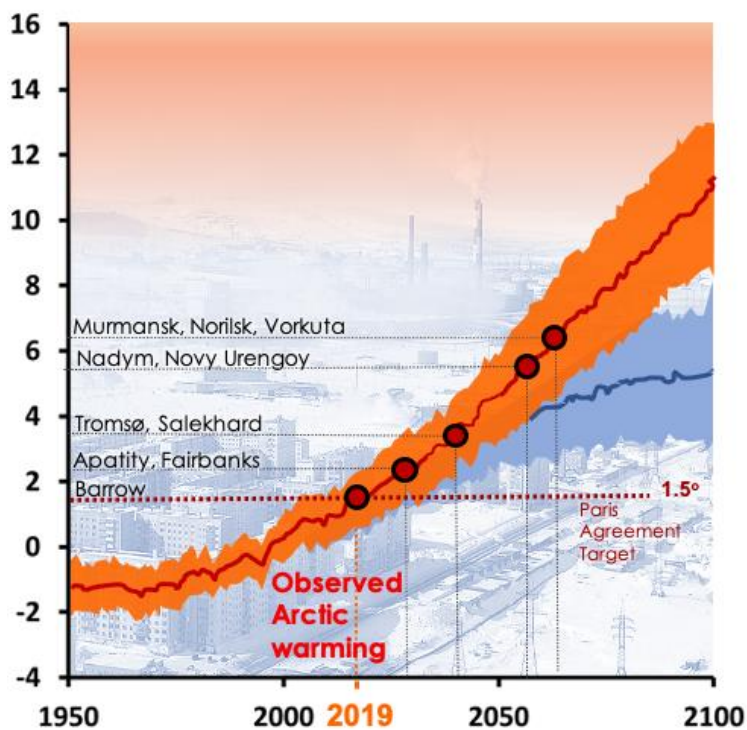
3385



3386

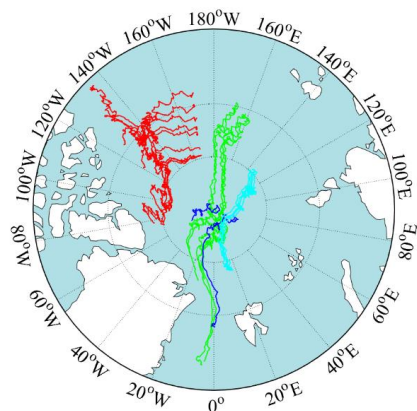
3387 Figure 3.

3388



3389

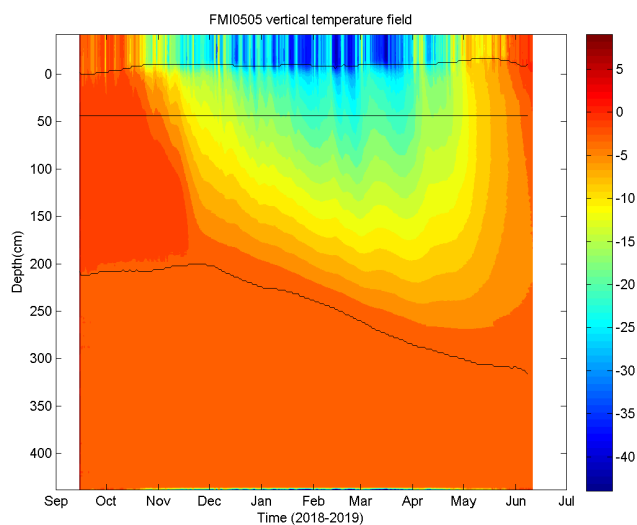
3390 Figure 4.



3391

3392 Figure 5.

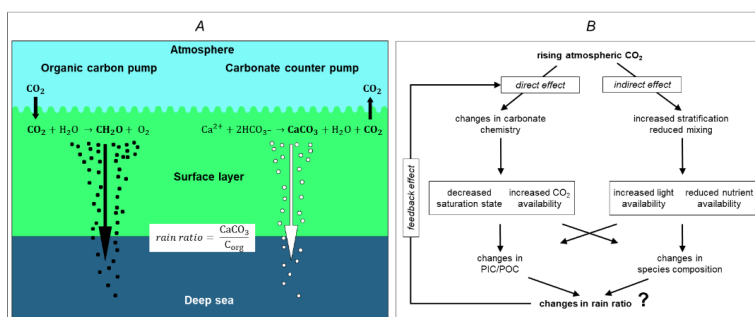
3393



3394

3395 Figure 6.

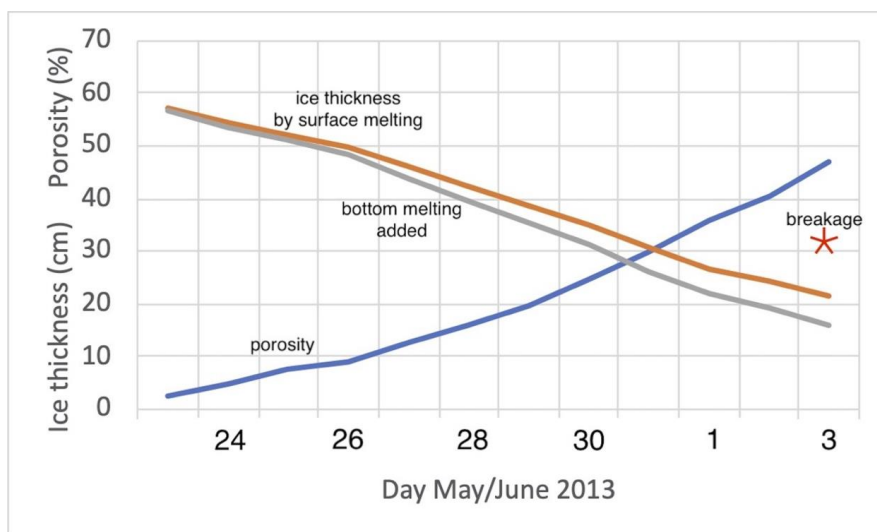
3396



3397

3398 Figure 7.

3399



3400

3401 Figure 8.

3402

A

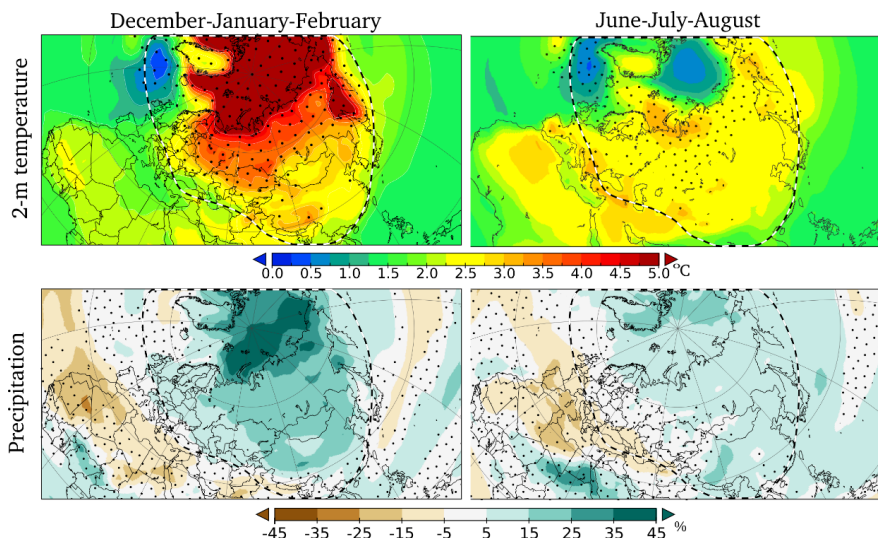
	Fe	Al	Mn	Pb	Bi	Co	Be	V	Ni	Cr	Cd	Cu	Zn	As	B	U	Mo	Sb	Ca	Sr	Sn
Russian part of the catchment	65	69	56	46	77	59	71	65	48	29	49	41	25	22	11	5	2	1	2	3	34
Mongolian part of the catchment	98	96	100	95	87	89	71	57	56	55	71	70	86	10	19	4	2	0	11	9	58

B

	Fe	Al	Mn	Pb	Bi	Co	Be	V	Ni	Cr	Cd	Cu	Zn	As	B	U	Mo	Sb	Ca	Sr	Sn
Russian part of the catchment	60	70	52	45	75	57	41	56	40	47	19	42	26	39	18	6	4	41	2	3	15
Mongolian part of the catchment	78	83	59	72	76	59	49	43	35	49	13	62	23	12	10	1	1	42	2	2	11

3403

3404 Figure 9.



3405

3406 Figure 10.

3407

3408

3409

3410

3411 **Figure 1.** A recent field and modelling study shows that cold soil decreases belowground hydraulic  
3412 conductance (i.e. less root water uptake), and further canopy conductance in mature, boreal trees in spring  
3413 (Lintunen et al. 2020). Cold temperature also decreases sink strength (i.e. less sugars are needed for metabolism  
3414 and growth). Low sink strength increases sugar concentration in leaves, which decreases photosynthesis due  
3415 to increased stomatal and non-stomatal limitations for photosynthesis (Hölttä et al., 2017; Salmon et al., 2020).

3416 **Figure 2.** Example of results from the state-of-the-art aerosol instruments NAIS and PSM displaying NPF  
3417 event at Fonovaya station, Siberia, on 22.09.2019. Particles of different polarity, NAIS (a), ions of different  
3418 polarity, NAIS (b), particle number distribution at the smallest sizes, PSM (c), number concentration of the  
3419 smallest particles in different size bins, PSM (d).

3420

3421 **Figure 3.** Linear trends of monthly mean temperature in Western Siberia ( $55^{\circ}$ - $65^{\circ}$ N,  $65^{\circ}$ - $90^{\circ}$ E) in years 1979-  
3422 2018. In (a), the red bars show the trend in the ERA5 reanalysis and the blue bars the circulation-related trend.  
3423 In (b), the residual trends are shown. The error bars indicate the 5-95% uncertainty range in the circulation-  
3424 related trend and the residual trend based on interannual variability. Redrawn from Räisänen (2020).

3425



3426 **Figure 4.** The northern urban heat islands are forerunners of the global warming. Winter season future  
3427 temperatures for the Arctic (60–90°N) averaged over 36 CMIP5 global climate models and expressed as  
3428 departures from the means for the 1981–2005 period. The red line is the ensemble mean for RCP8.5, the blue  
3429 line is for RCP4.5. Shaded areas denote  $\pm$  one standard deviation from the ensemble mean (Overland et al.,  
3430 2014; and Fig. 2.15 of AMAP, 2017). The observed surface UHIs are shown as red dots collocated with the  
3431 expected future Arctic temperature anomalies, e.g., the observed wintertime urban temperature anomaly in  
3432 Nadyim corresponds to the regional warming as expected to be reached by 2060. Observe that the present Arctic  
3433 climate is already 1.5°C warmer than the historical normals 1960-1990.

3434

3435 **Figure 5.** Trajectories of SIMBA buoys deployed in the Arctic in the period 2018-2019. Red: CHINARE (10  
3436 buoys), green: NABOS (5 buoys), dark blue: CAATEX (2 buoys), and light blue: MOSAiC (15 buoys).  
3437 SIMBA is a thermistor string-based ice mass balance (IMB) buoy. It measures high-resolution (2 cm) vertical  
3438 environment temperature (ET) profiles (4 times a day) through the air-snow-sea ice-ocean column. The heating  
3439 temperature (HT) measured by the thermistor string once per day is based on the use of a small identical heater  
3440 on each sensor. The ET and HT data are used to derive snow depth and ice thickness. SIMBA uses GPS module  
3441 to track the buoy location. The Iridium satellite is used for data transmission. A total 15 SIMBA buoys have  
3442 been deployed in the Arctic Ocean during the Chinese National Arctic Research Expedition (CHINARE) 2018  
3443 and the Nansen and Amundsen Basins Observational System (NABOS) 2018 field expeditions in late autumn.  
3444 In 2019 17 SIMBA buoys were deployed during the CAATEX (2) and MOSAIC expeditions (15, leg 1).

3445

3446 **Figure 6.** SIMBA observations on the temporal evolution of the snow depth, ice thickness, and the  
3447 temperature profile from the ocean through snow and sea ice to air. The results were obtained applying the  
3448 algorithm by Liao et al. (2018). The black lines are snow surface (top), Initial freeboard (middle) and ice base  
3449 (bottom). 0 level refers to snow/ice interface. The colors indicate the temperature in °C.

3450 **Figure 7. A:** Biological pumps resulting in (i) atmospheric CO<sub>2</sub> sink and(ii) calcium carbonate transport from  
3451 surface to deep ocean; **B:** anticipated forward and feedback alterations in ocean ecology driven by atmospheric  
3452 CO<sub>2</sub> increase. PIC=particulate inorganic carbon; POC=particulate organic carbon (modified after Rost &  
3453 Riebesell, 2004).

3454 **Figure 8.** Field data for ice decay in Lake Kilpisjärvi in 2013 showing decrease of ice thickness by surface  
3455 melting and bottom melting and increase of porosity until breakage of ice cover.

3456 **Figure 9.** Hydrogeochemical signature of large river system –Selenga River case study. The figure represent  
3457 metal(loid)s partitioning (Median values) in the Selenga river basin in the upper (Mongolian) and downstream  
3458 (Russian) part between 20 July -10 August 2011 under dominant high water (A) and 07 June -10 July 2012  
3459 under dominant low water conditions. Dark orange fill corresponds to the share of suspended forms of  
3460 elements > 75% (green), light orange – 75-50%, light blue – 50-25%, dark blue – < 25%. The figure indicate  
3461 that in the large river system some metals are mostly found in the dissolved form (84–96% of Mo, U, B, and



3462 Sb on an average), whereas many others predominantly existed in suspension (66–87% of Al, Fe, Mn, Pb, Co,  
3463 and Bi). A consistently increasing share of metals in suspended particulate modes (about 2–6 times) is observed  
3464 under high discharge conditions For details and other hydrological seasons refer to (Kasimov et al., 2020b).  
3465

3466 **Figure 10.** Changes in 2-meter temperature (°C, upper panels) and precipitation (% , lower panels) during the  
3467 21st century. Present-day climatology is averaged over years 1981–2010 and end-of-century climatology over  
3468 2070–2099. Winter (left) and summer (right) are shown separately. Dotted areas indicate high variability in  
3469 model ensemble (for temperature: standard deviation of 21st century change exceeds 1°C; for precipitation:  
3470 standard deviation of 21st century change exceeds 100% or present-day precipitation). The model results are  
3471 from IPCC AR5, based on 42 individual models in CMIP5 experiments under the RCP4.5 scenario.

3472

3473 **Table 1.** Systems, key topical areas, research question introduced in the PEEEX Science Plan (SP) (Kulmala et  
3474 al. 2015; 2016a, Lappalainen et al. 2018) connected to the addressed research themes over last 5 years by the  
3475 PEEEX questionnaire (APPENDIX 1). The addressed research themes and the results are overviewed in Chapter  
3476 3.

3477

3478

PEEX – SP System	PEEX - SP key topical area	PEEX - SP research question (Q-No)	Addressed research themes during the last 5 years
Land	Changing land ecosystem processes	<b>How could the land regions and processes that are especially sensitive to climate change be identified, and what are the best methods to analyze their responses? (Q-1)</b>	<ul style="list-style-type: none"><li>• high-latitude photosynthetic productivity and vegetation changes (greening, browning)</li><li>• new methodologies determining Earth surface characteristics</li></ul>
Land	Risk areas of permafrost thawing	<b>How fast will permafrost thaw proceed, and how will it affect ecosystem processes and ecosystem-atmosphere feedbacks, including hydrology and greenhouse gas fluxes ? (Q-2)</b>	<ul style="list-style-type: none"><li>• soil temperature evolution</li><li>• changing GHG fluxes, carbon sink-source dynamics due to permafrost thawing</li></ul>
Land	Ecosystem structural changes	<b>What are the structural ecosystem changes and tipping points in the future evolution of the Pan-Eurasian ecosystem? (Q-3)</b>	<ul style="list-style-type: none"><li>• changes in soil microbial activity e.g. effect of forest fires</li><li>• changes of the Northern soils and functioning of the Arctic tundra in global carbon cycling context</li></ul>



Atmosphere	Atmospheric composition and chemistry	<b>What are the critical atmospheric physical and chemical processes with large-scale climate implications in a northern context? (Q4)</b>	<ul style="list-style-type: none"> <li>• carbon (C) balance in the boreal forests; methane (CH<sub>4</sub>) balance at the Arctic; carbon monoxide (CO), ozone (O<sub>3</sub>) at the Northern Eurasian region</li> <li>• Sources and properties of atmospheric aerosols in boreal and Arctic environments</li> <li>• black carbon and dust in the atmosphere and on snow at the Northern high latitudes</li> <li>• methodological and model developments related to atmospheric chemistry and physics</li> </ul>
Atmosphere	Urban air quality and megacities, ABL	<b>What are the key feedbacks between air quality and climate at northern high latitudes and in China? (Q5)</b>	<ul style="list-style-type: none"> <li>• recent observations on air quality in China</li> <li>• Anthropogenic emissions and environmental pollution in Russia</li> </ul>
Atmosphere	Weather and atmospheric circulation	<b>How will atmospheric dynamics (synoptic scale weather, boundary layer) change in the Arctic-boreal regions? (Q6)</b>	<ul style="list-style-type: none"> <li>• cold &amp; warm episodes</li> <li>• cyclone density dynamics</li> <li>• circulation effect on temperature and moisture</li> <li>• cloudiness in Arctic</li> <li>• atmospheric boundary layer (ABL) dynamics</li> </ul>
Water	The Arctic Ocean in the climate system	<b>How will the extent and thickness of the Arctic sea ice and terrestrial snow cover change? (Q-7)</b>	<ul style="list-style-type: none"> <li>• Sea ice dynamics and thermodynamics with atmospheric and ocean dynamics</li> <li>• Snow depth/mass and sea ice thickness</li> <li>• Sea ice research supporting navigation</li> <li>• Ocean floor, sediments: composition and fluxes</li> <li>• River runoff effecting the hydrological processes at coastal marine environments in Russia</li> </ul>
Water	Arctic marine ecosystem	<b>What is the joint effect of Arctic warming, ocean freshening, pollution load and acidification on the Arctic marine ecosystem, primary production and carbon cycle? (Q-8)</b>	<ul style="list-style-type: none"> <li>• Living marine organisms weaken or even subdue CO<sub>2</sub> accumulation</li> </ul>
Water	Lakes and large-scale river systems	<b>What is the future role of Arctic-boreal lakes, wetlands and large river systems, including thermokarst lakes and running waters of all size, in biogeochemical cycles, and how will these changes affect societies? (Q-9)</b>	<ul style="list-style-type: none"> <li>• organic carbon, carbon balance, ice cover at lakes in the Northern high latitudes</li> <li>• specific characteristics of the Lake Baikal and Selenga River delta in Russia</li> <li>• specific characteristics of Asian water lakes</li> </ul>



Society	Anthropogenic impact	<b>How will human actions such as land-use changes, energy production, the use of natural resources, changes in energy efficiency and the use of renewable energy sources influence further environmental changes in the region? (Q-10)</b>	<ul style="list-style-type: none"> <li>• Mitigation e.g method for the natural risk assessment in Russia and new clean energy technologies</li> </ul>
Society	Environmental impact	<b>How do the changes in the physical, chemical and biological state of the different ecosystems, and the inland, water and coastal areas affect the economies and societies in the region, and vice versa? (Q-11)</b>	<ul style="list-style-type: none"> <li>• Reindeer grazing effects on the ground vegetation structure and biomass</li> </ul>
Society	Natural hazards	<b>In which ways are populated areas vulnerable to climate change? How can their vulnerability be reduced and their adaptive capacities improved? What responses can be identified to mitigate and adapt to climate change? (Q-12)</b>	<ul style="list-style-type: none"> <li>• Emerging zoonotic diseases</li> <li>• UV variation effects on health</li> <li>• Air pollution in different scales and environments (street-level urban air pollution, transported air pollution in urban environments, air pollution at the Arctic) and related health effects;</li> </ul>
Feedbacks	Key topics: Atmospheric composition, biogeochemical cycles: water, C, N, P, S	<b>How will the changing cryospheric conditions and the consequent changes in ecosystems feed back to the Arctic climate system and weather, including the risk of natural hazards? (Q-13)</b>	<ul style="list-style-type: none"> <li>• <i>Research needs:</i> quantification of the COntinental Biosphere-Aerosol-Cloud-Climate (COBACC) feedback loop at different Northern boreal environments</li> <li>• Gold &amp; high region quantification of BVOC – aerosols feedback loop at the Tibetan /Himalayan Plateau..</li> </ul>
Feedbacks	Key topics: Atmospheric composition, biogeochemical cycles: water, C, N, P, S	<b>What are the net effects of various feedback mechanisms on (i) land cover changes, (ii) photosynthetic activity, (iii) GHG exchange and BVOC emissions (iv) aerosol and cloud formation and radiative forcing ? How do these vary with climate change on regional and global scales? (Q-14)</b>	<ul style="list-style-type: none"> <li>• <i>Research needs:</i> The Arctic greening and browning calls for a multi-disciplinary scientific approach together, improved modelling tools and new data in order to solve scientific questions related to the net effects of various feedback mechanisms connecting the biosphere-atmosphere - human activities</li> </ul>



Feedbacks	Key topics: Atmospheric composition, biogeochemical cycles: water, C, N, P, S	<b>How are intensive urbanization processes changing the local and regional climate and environment? (Q-15)</b>	<ul style="list-style-type: none"><li>• <i>Research needs:</i> accelerating urbanization calls for studies on the effects of on air pollution, local climate and the effects these changes have on global climate. Integrated studies should lead to services for society, cities helping to mitigate hazards storms, flooding, heat waves, and air pollution episodes (see also 3.2.1)</li></ul>
-----------	--	---	---

3479

3480

3481 **Code/Data availability:** This is an review paper and the data availability is introduced in the  
3482 original articles.

3483 **Author contribution:** Co-authors have provided text and/or relevant references. Some of them  
3484 have been editors of the specific chapters of the manuscript.

3485 **Competing interests:** no specific competing interests